Identification and characterization of a new splice variant of the protein kinase DYRK4 and the role of DYRK1A during mitotic exit

Von der Fakultät für Mathematik, Informatik und Naturwissenschaften der RWTH Aachen University zur Erlangung des akademischen Grades eines Doktors der Naturwissenschaften genehmigte Dissertation

vorgelegt von

Diplom-Biologe

Chrisovalantis Papadopoulos

aus Wesel

Berichter:
Professor Dr.rer.nat Walter Becker
Univ.-Prof. Dr.rer.nat. Wilhelm Jahnen-Dechent

Tag der mündlichen Prüfung: 13.05.2011

Diese Dissertation ist auf den Internetseiten der Hochschulbibliothek online verfügbar.

Acknowledgements

First of all I want to thank Prof. Walter Becker for giving me the opportunity to do this interesting work in his lab, for allowing me to do “a free research” and to follow all the ideas that came to my mind. As my supervisor he was always willingly sharing his time to discuss not only all my scientific questions. I thank him for supporting my scientific career and my desires to gather experiences abroad, for his trust, and for his manner in general what let all of us working gladly in his lab.

I also want to thank Prof. Wilhelm Jahnen-Dechent. I was very glad when he willingly agreed to become my second supervisor.

Thank you to Dr. Susana de la Luna for her great support during my stay in Barcelona in her working group. It was a pleasure and a privilege to work with you. Together with Krisztina Arató, they encouraged me to believe in the potential of the DYRK4 paper and contributed with excellent experiments to finish this great work. Gracias Dr. Kriszti for your contribution not only in the scientific part, but also for Callus and much more ☺. Special thanks also to all Lunis and the Mus musculus of Marionas group. Thanks again for the warm reception in Barcelona!

I also thank Prof. Müller-Newen and Nico Chatain for the introduction to live cell imaging and for their contribution to the DYRK4 paper. Merci Nico! Thanks to Ulli from the group of Prof. Lüscher for the introduction to cell cycle analysis by FACS.

Thank you to everybody of the institute of pharmacology and toxicology, the scientist, the professors, the secretaries, the technicians, the colleagues, the friends…….. Thanks for being so open, for supporting me during my time here, for “problem solving” and for the coffee breaks spent together. Special thanks to Simone, to Ulf, to George and to the former and the present members of the DYRK group. I enjoyed all the “DYRK meetings” a lot. Also thanks to Annette and Nora for coffee, sports and smiling.

And last but certainly not least thanks to my parents for supporting me throughout my studies and making all this possible, to my sisters for helping me out and encouraging me. Thanks to my friends in Aachen, Wesel and all over the world. For their understanding, that a PhD student does not have enough time to be always present physically and/or mentally.

Abbreviation

APC/C	anaphase-promoting complex or cyclosome
ATP	Adenosine-5'-triphosphate
BSA	bovine serum albumin
CDK	cyclin-dependent kinase
CLK	CDK-like kinase
Cpm	counts per minute
CRM1	exportin-1
DAPI	4',6- diamidino-2-phenylindole
DH-box	DYRK homology-box
DMEM	Dulbecco´s modified Eagle medium
DMSO	dimethyl sulfoxide
dNTP	deoxynucleotide triphosphates
Dox	doxycycline
DS	Down syndrome
DSCR	Down syndrome critical region
DTT	Dithiothreitol
DYRK	dual-specificity tyrosine-phosphorylation regulated kinase
EDTA	ethylenediaminetetraacetic acid
ER	endoplasmatic reticulum
EST	expressed sequence tag
FACS	flow cytometry
Fig.	Figure
FLAG	octapeptide used as a tag in molecular biology
FLIP	fluorescence loss in photobleaching
FRT	Flp recombinase target sequence
GFP	green fluorescent protein
GSK	glycogen synthase kinase
GST	gluthathione S-transferase
HA	Human influenza hemagglutinin
HDAC	histone deacetylases
HEPES	4-(2-hydroxyethyl)-1-piperazineethanesulfonic acid
HRP	horseradish peroxidase
IgG	immunglobuline G

IMAC	immobilized-metal affinity chromatography
IP	immunoprecipitation
IPTG	isopropyl-β-D-thiogalactopyranoside
IVK	*in vitro* kinase
LB	medium after Luria Bertani
LSB	laemmli sample buffer
M-MLV	moloney murine leukemia virus
MAPK	mitogen-activated protein kinase
Mnb	minibrain
NAPA	N-terminal autophosphorylation accessory
NiNTA	nickel-nitrilotriacetic acid
NES	nuclear export signal
NLS	nuclear localization signal
OD	optical density
uORF	upstream open reading frame
PAGE	polyacrylamide gel electrophoresis
PEST	proline, glutamic acid, serine, threonine-rich region
PBS	phosphate buffered saline
PCR	polymerase chain reaction
PMSF	phenylmethylsulphonyl fluoride
PP	phosphoprotein phosphatase
qRT-PCR	quantitative real-time reverse transcription-PCR
RB	retinoblastoma protein
ROI	region of interest
Rpm	rounds per minute
RT	room temperature
RT-PCR	reverse transcription-PCR
SDS	sodium dodecyl sulphate
SF3B1	splicing factor 3B 1
TBS	Tris-buffered saline
TBS-T	TBS + 0.1% Tween-20
Tris	2-amino-2(hydroxymethyl)-1,3-propanediol
UPR	unfolded protein response
XBP1	X-box binding protein-1

Table of contents

Acknowledgements ---- I

Abbreviation ---- II

1. Introduction ---- 1

1.1 Protein kinases ---- 1

1.2 DYRK (dual-specificity tyrosine(Y)-phosphorylation regulated kinase) ---- 1
1.2.1 The DYRK family ---- 1
1.2.2 DYRK1A ---- 4
1.2.3 Autophosphorylation of DYRKs ---- 5
1.2.4 Substrate specificity of DYRKs ---- 6
1.2.5 Subcellular localization ---- 7

1.3 The cell cycle ---- 8
1.3.1 The retinoblastoma protein (RB), Cyclin D1 and histone H3 ---- 9
1.3.1.1 Phosphorylation level of the retinoblastoma protein ---- 10
1.3.1.2 Protein level of Cyclin D1 ---- 11
1.3.1.3 Phosphorylation level of histone H3 ---- 11
1.3.2 DYRKs and the cell cycle ---- 13

2. The aim of the study ---- 15

3. Material and Methods ---- 16

3.1 Materials ---- 16
3.1.1 Chemicals ---- 16
3.1.2 Frequently used buffers and chemical solutions ---- 16
3.1.3 Microorganisms ---- 17
3.1.4 Peptides ---- 17
3.1.5 Antibodies ---- 17
3.1.6 Plasmids ---- 19

3.2 Methods ---- 20
3.2.1 Preparation of bacterial expressed GST-DYRK1A variants ---- 20
3.2.2 Cell culture, transient and stable transfections ---- 22
3.2.3 Gene expression PCR analysis in tissues and cell lines ---- 23
3.2.4 Quantitative real-time reverse transcription-PCR (qRT-PCR) ---- 23
3.2.5 Fluorescence microscopy and shuttling analysis ---- 24
3.2.6 Immunoprecipitation ---- 25
3.2.7 Phosphatase treatment ---- 25
3.2.8 IMAC *(immobilized-metal affinity chromatography)* ---- 26
3.2.9 Protein purification using anti-GFPmag ---- 26
3.2.10 *In vitro* phosphorylation assay ---- 26
3.2.11 *In vitro* kinase (IVK) assay ---- 26
3.2.12 Whole cell lysates ---- 27

3.2.13 Western blot ----27
3.2.14 Synchronization for cell cycle analysis ----28
3.2.15 FACS analysis of synchronized cells ----29

4. Results ---------- 30

4.1 DYRK4 ---------- 30
4.1.1 Human and murine DYRK4 are expressed as multiple alternative splicing variants ----30
4.1.1.1 Exon-intron organization of the N-terminal region of DYRK4 ----30
4.1.1.2 Differential expression of DYRK4 variants in human tissues ----32
4.1.1.3 The transcript of the long human DYRK4 isoform is upregulated by tunicamycin in SH-SY5Y cells ----34
4.1.2 Alternative splicing alters the subcellular localization of DYRK4 ----35
4.1.2.1 DYRK4 is mainly localized in the cytosol ----35
4.1.2.2 CRM1-independent distribution of GFP-mDYRK4 ----36
4.1.2.3 Nucleocytoplasmic distribution of DYRK4 ----37
4.1.3 Kinase activity of DYRK4 ----40
4.1.3.1 DYRK4 is target of upstream kinases ----40
4.1.3.2 Long and short isoform of DYRK4 are catalytically active in vitro ---41
4.1.3.3 DYRK4 phosphorylates SF3B1 on Thr434 ----42
4.1.4 Substrate specificity of DYRK4 ----44
4.1.4.1 Pep285 is a specific substrate for DYRK4 ----44
4.1.4.2 Insertion of the NxGY motif does not significantly alter substrate selectivity of DYRK4 ----45

4.2 Posttranslational modifications of DYRK1A during the cell cycle ---------- 49
4.2.1 Harmine inhibits DYRK1A in cell culture ----49
4.2.1.1 Harmine inhibits the phosphorylation of SF3B1 ----49
4.2.1.2 Harmine inhibits the phosphorylation of Septin4 ----51
4.2.2 Phosphorylation of DYRK1A on Serine 748 ----52
4.2.2.1 Endogenous DYRK1A is not fully autophosphorylated in cells ----52
4.2.2.2 Autophosphorylation of exogenous DYRK1A is inducible by Calyculin A ----53
4.2.2.3 Generation of a phospho-specific anti-pSer748 antibody ----55
4.2.2.4 Phosphorylation on Ser748 is an autophosphorylation event ----57
4.2.2.5 DYRK1A autophosphorylation on Ser748 is inhibited by harmine ---58
4.2.2.6 DYRK1A autophosphorylates on Ser748 in vitro ----59
4.2.2.7 Calyculin A does not elevate DYRK1A phosphorylation on Ser748 --61
4.2.2.8 Ser748 autophosphorylation occurs via an intermolecular mechanism ----62
4.2.2.9 Ser748 phosphorylation alters DYRK1A activity ----64
4.2.2.10 Ser748 phosphorylation of DYRK1A in mitotic cells ----66
4.2.3 Posttranslational modifications of DYRK1A during mitotic exit ----70
4.2.3.1 Establishment of cell cycle synchronization ----70
4.2.3.2 Ser748 phosphorylation of DYRK1A during the cell cycle ----72
4.2.3.3 Degradation of DYRK1A during mitotic exit ----72
4.2.3.4 Degradation of DYRK1A during mitotic exit is inhibited by MG132 --75
4.2.3.5 Degradation of overexpressed DYRK1A is independent of its kinase activity ----75
4.2.3.6 Catalytically active DYRK1A interferes with RB dephosphorylation -78

4.2.3.7 The C-terminus of DYRK1A is essential for interference with RB and histone H3 dephosphorylation ----------79

5. Discussion ---------- 84

5.1 DYRK4 ---------- 84
5.1.1 Alternative promoter use and alternative splicing of DYRK4 ----------84
5.1.2 DYRK4 gene expression ----------85
5.1.3 A putative role of DYRK4 in the unfolded protein response----------86
5.1.4 The subcellular localization of DYRK4 could represent a regulatory mechanism ----------86
5.1.5 DYRK4 is phosphorylated by cellular kinases ----------87
5.1.6 Substrate specificity of DYRK4 ----------88

5.2 DYRK1A ---------- 89
5.2.1 Different phosphorylation level of endogenous DYRK1A and GFP-DYRK1A----------90
5.2.2 Harmine and the Ser748 autophosphorylation of DYRK1A ----------91
5.2.3 Inter- and intramolecular autophosphorylation of DYRK1A ----------92
5.2.4 Ser748 phosphorylation of DYRK1A may modulate its activity ----------93
5.2.5 Ser748 phosphorylation of DYRK1A during mitosis ----------95
5.2.6 Degradation of DYRK1A during mitotic exit----------96
5.2.7 The effect of overexpressed DYRK1A on cell cycle proteins ----------98
5.2.7.1 The retinoblastoma protein (RB)----------98
5.2.7.2 Protein level of Cyclin D1----------99
5.2.7.3 Phosphorylation level of histone H3 ----------99

6. Summary ---------- 100

7. Zusammenfassung ---------- 102

8. References ---------- 104

9. Curriculum Vitae ---------- 113

10. Publication List ---------- 114

1. Introduction

1.1 Protein kinases

Protein kinases are enzymes that phosphorylate proteins, and thereby regulate essential processes in the eukaryotic cell. They transfer a phosphate group from a nucleoside triphosphate and covalently attach it to a serine, threonine or tyrosine residue replacing the hydroxyl group. The human genome contains about 500 protein kinase genes and kinases were classified by sequence comparison of their catalytic domains (Hanks and Hunter, 1995), which are highly conserved in closely related kinases. Protein kinases also can be divided into groups by the residues they phosphorylate. Some only phosphorylate tyrosine residues (Tyr kinases), others only serine or threonine residues (Ser/Thr kinases), and few kinases can phosphorylate both aliphatic and aromatic residues (dual-specificity kinases). Often the members of kinase families not only share similar amino acid sequence, but also functional properties.

1.2 DYRK (dual-specificity tyrosine(Y)-phosphorylation regulated kinase)

1.2.1 The DYRK family

Together with cyclin-dependent kinases (CDK), mitogen-activated protein kinases (MAPK), glycogen synthase kinases (GSK) and CDK-like kinases (CLK), the dual-specificity tyrosine(Y)-phosphorylation regulated kinases (DYRKs) belong to the CMGC group of protein kinases. This evolutionarily conserved family of protein kinases play key roles in the regulation of cell differentiation, proliferation and survival (Park et al. 2009). DYRKs share a conserved kinase domain and a adjacent N-terminal DYRK homology (DH)-box (DDDNXDY), although they differ in their N- and C-terminal extensions (Becker and Joost, 1999). From a phylogenetic point of view, DYRKs are divided into two subclasses (Fig. 1*A*) which can be distinguished by the presence of specific protein motifs (Aranda et al. 2010).

Class I DYRKs harbour a functional, bipartite nuclear localization signal (NLS) N-terminal to the DH-box, and a C-terminal PEST-region, a motif rich in proline, glutamic acid, serine, and threonine which is believed to initiate a rapid degradation of the protein (Rogers et al. 1986). This class includes the *Drosophila melanogaster* minibrain kinase (*mnb*), *Caenorhabditis elegans* MBK-1, and mammalian DYRK1A

and DYRK1B (also called Mirk) (Tejedor et al. 1995; Raich et al. 2003; Becker et al. 1998). Although DYRK1A and DYRK1B show 85% identity in their amino acid sequence within the catalytic domain, they differ in their C-terminal region (Leder et al. 1999). DYRK1A harbours a stretch of 13 consecutive histidine residues (His) and a domain containing a high portion of serine and threonine residues (Ser/Thr) (Fig. 1*A* and *B*). The histidine-rich region targets DYRK1A to the nuclear speckle compartment (Alvarez et al. 2003). An alternative splicing event in the N-terminal domain of DYRK1A gives rise to two protein isoforms that differ by the presence or absence of a 9 amino acid segment (Kentrup et al. 1996; Guimerá et al. 1999; Aranda et al. 2010). These splice variants seem to be expressed at similar levels and show no apparent functional differences. In this study, the numbering of the amino acids refers to the long splicing variant. Alternative splicing is observed in all human DYRKs (Aranda et al. 2010).

Class II DYRKs do not contain any known protein domain within the N- and C- terminal extensions, except for the N-terminal autophosphorylation accessory (NAPA) regions, NAPA1 and NAPA2, N-terminal to the DH-box (Kinstrie et al. 2010). They include mammalian DYRK2, DYRK3 (also called REDK) and DYRK4, *Drosophila melanogaster* dDYRK2 (*smi35*), *Caenorhabditis elegans* MBK-2 and *Schizosaccharomyces pombe* Pom1p (Becker et al. 1998; Raich et al. 2003; Bähler and Pringle, 1998; Lochhead et al. 2003).

The mammalian class I DYRKs differ in tissue expression, with DYRK1A being ubiquitously expressed in adult and fetal tissues (Guimera et al. 1999; Okui et al. 1999) and DYRK1B predominantly found in testis, but also in muscle tissue (Becker et al. 1998; Deng et al. 2003). Among the mammalian class II DYRKs, which are predominantly expressed in testis in rodents, DYRK2 and DYRK3 are most closely related and they are encoded by paralogous genes that originated by gene duplication (Zhang et al. 2005). Despite this close relationship, they have acquired very different functions. DYRK2 is involved in the response to DNA damage through p53 phosphorylation (Taira et al. 2007), whereas DYRK3 regulates erythropoiesis through as yet unknown molecular pathways (Geiger et al. 2001; Lord et al. 2000).

In contrast to DYRK2 and DYRK3, very little is known about the function of the other mammalian class II DYRK, DYRK4, and no substrate has been identified for this kinase. Rat and murine DYRK4 were reported to be testis-specific kinases expressed only in stage VIII post-meiotic spermatids (Becker et al. 1998;

Sacher et al. 2007). However, *Dyrk4* deficient mice are fertile (Sacher et al. 2007), which could possibly reflect some redundancy in function of the class II DYRKs, all of which are strongly expressed in the testis. Conversely, it remains unclear whether DYRK4 can phosphorylate the same substrates as other DYRKs and thus, substitute for a loss of DYRK3 or DYRK2.

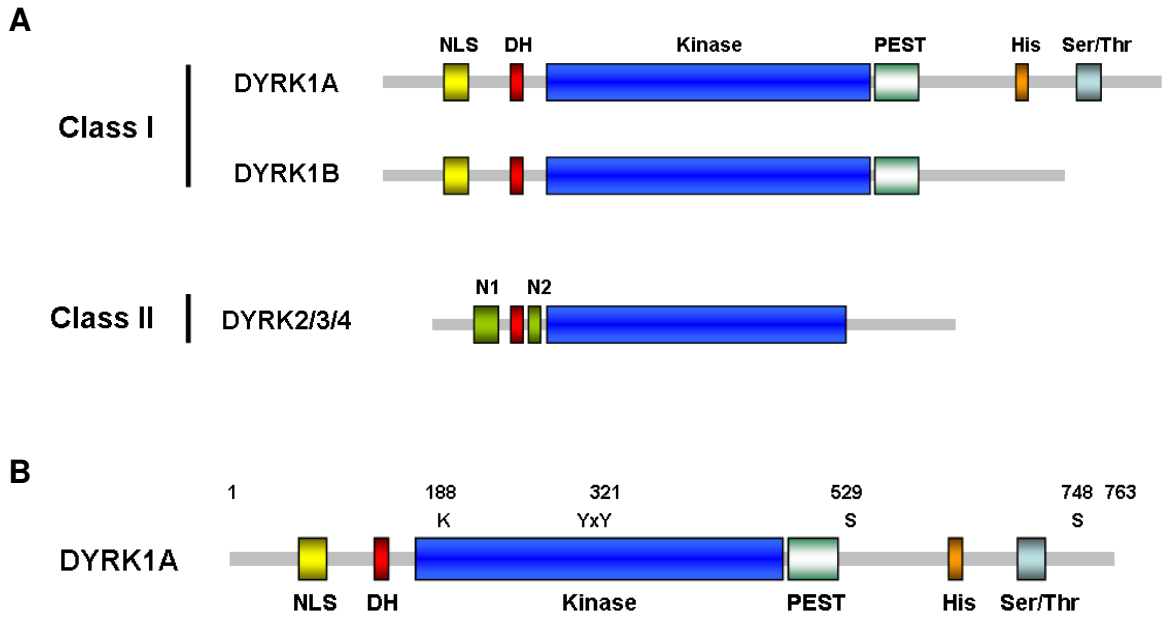

Figure 1: Schematic representation of DYRK protein structure in mammals.
A. Schematic representation of class I (DYRK1A/1B) and class II (DYRK2/3/4) DYRKs showing the different protein motifs identified. NLS, nuclear localization signal; DH, DYRK homology-box; Kinase, kinase domain; PEST, motif rich in proline, glutamic acid, serine, and threonine residues; His, polyhistidine stretch; Ser/Thr, region enriched in serine and threonine residues; N1 and N2, N-terminal autophosphorylation accessory region (NAPA). **B.** Schematic representation of the full-length DYRK1A protein. Accompanying numbers indicate the first and the last amino acids, and amino acids relevant in this study. K, lysine residue; Y, tyrosine residue; S, serine residue.

1.2.2 DYRK1A

Mammalian DYRK1A and the orthologous gene in *Drosophila*, called *minibrain* (*mnb*), are the best characterized members of the DYRK family and are highly conserved from insects to humans (Galceran et al. 2003). The human *DYRK1A* gene is located within the so called Down syndrome critical region (DSCR) on chromosome 21, its overexpression in Down syndrome (DS) is suggested to contribute to developmental brain defects and the early onset neurodegeneration in individuals with trisomy 21. In particular, the phosphorylation of microtubule-associated protein tau by DYRK1A suggests the involvement of DYRK1A in neurofibrillary degeneration in DS (Wegiel et al. 2010). Analyses of mouse models overexpressing *DYRK1A* are consistent with its proposed contribution to neuropathological traits of DS (Park et al. 2009). Heterozygous *DYRK1A*$^{+/-}$ mice show reduced body weight, brain size and total number of neurons (Fotaki et al. 2002) and strongly indicate the importance of *DYRK1A* gene dosage. *DYRK1A*$^{-/-}$ mice embryos show a severe developmental delay, reduced body size and die around embryonic day 10.5 (Fotaki et al. 2002), indicating that DYRK1A plays a vital role in cellular mechanisms. Indeed, numerous studies have revealed that DYRK1A is a pleiotropic protein kinase with a broad substrate range and diverse functions in cellular regulation (Fig. 2).

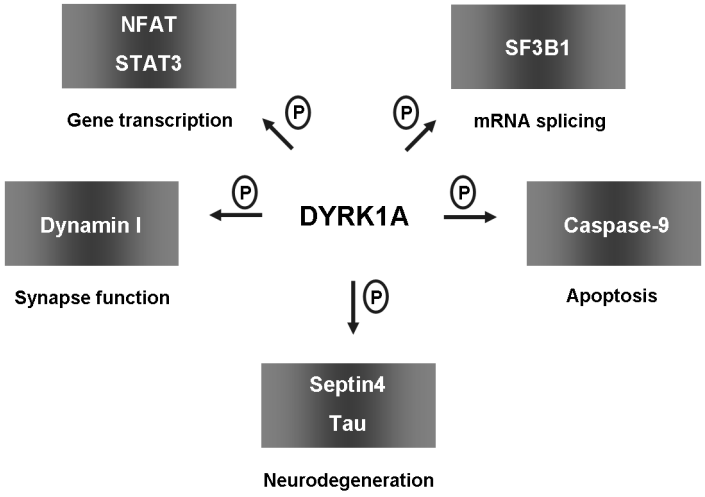

Figure 2: DYRK1A is a pleiotropic protein kinase.
Examples of known substrates and putative functions of DYRK1A (reviewed in Aranda et al. 2010).

1.2.3 Autophosphorylation of DYRKs

The dual-specificity tyrosine(Y)-phosphorylation regulated kinases (DYRKs) belong to the dual-specificity protein kinases, which are able to phosphorylate aliphatic (serine and threonine) and aromatic (tyrosine) residues. DYRK kinases contain a conserved Tyr-X-Tyr motif in the activation loop (Fig. 1*B*), and the phosphorylation of the second tyrosine residue (Tyr321) is essential for full catalytic activity of all DYRKs tested to date (reviewed in Aranda et al. 2010; Becker and Sippl, 2011). In contrast to e.g. the mitogen-activated protein kinase family, in DYRK kinases the phosphorylation of Tyr321 is not catalysed by upstream kinases, but is an autophosphorylation event (Fig. 3*A*). This event takes place during translation and is called “one-off autophosphorylation”. It leads to a constitutive active kinase and has been found using dDYRK2 as a model (Lochhead et al. 2005).

Class I and class II DYRKs show mechanistical differences in their tyrosine autophosphorylation process, because class II DYRKs require the NAPA domain for this one-off event (Kinstrie et al. 2010), which provides a chaperone-like function. Mature DYRKs are incapable of phosphorylating themselves on tyrosine residues and phosphorylate exogenous substrates only at serine or threonine residues. Using a mutant version of DYRK1A, where the tyrosines of the Tyr-X-Tyr motif in the activation loop are mutated to phenylalanine (Y319F/Y321F), it has been shown that DYRK1A autophosphorylates not only its tyrosines in the activation loop, as this mutant is still detectable with a phosphotyrosine specific antibody (Himpel et al. 2001).

A second autophosphorylation site reported for mammalian DYRK1A is located close to the PEST domain, Ser529 (RAR**S**DP) (Fig. 1*B*) (Alvarez et al. 2007). Autophosphorylation on Ser529 occurs via an intramolecular mechanism. Alvarez et al. showed that phosphorylation of this residue does not affect the intrinsic kinase activity on its own, but mediates the interaction of DYRK1A with 14-3-3β. Binding of 14-3-3β increases the catalytic activity of DYRK1A (Alvarez et al. 2007).

All protein kinases have a conserved lysine in the ATP-binding motif, which is involved in binding of ATP and facilitates transfer of ATP γ–phosphate to the target amino acid. Mutation of this lysine to arginine (in the case of DYRK1A: K188R), leads to a loss of phosphorylation on tyrosine residues and on Ser529 in DYRK1A. Such a mutant is a valuable tool for autophosphorylation analysis.

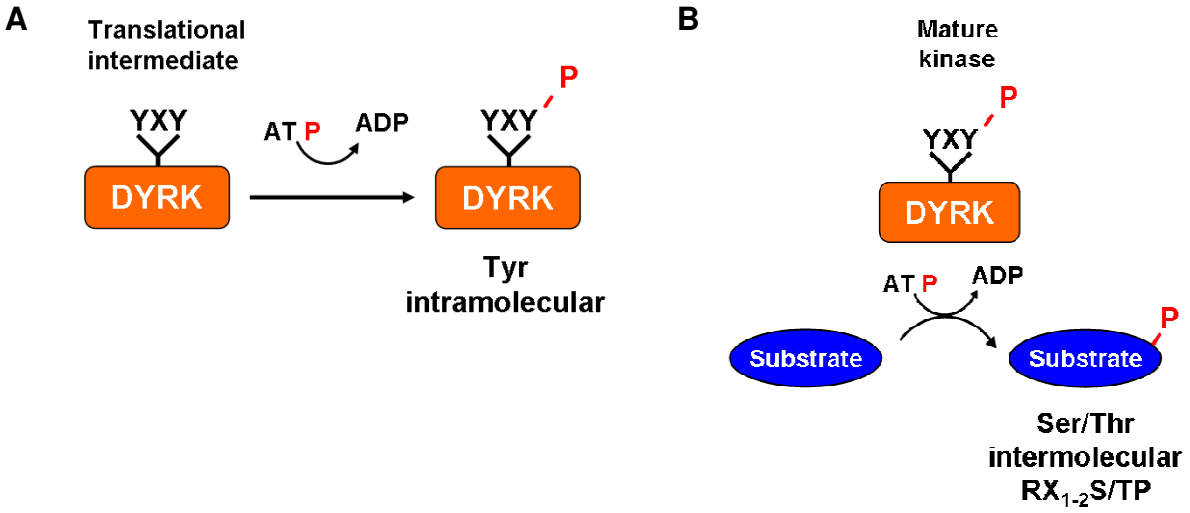

Figure 3: Dual-specificity of DYRK kinases.
A. Autophosphorylation of the conserved tyrosine in the activation loop (YXY motif) is catalysed by a translational intermediate form of DYRK1A. **B.** Substrate phosphorylation by mature DYRK1A occurs only on serine or threonine residues. Consensus sequence for substrate recognition by DYRK1A is given ($RX_{1-2}S/TP$).

1.2.4 Substrate specificity of DYRKs

Mature DYRKs phosphorylate substrates only at serine or threonine residues (Fig. 3*B*). The definition of a consensus phosphorylation sequence for DYRK1A, ($RX_{1-2}(S/T)P$) (Himpel et al. 2000) has stimulated the identification of numerous phosphorylation sites in DYRK1A substrates (see UCSD-Nature Molecule Pages: Protein A000796; Aranda et al. 2010). Some DYRK1A substrates, such as eukaryotic initiation factor 2Bε, the microtubule associated protein tau or glycogen synthase are also phosphorylated by DYRK2 *in vitro* (Skurat and Dietrich, 2004; Woods et al. 2001), whereas histone H2B is only phosphorylated by DYRK2 and DYRK3 but not by DYRK1A (Becker et al. 1998). A comparative analysis of peptide substrates has also revealed both similarities and differences in the substrate specificity of DYRK1A and DYRK2 or DYRK3 (Campbell and Proud, 2002). However, to date the substrate specificities of different members of the DYRK family have not been systematically compared.

1.2.5 Subcellular localization

Since no activating kinase appears to be required, other control mechanisms may regulate the biological activity of DYRK kinases. Indeed, the subcellular localization of DYRKs has emerged as one such mechanism. DYRK1A and DYRK1B possess a bipartite nuclear localization signal (NLS) in their N-termini (Fig. 1*A*) that targets overexpressed GFP (green fluorescent protein)-fused DYRK1A and DYRK1B to the nucleus (Becker et al. 1998). Further, DYRK1A contains a histidine-rich region in the C-terminus that targets DYRK1A to the nuclear speckle compartment (Alvarez et al. 2003). However, in neurons endogenous DYRK1A has been found both in the nucleus and the cytoplasm (Martí et al. 2003). Similar localization has been observed with exogenous GFP-DYRK1A when expressed at low levels in rat pheochromocytoma cells (PC12) cells (Fig. 4; unpublished data). Furthermore, an inducible re-distribution of overexpressed DYRK1A from the nucleus to the cytoplasm has been observed in PC12 cells (Bescond and Rahmani, 2005). Consistently, nuclear and cytoplasmic substrates have been identified for DYRK1A (Fig. 2). The yeast homolog of DYRK1A, Yak1p, translocates to the nucleus in response to glucose availability (Moriya et al. 2001). DYRK1B accumulates in the cytosol of cells from rhabdomyosarcoma tumors, whereas it is predominantly found in the nucleus of undifferentiated NIH-3T3 cells (Mercer et al. 2006).

Several class II kinases have been reported to be predominately localized in the cytoplasm (*e.g.*, MBK-2; Raich et al. 2003); but changes in MBK-2 localization from the cortex to the cytoplasm have been described during *Caenorhabditis elegans* zygote maturation (Cheng et al. 2009). DYRK2 has been shown to enter the nucleus upon exposure to genotoxic stress (Taira et al. 2007). DYRK3 has been found predominantly in nuclear protein extracts of human erythropoietin-responsive cells (UT7-EPO) (Lord et al. 2000) and interaction with cAMP response element (CRE)-binding protein (CREB) predicts a nuclear localization (Li et al. 2002). The *Drosophila* homolog of DYRK4, dDYRK2, has also been suggested to translocate into the nucleus, because it phosphorylates the nuclear protein SNR1 (Kinstrie et al. 2006).

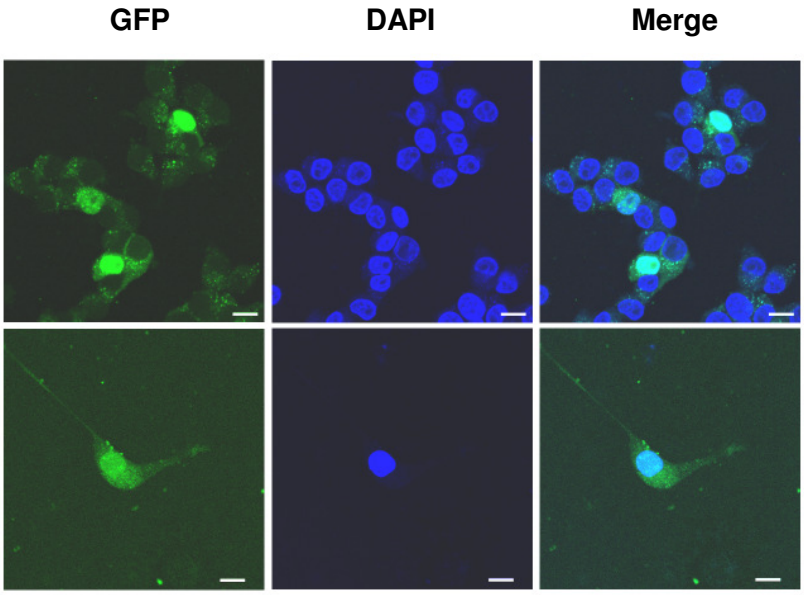

Figure 4: GFP-DYRK1A is localized both in the nucleus and the cytoplasm in PC12 cells.
Expression of GFP-tagged DYRK1A was induced with doxycycline (2 µg/ml) and PC12_GFP-DYRK1A cells were stimulated to differentiate with NGF (nerve growth factor; 100 ng/ml) for 24 h (lower panel) or 72 h (upper panel). Subcellular localization was analyzed by fluorescence microscopy. Nuclei were stained with DAPI. Scale bars, 10 µm.

1.3 The cell cycle

In a large scale phosphoproteomic screening of protein kinase, DYRK1A phosphorylation on serine 748 and 758 has been found to be upregulated in mitotic cells (Daub et al. 2008). In this study, synchronized human cervix carcinoma cells (HeLa) arrested in M phase were compared to cells arrested in S phase of the cell cycle.

The cell cycle is an ordered series of events that begins with cell growth and ends with division into two daughter cells. The cell cycle consists of four phases: G_1, S, G_2 and M phase (Fig. 5*A*). After cell growth, with a great amount of protein synthesis during G_1 phase (first gap phase), cells can exit the cell cycle to enter G_0 phase, where cells can differentiate or rest in a so called “quiescent state” and re-enter the cell cycle mediated by specific stimulators. At the end of the G_1 phase there is a checkpoint called “restriction point”, where e.g. DNA damage is assessed. Once cells passed this restriction point, they are committed to enter S phase (synthesis phase) where DNA synthesis and replication occurs. In the following G_2 phase (second gap phase), cells synthesize proteins and may continue to increase in size.

At the end of G_2 phase, cells pass the G_2 checkpoint and enter M phase (mitotic phase: mitosis and cytokinesis). The mitotic phase is a short period of the cell cycle, but nevertheless is a highly regulated process. Mitosis is divided into five stages (Fig. 5*B*). During mitosis the pairs of chromosomes condense, the mitotic spindle is formed and the sister chromatids are separated and driven to opposite ends of the cell. Finally, chromosomes unfold back into chromatin. Cytokinesis (division of the cytoplasm and formation of two identical daughter cells) begins during telophase and marks the end of M phase, but is not part of mitosis.

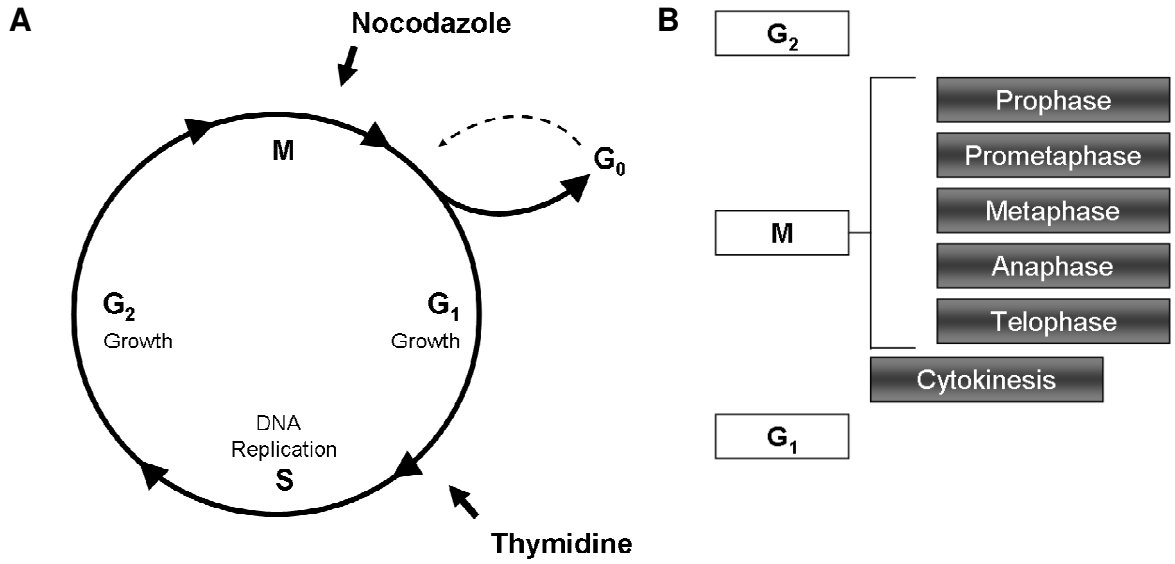

Figure 5: The phases of the cell cycle.
A. Scheme of the cell cycle. M, Mitosis; G_0, Gap 0/Resting; G_1, Gap 1; S, Synthesis; G_2, Gap 2. Two compounds (nocodazole, thymidine) used in this study to arrest cell cycle at indicated phases are shown. Nocodazole inhibits spindle formation and arrests cells in M phase; Thymidine indirectly blocks the ribonucleoside diphosphate reductase, inhibits DNA synthesis and arrests cells in S phase. **B.** The mitotic phase which is divided into mitosis and cytokinesis. The five stages of mitosis are listed.

1.3.1 The retinoblastoma protein (RB), Cyclin D1 and histone H3

There are several ways to follow the progression through the stages of the cell cycle of synchronized cells. A simple method is the analysis of phosphorylation levels of specific proteins, such as retinoblastoma protein (RB) or histone H3, as well as the analysis of protein level of different cyclins, such as Cyclin D1. A summary of these three proteins is given that have been examined during cell cycle analysis in this study.

1.3.1.1 Phosphorylation level of the retinoblastoma protein

The RB protein is a well studied substrate of CDKs containing over 16 consensus phosphorylation sites for CDKs (Tamrakar et al. 2000). Located in the nucleus, RB acts as a transcriptional repressor by binding transcription factors like E2F, ATF-2 or c-ABL. Sequential phosphorylation at different sites of RB by different CDKs leads to the release of distinct transcription factors (Knudsen and Wang, 1996; Zarkowska and Mittnacht, 1997). For instance, the release of members of the E2F family regulates several genes required for DNA replication (Fig. 6*A*) as well as Cyclin D1 and Cyclin E (Ohtani et al. 1995) that must be expressed before the S phase of the cell cycle.

In general, hyperphosphorylation of RB is present from late G_1 phase up to the end of M phase (Fig. 6*A*) (reviewed in Giacinti and Giordano, 2006). In mitotic cells, Cyclin B/cdc2 is the principle RB kinase (Fig. 6*A* and *B*). Cyclin B level reach a maximum at the G_2-M boundary (Evans et al. 1983; Standart et al. 1987), and in complex with cdc2 Cyclin B maintains the hyperphosphorylation level of RB in mitotic cells (Lin and Wang, 1992). At the end of mitosis Cyclin B is destroyed, what results in the inactivation of the cdc2 protein kinase and allows cells to leave M phase. Cells expressing a stable Cyclin B arrest during mitosis (Murray et al. 1989; Ghiara et al. 1991; Luca et al. 1991).

The release of the c-ABL tyrosine kinase occurs due to phosphorylation of RB on Ser807 and Ser811 by Cyclin D1/CDK4 and Cyclin E1/ CDK2 (Knudsen and Wang, 1996). Nuclear c-ABL tyrosine kinase activity is suppressed by RB, which binds to the tyrosine kinase domain of c-ABL. A number of reports have shown that the nuclear c-ABL tyrosine kinase plays an important role in the activation of apoptosis by DNA damage (Wang, 2000). As the phospho-specific anti-pRB antibody used in the present study recognizes phosphorylation at Ser807/811, it is possible to determine if the tyrosine kinase c-ABL is bound and thus inactivated (dephosphorylation of RB at Ser807/811) or c-ABL is released and thus active (phosphorylation of RB at Ser807/811).

Dephosphorylation of RB occurs in the anaphase by phosphoprotein phosphatase 1 (PP1) which removes the inhibitory phosphate groups (Ludlow et al. 1993). Mitotic RB dephosphorylation is reported to be a sequential, temporally-regulated event (Rubin et al. 2001) with Cyclin D/CDK4 sites, such as Ser807, being dephosphorylated at a rapid rate.

The protein $p27^{Kip}$ is an inhibitor of Cyclin E/CDK2 activity. Thus the hyperphosphorylation of RB can also be regulated by modulation of $p27^{Kip}$ protein levels directly or indirectly, since high CDK2 activity has been shown to induce the proteolytic destruction of $p27^{Kip}$ (Sheaff et al. 1997; Vlach et al. 1997).

1.3.1.2 Protein level of Cyclin D1

Cyclins exhibit distinct expression and degradation patterns to coordinate the cell cycle and function as regulators of CDKs together with CDK inhibitors (such as $p21^{Cip}$ or $p27^{Kip}$) (Fig. 6*B*) (reviewed in Johnson and Walker, 1999). Cyclin D1 functions as a regulatory subunit of CDK4 or CDK6, whose activity is required for G_1/S transition. The protein level of Cyclin D1 (Fig. 6*B*) decreases upon entry into the S phase (Diehl et al. 1998). Accordingly, detection of Cyclin D1 protein level can be used to determine cells arrested in S phase. The degradation of Cyclin D1 is essential for DNA replication and regulated by phosphorylation of Cyclin D1 at Thr286 by GSK-3β (Alt et al. 2000) or $p38^{SAPK2}$ (Casanovas et al. 2000) and at Thr288 by DYRK1B (Zou et al. 2004).

1.3.1.3 Phosphorylation level of histone H3

Histones (H2A, H2B, H3 and H4) are components of the nucleosomes and their N-terminal tail domain is subjected to multiple posttranslational modifications such as methylation, acetylation, ubiquitination, ADP-ribosylation and phosphorylation. A simple method to determine mitotic cells is to detect the phosphorylation level of histone H3 at Ser10. Phosphorylation on Ser10 correlates with chromatin condensation in mitosis and upon mitotic exit a global dephosphorylation of histone H3 takes place (reviewed in Hans and Dimitrov, 2001).

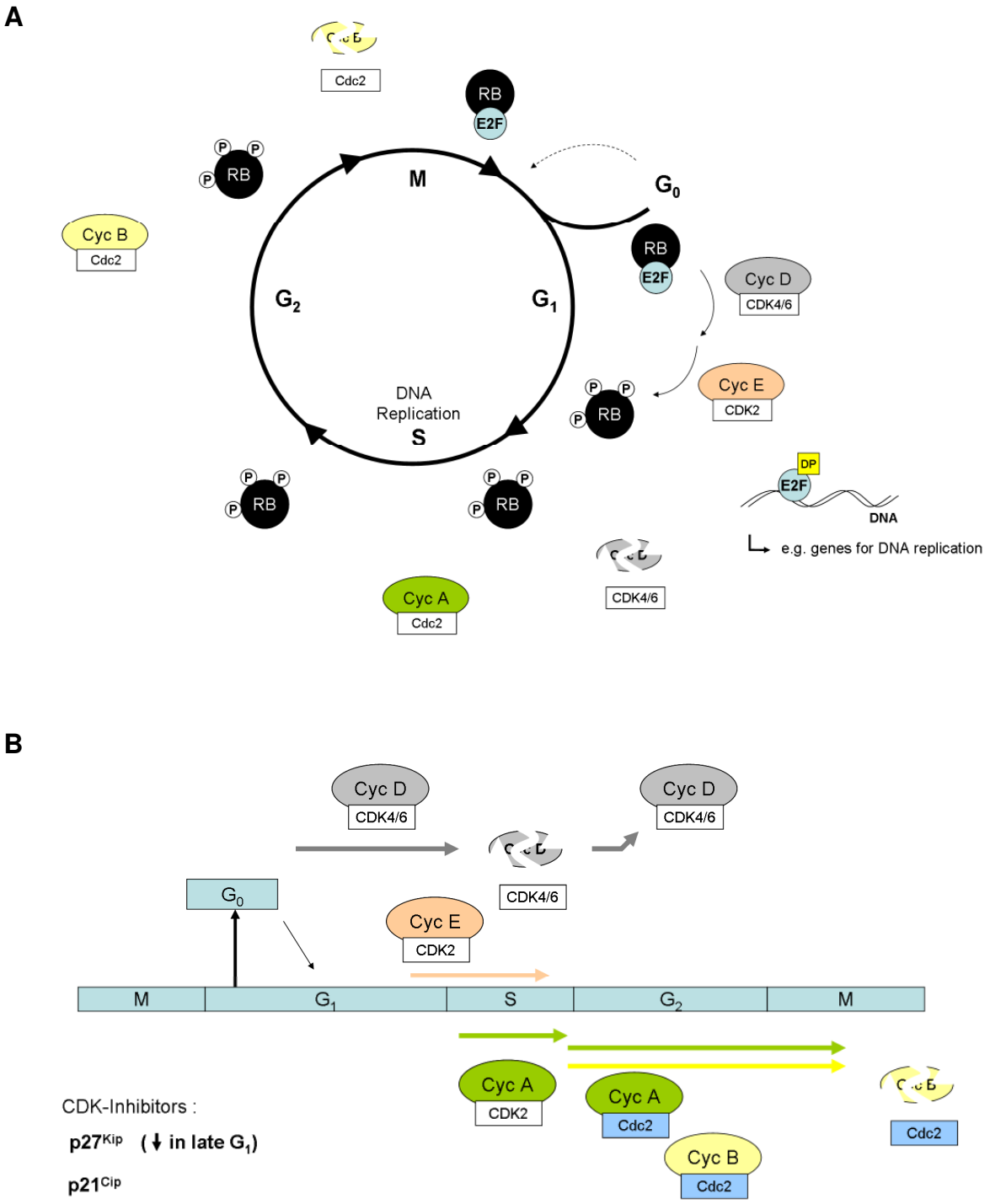

Figure 6: Schematic of RB and Cyclin D1 in cell cycle control.
A. Simplified regulation model of the RB phosphorylation by the indicated cyclin-dependent kinases Cyclin/CDK complexes during the cell cycle. As example of RB inactivation its association with E2F is shown. Most E2F polypeptides interact with DP polypeptides to act as transcriptional factors. Crucial degradation of Cyclin D and B is indicated. RB, retinoblastoma protein; E2F, transcription factor; DP, transcription factor. **B.** Expression of cyclins through the cell cycle. The oscillations of different cyclins due to regulated gene expression and protein destruction by proteolysis is shown. Interaction of each cyclin with its specific CDK or Cdc2 is indicated. Two main CDK inhibitors are listed.

1.3.2 DYRKs and the cell cycle

The identification, that Ser748 phosphorylation of DYRK1A is upregulated in mitotic cells is not the first report bringing together DYRKs and the cell cycle. The DYRK kinase homolog in *Dictyostelium*, YakA, has been reported to be essential for both a starvation-induced growth arrest and initiation of a developmental response, and has been suggested to function as a specific cell-cycle regulator to facilitate exit from the cell cycle and to mediate developmental events (Souza et al. 1998). The DYRK family members Yak1p (DYRK homolog in *S. cerevisiae*), Pom1 (DYRK homolog in *S. pombe*) and DYRK1B are all active G_0/G_1 kinases that can arrest cells in G_1 phase of the cell cycle (Bähler and Nurse, 2001; Souza et al. 1998; Deng et al. 2003). MBK-2 (class II DYRK in *C. elegans*) kinase activity is also regulated during the cell cycle (Cheng et al. 2009). DYRKs have been shown to interact with cell cycle control genes such as SNR1 (chromatin remodelling factor) and TRX (trithorax; a chromatin component) (Kinstrie et al. 2006), including phosphorylation of class II histone deacetylases (HDACs) (Deng et al. 2005). Various other studies have identified a number of potential DYRK family substrates including the cell-cycle regulator, Cyclin D1, the cyclin-dependent inhibitor $p27^{Kip1}$ and the cell-cycle inhibitor and survival molecule $p21^{Cip1}$ (Table 1).

Mammalian DYRK2 is reported to participate in M phase progression as knockdown of DYRK2 induces G_2-M arrest. DYRK1B, a G_0/G_1-active kinase, stabilizes the CDK inhibitor $p27^{Kip}$ by phosphorylating it at Ser10 (Deng et al. 2004), whereas mitogen stimulation reduces DYRK1B levels and allows cells to enter G_1 (Deng et al. 2003). DYRK1B does not enhance turnover only of $p27^{Kip}$ but also of the G_1 phase cyclin Cyclin D1 via phosphorylation on Thr288 (Zou et al. 2004). DYRK1A has been related to the cell cycle as it causes an increase in phosphorylation of the transcription factor Forkhead (FKHR) and high levels of Cyclin B1 in transgenic mice overexpressing DYRK1A (Branchi et al. 2004), which is also observed in hippocampal neurons of DS patients (Nagy et al. 1999; Nagy et al. 1997). Furthermore, overexpression of DYRK1A leads to an aberrant mitosis (Funakoshi et al. 2003) and thereby a disturbance of cell cycle progression through the G_2-M phase due to alteration in Cyclin B expression. A recent study showed that overexpression of DYRK1A leads to the degradation of Cyclin D1 in neural progenitor cells and thereby facilitates exit from the cell cycle (Yabut et al. 2010). An indirect effect of

DYRK1A on the cell cycle is mediated by phosphorylation of the transcription factor p53 on Ser15 and the subsequent induction of $p21^{Cip1}$ expression (Park et al. 2010).

Taken together, all these findings strongly indicate a potential role of DYRK1A in the cell cycle.

Table 1: Mammalian DYRKs and the cell cycle.
Examples for reports that implicate DYRK family members in cell cycle control.

Kinase	Mechanism	Effect	Reference
DYRK1A	Degradation of Cyclin D1	Exit from the cell cycle → G_0 , Differentiation	Yabut et al. 2010
DYRK1A	Ⓟ of p53	Induction of $p21^{Cip1}$ → Cells arrest in G_0/G_1	Park et al. 2010
DYRK1B	Ⓟ of Cyclin D1, D3	Degradation of Cyclin D → Cells arrest in G_0/G_1	Zou et al. 2004
DYRK1B	Ⓟ of $p27^{Kip}$	Inhibition of Cyclin/CDK → Cells arrest in G_0/G_1	Deng et al. 2004
DYRK2	Knockdown of DYRK2	Stabilization of katanin p60 → Cells arrest in G_2/M	Maddika and Chen, 2009

Circled P, phosphorylation.

2. The aim of the study

The members of the dual-specificity tyrosine(Y)-phosphorylation regulated kinase (DYRK) family play key roles in a great variety of cellular processes. The best characterized member is DYRK1A as its gene is located in the Down syndrome critical region (DSCR) on chromosome 21 in humans and it is overexpressed in Down syndrome individuals. DYRK1A is a candidate for drug target development. In contrast, DYRK4 has remained essentially uncharacterized.

This study aimed to clarify the function, subcellular localization, substrate specificity and tissue distribution of DYRK4. Further, it should be answered whether DYRK4 is able to target the same substrates as DYRK1A.

The second aim of the study was to elucidate the role of DYRK1A in the cell cycle. As a recent study revealed that DYRK1A phosphorylation at Ser748 is induced in mitotic HeLa cells (Daub et al. 2008), this study intended to illuminate the mechanism and function of Ser748 phosphorylation during the cell cycle. Finally, the fate of DYRK1A during the cell cycle should be followed and the effect of its overexpression on the cell cycle should be figured out.

3. Material and Methods

3.1 Materials

3.1.1 Chemicals

Chemicals were obtained from Sigma-Aldrich (Munich, Germany), Merck Eurolab (Darmstadt, Germany), AppliChem (Darmstadt, Germany) or from companies as indicated.

3.1.2 Frequently used buffers and chemical solutions

Chemiluminiscence detection solution:

Component A: 1 mL 1 M Tris-HCl (pH 8.5); 40 µL H_2O_2 (30% v/v); 9 mL H_2O

Component B: 1 ml 1 M Tris-HCl (pH 8.5); 100 µL 250 mM Luminol;
44 µL 90 mM *p*-Coumaric acid; 10 ml H_2O

Glutathione elution buffer: 50 mM Tris-HCl (pH 8.0); 10 mM reduced Glutathione

6 M GuHCL lysis buffer: 100 mM NaH_2PO_4; 10 mM Tris-HCl (pH 8.0);
6 M Guanidine-HCl; 30 mM Imidazole

IP lysis buffer: 50 mM Tris-HCL (pH 7.5); 150 mM NaCl; 1 mM EDTA;
0.5% v/v Igepal;
supplemented with 100 mM $NaVO_4$; 100 mM Phenylmethylsulphonyl fluoride (PMSF); 2.5 µg/µl Aprotinin; 1 µg/µl Pepstatin;
10 µg/µl Leupeptin

IP washing buffer (+Igepal): 50 mM Tris-HCl (pH 7.5); 150 mM NaCl; 2 mM EDTA;
(0.1% v/v Igepal)

10x kinase buffer: 250 mM HEPES (pH 7.4); 50 mM $MgCl_2$; 5 mM DTT

2x LSB: 20% v/v Glycerol; 4% w/v SDS; 10 mM EDTA; 0.125 M Tris (pH 6.8);
0.02 % v/v Bromophenol blue

LSB: 6 mg DTT/100 µl 2x LSB

PBS (pH 7.4): 140 mM NaCl; 3 mM KCl; 8 mM Na_2HPO_4; 1.8 mM KH_2PO_4

SDS lysis buffer: 20 mM Tris (pH 7.4); 1% w/v SDS

TBS (pH 7.6): 150 mM NaCl; 20 mM Tris

TBS-T buffer: 0.1 % v/v Tween-20 in TBS

8 M Urea washing buffer: 100 mM NaH_2PO_4; 10 mM Tris-HCl (pH 6.3); 8 M Urea; 60 mM Imidazole

3.1.3 Microorganisms

E. coli DH5α [F' *ProA+B+ lacIq Δ(lacZ)M15 zzf::Tn10 (tetR)/fhuA2Δ (argFlacZ) U169 phoA glnV44 Φ80 Δ(lacZ)m15 gyrA96 recA1relA1 endA1 thi-l hsdR17*]

3.1.4 Peptides

Peptides were obtained from JPT Peptide Technologies (Berlin, Germany), Deutsches Wollforschungsinstitut (DWI, RWTH Aachen University, Germany) and GBF (Braunschweig, Germany). Biotinylated Pep285 (1mM), biotinylated Pep3 (1mM) and DYRKtide (2mM) were dissolved in H_2O, while SAPtide (2mM) was dissolved in water with 5% DMSO. Aliquots were stored at -20°C.

Table 2: Peptides used in this study.

Name	Sequence	Mimic	Supplier
Pep285	Biotin-Ttds-VGLLKLA<u>S</u>PELER	Ser73 c-Jun protein	JPT
Pep3	Biotin-Ttds-TPGSRSR<u>T</u>PSLPT	Thr212 tau protein	JPT
SAPtide	RRARKLTA<u>T</u>PTPLGG	Thr434 SF3B1 protein	DWI
DYRKtide	RRRFRPA<u>S</u>PLRGPPK	artificial	GBF

3.1.5 Antibodies

All primary and secondary antibodies used in this study are listed in Table 3, ordered by name.

Rabbit polyclonal phospho-specific antibody for DYRK1A phosphorylated at Ser748 (anti-pS748) was generated by immunizing rabbits with the phosphopeptide GADREEpSPMTGVC (where pS is a phospho-Ser residue) conjugated to LPH (hemocyanine from *Limulus polyphemus*). Custom immunisation and antibody purification was performed by BioGenes, Berlin, Germany.

Table 3: Antibodies and conjugates.

Target	Host	Specification and application[a)]	Reference
anti-β-Actin	mouse	monoclonal, 1:3000 WB	Sigma, St. Louis, MO, USA
anti-Cyclin D1	mouse	monoclonal, 1:1000 WB	Cell Signaling Technology, Danvers, MA, USA
anti-DYRK1A	mouse	monoclonal, 1:1000 WB, 1µg IP	Abnova, Taipei City, Taiwan
anti-FLAG BioM^2	mouse	monoclonal, 2µg/ml WB	Sigma, Munich, Germany
anti-GFP	goat	polyclonal, 1:1000 WB	Rockland, Gilbertsville, PA, USA
anti-GFP	rabbit	polyclonal, 1µg IP	Rockland, Gilbertsville, PA, USA
anti-HA	mouse	monoclonal, 1:500 WB, 1µg IP	Covance, Richmond, CA, USA
anti-pH3 (pS10)	rabbit	polyclonal, 1:1000 WB	Cell Signaling Technology, Danvers, MA, USA
anti-pRB (pS807/811)	rabbit	polyclonal, 1:1000 WB	Cell Signaling Technology, Danvers, MA, USA
anti-pSer748	rabbit	polyclonal, 0.38µg/ml WB	this study
anti-pThr434	rabbit	polyclonal, 1:250 WB	de Graaf et al. 2006
anti-pTyr (PY99)	mouse	monoclonal, 1:200 WB	Santa Cruz Biotechnology, Santa cruz, CA, USA
anti-SF3B1	rabbit	polyclonal, 1:500 WB	custom immunization[b)]
anti-biotin	goat	polyclonal, HRP-linked 1:2000 WB	Cell Signaling Technology, Danvers, MA, USA
anti-mouse	goat	polyclonal, HRP-linked 1:5000 WB	Pierce, Rockland, IL, USA
anti-goat	rabbit	polyclonal, HRP-linked 1:3000 WB	Dianova, Hamburg, Germany
anti-rabbit	goat	polyclonal, HRP-linked 1:5000 WB	Pierce, Rockland, IL, USA

[a)] HRP, horseradish peroxidase; IP, immunoprecipitation; WB, Western blot.
[b)] Polyclonal antibody raised against the N-terminal region (MAKIAKTHEDIEAQIC) of SF3B1

3.1.6 Plasmids

The expression plasmids encoding GFP-, GST- and HA-tagged wild-type DYRK1A and the kinase deficient mutants K188R and Y321F have been described previously (Kentrup et al. 1996; Becker et al. 1998; Becker and Joost, 1999; Himpel et al. 2000). Point mutations of GFP-tagged DYRK1A used in the present study were generated by site-directed mutagenesis using corresponding oligonucleotides listed in Table 4. The point mutant GFP-DYRK1A S748A was generated by Simone Bamberg-Lemper. GFP-tagged deletion mutants of DYRK1A have been generated by Katharina Kolanowski under my supervision and are described in her diploma thesis[1] (GFP-DYRK1A ΔC (amino acids 1-481); GFP-DYRK1A ΔN (amino acids 135-763); GFP-DYRK1A ΔCΔN (amino acids 135-481)).

The pcDNA5/FRT/TetOn/GFP-DYRK1A construct was generated by cloning rat GFP-DYRK1A cDNA into pcDNA5/FRT/TO vector (Invitrogen, Darmstadt, Germany) using HindIII and NotI and then by replacing the promoter with that of pTRE-d2EGFP (Clontech Mountain View, CA, USA) using SpeI and HindIII in order to make the vector compatible with the Tet-on system from Clontech.

Plasmids pHA-hDYRK4^{520} and the kinase deficient mutants pHA-hDYRK4^{520} K133R and pHA-hDYRK4^{520} Y264F; pGFP-hDYRK4^{520}, pGFP-hDYRK4^{644}, pGFP-mDYRK4^{594}, pGFP-mDYRK4^{642} have been described (Papadopoulos et al. 2011). Generation of pGFP-hDYRK4^{NLGY} was generated by site-directed mutagenesis using pGFP-hDYRK4^{520} and the corresponding oligonucleotides listed in Table 4. Position of the amino acids NLGY insertion can be seen in Figure 15*A*. pGFP-mDYRK4$^{L191A/L193A}$ was generated by site-directed mutagenesis using pGFP-mDYRK4^{642} and the corresponding oligonucleotides listed in Table 4. All oligonucleotides were purchased from Eurogentec and all site-directed mutageneses have been performed using the QuikChange Site Directed Mutagenesis kit according to manufacturer's instructions (Stratagene). All mutations generated were verified by DNA sequencing (GATC, Konstanz, Germany).

GFP-SF3B1-NT (amino acids 1-492) (de Graaf et al. 2006) and GFP-SF3B1 Δ256-382 (deletion of amino acids 256-382 of GFP-SF3B1-NT) (Becker; unpublished data) were available in the laboratory. FLAG-Septin4 has been previously described (Sitz et al. 2006).

[1] Kolanowski, Katharina (2011) Posttranslational Modification of the protein kinase DYRK1A, diploma thesis, RWTH Aachen University

To express STAT5A as a yellow fluorescent fusion protein (STAT5A-YFP), mouse STAT5A cDNA was fused to YFP and subcloned into pcDNA5/FRT/TO (Invitrogen). STAT5A-YFP was a kind gift of Nicolas Chatain (Institute of Biochemistry, RWTH Aachen, Germany).

3.2 Methods

3.2.1 Preparation of bacterial expressed GST-DYRK1A variants

180 ml of LB medium with ampicillin (100 µg/ml) were inoculated with 5 ml of over-night culture of transformed *E.coli* DH5α. The cultures were left to grow till an OD of 0.7-0.8 at 37°C and protein expression was then induced by addition of IPTG (final concentration of 0.1 mM). After 2 h of induction at RT, cells were collected by centrifugation (10 min, 4°C, 5000 rpm) and then thoroughly resuspended in 6 ml phosphate buffered saline (PBS) containing 80 µl Lysozyme (10 mg/ml) and 60 µL PMSF (17.5 mg/ml) for 5 min at RT. Afterwards cells were sonified for 30 sec, and 300 µL of 20% Triton X-100 were added. The mixture was incubated on ice for 15 min, and mixed every 5 min. Next, the remaining cell debris was removed by centrifugation (10 min, 4°C, 10000 rpm) and the supernatant was mixed with 200 µL of Glutathione sepharose 4B (Amersham Bioscience, Piscataway, NJ, USA). For binding of the protein to the sepharose, the batch was incubated for 30 min at 4°C, and after centrifugation (4 min, 4°C, 1600 rpm) the supernatant was discarded. The pellet was washed three times in 1 ml cold PBS. The protein was eluted three times with 150 µl Glutathione elution buffer each, the first two times for 10 min at RT and the last time for 20 min on ice. Eluates and aliquots were stored at -80°C.

Table 4: Oligonucleotides used in this study.

Primer	sequence 5'→ 3'	rest. site[c)]	plasmid name
Primers for site-directed mutagenesis (only the sequence for the forward primers given)			
2009MA15	- GATAGAGAAGAGGCGCCCATGACAGGAG-	*KasI*	GFP-DYRK1A S748A
2010JA01 2010JA03	-GCTGATAGAGAAGAGGAGCCCATGACAGGAG- - GTGTGCAACAGGAGCCTGTAGCTAGCTCG-	- -	GFP-DYRK1A S748E/S758E
2010JA01 2009SE25	-GCTGATAGAGAAGAGGAGCCCATGACAGGAG- -TTTGTGTGCAACAGGCCCCTGTGGCTAGCTCGT-	- *BglI*	GFP-DYRK1A S748E/S758A
2009SE23 2009SE25	- GAAGAGTCTCCCATGGCCGGCGTTTGTGTGC- -TTTGTGTGCAACAGGCCCCTGTGGCTAGCTCGT-	*NaeI* *BglI*	GFP-DYRK1A T751A/S758A
2009SE27	- GCAAGGGGCTGACTAGTAAGAGTCTCCCATGAC-	*SpeI*	GFP-DYRK1A ΔC19
2009DE34	-CTCAGAGCTGTGGTTCGCCGGCGCTGAAGCCA AGAAGCTCG-	*NaeI*	GFP-mDYRK4^{642} L191A/L193A
2008NO21	-GCAAGACGAGTAACCTAGGCTATGATGATGAGC ATGGC-	*AvrII*	GFP-hDYRK4^{NLGY}
RT-PCR and qRT-PCR of the long variant human DYRK4 (primers match exons 5 and 11 as shown in Fig. 7*A*)			
hD4L-f	-GGAAATGTGATTTGACTCCCTTCCTG-		
hD4L-r	-CTGAGGCCGGCATCTGATTG-		
RT-PCR of the short variant human DYRK4 (primers match exons 9 and 11 as shown in Fig. 7*A*)			
hD4S-f	-GCTGTTGAAAGCCTGCAGC-		
hD4S-r	-GACTTCTCCTCTGCCTTGGG-		
RT-PCR and qRT-PCR of total human DYRK4 (primers match exons coding for the catalytic domain)			
hD4Cat-f	-CGCTTCACTCTCTCTGTTTTG-		
hD4Cat-r	-TCACTTCTGGGGATCGGTAG-		
RT-PCR of human GAPDH also used in qRT-PCR			
GAPDH-f	-CGGGGCTCTCCAGAACATCATCC-		
GAPDH-r	-CCAGCCCCAGCGTCAAAGGTG-		

[c)] rest., restriction;

3.2.2 Cell culture, transient and stable transfections

COS-7, HEK_GFP-DYRK1A and SH-SY5Y cells were cultured in Dulbecco´s modified Eagle medium (DMEM) High Glucose ([4.5 g/L], with L-Glutamine and sodium pyruvate) (PAA) containing 10% fetal bovine serum (PAA) and supplemented with L-glutamine plus antibiotics (100 units/ml penicillin and 100 µg/ml streptomycin). SH-SY5Y cells were kindly provided and kept in culture by Ulf Soppa. HeLa cells were cultured in Quantum 101 for HeLa Cells with L-glutamine (PAA Laboratories GmbH). PC12_GFP-DYRK1A cells were cultured in DMEM High Glucose containing 10% horse serum (PAA), 5% fetal bovine serum and 25 mM HEPES (Sigma). All cells were cultured at 37°C and 5% of CO_2.

Transient transfections were performed by using FUGENE HD Transfection Reagent (Roche Molecular Biochemicals, Mannheim, Germany), and the cells were washed after 24 h and processed 24 h later. For live cell imaging, COS-7 cells were transiently transfected and 24 h later, they were subcultured on 42-mm glass coverslips. After 48 h, the coverslips were placed into a thermostat-controlled (37°C) and CO_2-controlled perfusion chamber (Pecon), and covered with DMEM culture medium. To block CRM1-mediated nuclear export leptomycin B (Calbiochem, San Diego, CA, USA) was added to the culture medium at 10 ng/ml for 4 h.

For inducible expression of GFP-DYRK1A, PC12 Tet-on cells (Clontech) were stably transfected with the pFRT/lacZeo (Invitrogen) construct to introduce the Flp recombinase target sequence (FRT) using JetPEI (PEQLAB, Erlangen, Germany). Positive clones were then transfected with pcDNA5/FRT/TetOn/GFP-DYRK1A to stably integrate GFP-DYRK1A cDNA by Flp-mediated recombination (Invitrogen). Positive cells were selected in the presence of 100 µg/ml hygromycin B (PAA). Finally, doxycycline-induced GFP-DYRK1A expressing cells were further selected for GFP fluorescence using FACS Vantage SE with DIVA Software (Becton Dickinson, Heidelberg Germany) at the CRG/UPF FACS Unit (Barcelona, Spain). The generation of stably transfected HEK293 cells expressing GFP-DYRK1A under the control of a tetracycline-regulated promoter (HEK_GFP-DYRK1A) has been described earlier (Sitz et al. 2008). Expression of GFP-DYRK1A in PC12 or HEK293 cells was induced with 2 µg/ml doxycycline (Sigma) for two days if not stated otherwise. Harmine (Fluka, Buchs, Switzerland), DMAT (Calbiochem, San Diego, CA, USA), Calyculin A (Tocris Bioscience, Avonmoth, UK), MG132 (Sigma), nocodazole (Sigma) and thymidine (Sigma) were added to the cells as indicated.

3.2.3 Gene expression PCR analysis in tissues and cell lines

A panel of human cDNAs normalized to the expression of housekeeping genes was purchased from Clontech (Human MTC Panel I). Total RNA from cell lines was isolated using the NucleoSpin RNA II Kit (Macherey-Nagel, Düren, Germany) according to the manufacturers instructions and subjected to reverse transcription using an oligo(dT) 12-18 primer and Superscript II Reverse Transcriptase (Invitrogen). The sequences of the oligonucleotides used for the specific detection of *DYRK4* splice variants are provided in Table 4. PCR reactions were performed with the GoTaq DNA polymerase (Promega, Mannheim, Germany) at an annealing temperature of 57°C. The identity of the PCR products was verified by DNA sequencing (GATC, Konstanz, Germany).

3.2.4 Quantitative real-time reverse transcription-PCR (qRT-PCR)

SH-SY5Y cells were treated for 8 h with 3 µM tunicamycin (Sigma) or DMSO. Isolation of total RNA from SH-SY5Y was carried out on the QIAcube using the RNeasy Mini Kit (Qiagen, Hilden, Germany). $2x10^6$ cells were lysed in RLT-buffer on ice and transferred to 2 ml reaction tubes. Tubes were placed in the QIAcube and automated RNA isolation was performed following the manufacturer's instructions. Total RNA was eluted in 60 µl endvolume and concentration was determined by photometry (NanoDrop ND-1000, NanoDrop Technologies, Wilmington, USA). M-MLV (moloney murine leukemia virus) reverse transcriptase (Promega, Mannheim, Germany) was used forcDNA synthesis. Quantitative real time PCR (qRT-PCR) was performed using the LightCycler 480 DNA SYBR Green I Master (Roche). Details can be seen in Table 5 and 6. Gene expression level of *DYRK4* variants were analyzed using the LightCycler 480-Software 1.5 and normalized to *GAPDH*. All samples were performed as triplicates.

Table 5: cDNA synthesis and master mix for qRT-PCR.

RNA	1 µg
Oligo(dT)-Primer [0.5 µg/µl]	1 µl
ad 12 µl nucleasefree H_2O	
10' at 65°C, then store at 4°C	
5x M-MLV RT reaction buffer	4 µl
dNTP-mix [10 mM]	2 µl
RNasin [40 U/µl]	1 µl
M-MLV RT [2000 U/µl]	1 µl
90' at 37°C, 2' at 95°C	
nucleasefree H_2O	30 µl

cDNA	1 µl
SYBR Green I Master	5.5 µl
forward primer	6 µM
reverse primer	6 µM
	ad 11 µl H_2O

Table 6 : qRT-PCR program.

Gene	Denaturation	Annealing	Elongation	Cycles
DYRK4 Long	10'' 95°C	10'' 58°C	15'' 72°C	55
DYRK4 Cat	10'' 95°C	10'' 62°C	15'' 72°C	50
GAPDH	10'' 95°C	10'' 66°C	20'' 72°C	45

3.2.5 Fluorescence microscopy and shuttling analysis

To detect GFP-tagged proteins in the transfected cells, they were first fixed in 4% paraformaldehyde in PBS for 15 min at RT. The coverslips were then mounted in Vectashield (Vector Laboratories) containing 500 ng/ml 4',6-diamidino-2-phenylindole (DAPI), analyzed under a Zeiss Observer.Z1 and images were acquired with an AxioCam MRm camera (Zeiss, Göttingen, Germany). Confocal imaging and the fluorescence loss in photobleaching (FLIP) assays were performed using a Zeiss LSM 510 Meta confocal microscope equipped with an argon laser. Cells were examined with a 63x1.2 NA Zeiss water immersion objective. GFP was excited at λ= 488 nm and detected using a 505-530 bandpass filter. YFP was excited at λ= 514 nm and using a 530-600 bandpass filter. In the FLIP assay, bleaching was performed with 14 pulses each consisting of 50 iterations in a cytoplasmic region of

interest (ROI) until most of the cytoplasmic fluorescent protein was bleached. Data were recorded after each bleach pulse and subsequently every 30 sec. Four ROIs were used to measure the fluorescence intensities. The first ROI was taken from the bleached region (ROI) and a second ROI from the nucleus (Nuc) of the bleached cell. A third ROI was taken from a non-bleached neighbouring cell to measure the loss of fluorescence during image acquisition (Con), while the fourth ROI monitored the background fluorescence (BG). Normalized fluorescence intensities were calculated from five representative FLIP measurements as follows: 1) Background subtraction: ROI (t) – BG (t), Nuc (t) – BG (t), Con (t) – BG (t) 2) Correction: (ROI (t) – BG (t))/ (Con (t) – BG (t)), (Nuc (t) – BG (t))/ (Con (t) – BG (t)) 3) Normalization: ((ROI (t) – BG (t))/ (Con (t) – BG (t))) * ((ROI (0) – BG (0))/ (Con (0) – BG (0))).

3.2.6 Immunoprecipitation

Transfected cells were washed twice in cold PBS and lysed in immunoprecipitation (IP) lysis buffer. After centrifugation the supernatant was obtained and incubated with 1 µg/sample of rabbit anti-GFP (Rockland) or mAb anti-HA (Covance) for 1 h at 4°C. Equilibrated Ezview Protein G Affinity Gel (Sigma) was added to each sample and incubated at 4ºC overnight. Immuno-complexes were then washed twice with IP washing buffer containing Igepal and twice with washing buffer without Igepal. The samples recovered were analyzed in Western blot, in *in vitro* phosphorylation assay, in *in vitro* kinase assays or treated with phosphatase (as described below).

3.2.7 Phosphatase treatment

Extracts from transfected cells expressing HA-hDYRK4^{520} or its kinase deficient derivatives were subjected to anti-HA immunoprecipitation. Immuno-complexes were incubated for 1 h at 37°C in a total volume of 10 µl with phosphatase buffer and 2 µl of calf intestinal alkaline phosphatase (CIP) (10,000 U/ml, New England Biolabs, Schwalbach, Germany). The reaction was terminated by heating for 10 min at 65°C and washing twice with 50 mM Tris-HCl (pH 8) and 150 mM NaCl. Control reactions from the same immuno-complexes were treated similarly but in the absence of phosphatase.

3.2.8 IMAC *(immobilized-metal affinity chromatography)*

Transfected cells were washed once with ice cold PBS and lysed in 6 M GuHCL (guanidine hydrochloride) lysis buffer. After centrifugation supernatant was obtained, equilibrated nickel-nitrilotriacetic acid (Ni-NTA) agarose (Qiagen) was added to each sample and incubated for 2 h at 4ºC, and the agarose-complexes were then washed three times with 8 M urea washing buffer.

3.2.9 Protein purification using anti-GFPmag

Transfected cells were washed twice in ice cold PBS and lysed in IP lysis buffer. After centrifugation the supernatant was obtained and incubated with equilibrated 30µl/sample of anti-GFPmag (GFP-Trap coupled to magnetic particles; ChromoTek, Martinsried, Germany) for 3 h at 4°C. Proteins bound to GFP-mag were then washed twice with IP washing buffer with Igepal and twice with washing buffer without Igepal using a magnetic rack. The samples recovered were analyzed in Western blot, in *in vitro* phosphorylation assays or in *in vitro* kinase assays (as described below).

3.2.10 *In vitro* phosphorylation assay

Endogenous DYRK1A or overexpressed GFP-DYRK1A were immunoprecipitated with anti-DYRK1A antibody or by anti-GFPmag from HeLa, HEK_GFP-DYRK1A or PC12_GFP-DYRK1A cells. Immuno-complexes were split and incubated for 2 h at 37°C in the presence or absence of 1 mM ATP in 1x kinase buffer. Where indicated 4 µM harmine was added to the reaction. Reaction was stopped by adding LSB, proteins were eluted by heating at 98°C for 10 min and then analyzed in Western blot.

3.2.11 *In vitro* kinase (IVK) assay

For *in vitro* kinase (IVK) assays from mammalian cells, immuno-complexes were incubated for 30 min at 30ºC in 20 µl of 1x kinase buffer at a final concentration of 10 µM ATP and [γ^{33}-P]ATP (100–150 mCi/pmol) and with 100 µM of peptide. Incorporation of ^{33}P into DYRKtide and SAPtide was determined in triplicate by dotting aliquots of the reaction mixture onto Whatman P-81 ion exchange paper (Whatman, Maidstone, UK), washing in 5% phosphoric acid and counting by liquid scintillation in LS 6000SC (Beckman, Krefeld, Germany). Incorporation of ^{33}P into Pep285 and Pep3 was determined by dotting aliquots of the reaction onto a SAM²

biotin capture membrane (Promega, Mannheim, Germany), washing twice in 2 M NaCl for 2 min, twice in 2 M NaCl in 1% phosphoric acid for 3 min, twice in H_2O for 30 sec, once in 70% ethanol for 30 sec and subsequently counting by liquid scintillation. To ensure equal expression of the fusion proteins and autophosphorylation, the kinases were eluted from the beads in the presence of LSB by heating for 10 min at 98°C and analyzed in Western blot and subsequently by autoradiography using a Storage Phosphor Sreen and a Storm 820 PhosphorImager (Amersham Biosciences, Freiburg, Germany). The absolute counts per minute (cpm) obtained from unfused GFP transfected cells immuno-complexes were subtracted from cpm of each sample as background. Then cpms of each sample were normalized to the corresponding intensity of the signal obtained in the immunoblots (total protein).

3.2.12 Whole cell lysates

All steps were carried out on ice. Cells were washed twice with ice cold PBS and lysed with boiling SDS lysis buffer. The cells were then dispensed using a scraper, the solution was transferred to a 1.5 ml reaction tube, boiled for 5 min at 98°C and then sonificated for 30 sec. After centrifugation (5 min, 4°C, maximum rpm) the supernatant containing the proteins was stored at -20°C until further use. In the case of Calyculin A and nocodazole treatment, detached cells were transferred to a reaction tube, recovered by centrifugation (2 min, 4°C, 2000 rpm) and washed twice with ice cold PBS. Cell pellets were resuspended in 30 µl ice cold PBS and SDS lysis buffer was added. Cell lysates were then boiled, sonificated and centrifuged like above.

3.2.13 Western blot

Samples were resolved by SDS-PAGE using 10% SDS-polyacrylamide gels if not stated otherwise. The proteins were transferred to Protran Nitrocellulose membrane (Whatman, Dassel, Germany) that was then blocked with 5% skimmed milk in Tris-buffered saline (TBS) plus 0.1% Tween-20 (TBS-T) or with 3% bovine serum albumin (BSA) in TBS-T, when a phospho-specific antibody was used as primary antibody. The membranes were incubated overnight at 4ºC with primary antibodies (5% BSA in TBS-T + 0.02% NaN_3) and after washing with TBS-T the membranes were incubated for 45 min at RT with corresponding secondary antibodies (5% skimmed

milk in TBS-T + anti-biotin). After washing again with TBS-T, chemiluminiscence detection solution was added and the membrane was incubated for 1 min at RT in the dark. Antibody binding was detected by enhanced chemiluminiscence using a LAS-3000 CCD imaging system (Fujifilm, Düsseldorf, Germany) and the data was quantified using AIDA Image Analyzer (v4, Fuji UK). The antibodies and conjugates used are listed in Table 4.

3.2.14 Synchronization for cell cycle analysis

Double thymidine block (early S phase block): HeLa or PC12_GFP-DYRK1A cells were treated with 2 mM thymidine for 19 h (first block), then medium was removed and cells were washed twice with PBS and fresh medium was added for 9 h. The second thymidine block was then initiated by adding 2 mM thymidine to the medium for 17 h. Finally, cells were washed twice with PBS and detached from the tissue culture dish by either treatment with trypsine (HeLa cells) or by pippeting with fresh medium (PC12_GFP-DYRK1A cells). Suspended cells were split to p35 Falcon Easy Grip tissue culture dishes (Becton Dickinson and Company, Franklin Lakes, NJ, USA) and harvest at different time points for Western blot (whole cell lysates) or for flow cytometry (FACS) analysis. Transient transfection (5 µg DNA/tissue culture dish 100x20 mm) of HeLa cells during synchronization took place 2 h after the first thymidine block using FuGENE HD for 2 h. Cells were then washed and fresh medium was added for additional 5 h before initiating the second thymidine block (see Fig. 32*E* and *F*).

Thymidine-Nocodazole block (mitotic block): HeLa or PC12_GFP-DYRK1A cells were treated with 2 mM thymidine for 24 h (S phase block), then washed twice with PBS and released in fresh medium for 3 h. Cells were arrested in prometaphase by adding 100 ng/ml nocodazole to the medium for 12 h. Mitotic cells in suspension were then collected in a reaction tube, centrifuged (2 min, RT, 2000 rpm), washed twice with PBS, resuspended in fresh medium and split to p35 Falcon Easy Grip tissue culture dishes. Cells were harvested at the indicated time points for Western blot (whole cell lysates) or FACS anaylsis.

3.2.15 FACS analysis of synchronized cells

Cells were synchronized and released as described above. For FACS analysis, cells were detached from p35 Falcon Easy Grip tissue culture dishes (Becton Dickinson and Company, Franklin Lakes, NJ, USA) by pipetting in case of PC12_GFP-DYRK1A cells or by trypsinization in case of HeLa cells, washed with 1 ml PBS and resuspended in 100 µl PBS in a 1.5 ml reaction tube. 1.3 ml cold (< -20°C) Ethanol 80% was added dropwise to the tube while vortexing and then tubes were kept at -20°C overnight. Cells were centrifuged (2 min, 4°C, 1500 rpm) and washed twice with 1 ml PBS. Finally, cell pellets were incubated with 200 µl RNAse (20 µg/ml in PBS) for 5 min at RT, then replaced in FACS tubes and 400 µl propidium iodide (50 µg/ml in PBS) was added for additional 30 min at RT in the dark. Cells were then vortexed and DNA content was measured using the BD FACS Canto II and BD FACS Diva Software (BD Biosciences, Franklin Lakes, NJ, USA).

4. Results

4.1 DYRK4

4.1.1 Human and murine DYRK4 are expressed as multiple alternative splicing variants

4.1.1.1 Exon-intron organization of the N-terminal region of DYRK4

Database mining indicates that at least two different murine *Dyrk4* transcripts exist (Fig. 7*A*). One of them encodes a protein product of 594 amino acids (mDYRK4^{594}, corresponding to Accession Number [Acc. Nº] NM_207210), while the other (Acc. Nº AK077117) has a different 5'-terminal sequence and encodes a protein of 632 amino acids. Similarly, two different human DYRK4 protein products can be predicted: a 520 amino acid protein described previously (hDYRK4^{520}, translated from Acc. Nº NM_003845: (Sacher et al. 2007), and a 635 amino acid protein (hDYRK4^{635}, translated from Acc. Nº AK308260). The N-terminal regions of the long murine and human DYRK4 isoforms are encoded by orthologous exons (Fig. 7*A* and *B*). In contrast, the short isoform of mouse *Dyrk4* starts with a 5'-exon that is not conserved in human *DYRK4* (Fig. 7*A*). Thus, the longer isoform can be considered as the reference sequence for DYRK4, because the additional N-terminal sequence is conserved in mammals (Fig. 7*C*). By contrast, the corresponding first exon of the short variants appears to be species-specific, at least in human and mouse.

In summary, both human and murine DYRK4 genes express several transcripts as a result of alternative splicing, with the two main protein products differing in their amino-terminal domain.

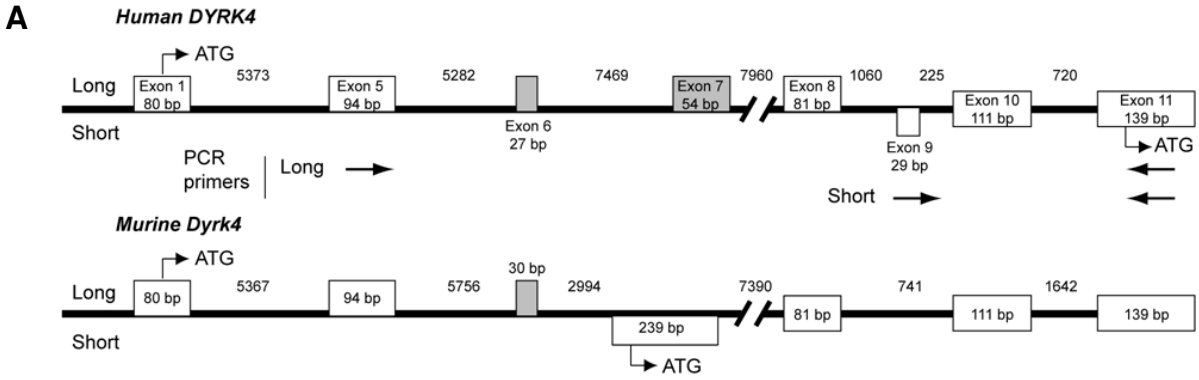

B

```
Mm DYRK4-S      1 ------------------------------------MCFLLQTSQMRTSKAQSEVESKPL  24
Mm DYRK4-L      1 MQLLRLPALTRTETSMDTNKARKRSLTTFPILKARKKQSFTSVKGPTLPPEIYMVESKPL  60
Hs DYRK4-L      1 MQLLPPPIRTGTKTQMDAKKPRKCDLTPFLVLKARKKQKFTSAKGPTLS-EIYMVGSKLS  59
                                  NLS                  Exon 6

Mm DYRK4-S     25 GHLQKPSSKNKKLRVNRCPQKIPSNTAFPFVDTKGKRNTVNFPQIGNKVPSKGPMQYQEN  84
Mm DYRK4-L     61 GHLQKPSSKNKKLRVNRCPQKIPSNTAFPFVDTKGKRNTVNFPQIGNKVPSKGPMQYQEN 120
Hs DYRK4-L     60 VQIQKPPSNIKNSRMTQVFHKNTSVTSLPFVDTKGKKNTVSFPHISKKVLLKSSLLYQEN 119

Mm DYRK4-S     85 QIHNQVLSSELKTSEIPFNINTKAQDTKPHPELQKKHKVPLTVAEALKFFKNQLSPYEQS 144
Mm DYRK4-S    121 QIHNQVLSSELKTSEIPFNINTKAQDTKPHPELQKKHKVPLTVAEALKFFKNQLSPYEQS 180
Hs DYRK4-L    120 QAHNQMPASELKASEIPFHPSIKTQDPKAEEKSPKKQKVTLTAAEALKLFKNQLSPYEQS 179
Hs DYRK4-S      1 -----MPASELKASEIPFHPSIKTQDPKAEEKSPKKQKVTLTAAEALKLFKNQLSPYEQS  55
```

C

```
Homo sapiens                TQMDAKKPRKCDLTPFLVLKARKKQKFTSAKV
Pan troglodytes             TQMDAKKPRKCDLTPFLVLKARKKQKFTSAKV
Macaca mulatta              TQMDAKKPRKCDLTPFLVLKARKKQKLTSVKV
Mus musculus                TSMDTNKARKRSLTTFPILKARKKQSFTSVKV
Rattus norvegicus           TKMDTNKARKRSLTTFPVLKARKKQSFTSVKV
Equus caballus              TEMDAKEPKKCNLTSFPILKGRKKQNLTSVKV
Bos taurus                  TEMDAKKPRKGSLTSFPMLKATKKQNLASVKV
Oryctolagus cuniculus       TQMDAKKPLKKSVTSFPILKTRKKQNFTSVKV
Canis familiaris            TKMDAKKPRKCSLTSFPSLKAKKKQNLSPGKV
Monodelphis domestica       TKMNARKLGKRSTTSFPILKPRKKYNFSSIKV
```

Figure 7: Exon-intron organization of DYRK4.
A. Schematic representation of the exon–intron structure of the 5' end of the human and murine *DYRK4* gene. Exons are indicated by boxes and the translation start point of the different isoforms is marked (ATG). The length of the exons and introns (in bp) was determined using either the Ensembl or University of California, Santa Cruz (UCSC) servers. The alternatively spliced exons are shaded. The position of the PCR primers used in Fig. 8 is indicated. **B.** Alignment of the N-terminal regions of human (Hs) and murine (Mm) DYRK4. Translation of the different exons is shown in alternating colors (black and grey), and the alternatively spliced exon 6 is underlined. A predicted bipartite nuclear localization signal (NLS) is shown (bold underlined) and the basic amino acid residues are highlighted in bold. S, short; L, long. **C.** Conservation of the predicted protein sequence encoded by exon 5 of the *DYRK4* gene. *DYRK4* genes in mammalian genome sequences were identified using the tblastn algorithm at http://blast.ncbi.nlm.nih.gov/Blast.cgi. Basic residues of the putative NLS are shown underlined in bold. *Homo sapiens* chromosome (chr) 12 (NC_000012.11); *Pan troglodytes* chr 12 (NC_006479.2); *Macaca mulatta* chr 11 (NC_007868.1); *Mus musculus* chr 6 (NC_000072.5); *Rattus norvegicus* chr 4 (NC_005103.2); *Equus caballus* chr 6 (NC_009149.2); *Bos taurus* chr 5 (NC_007303.3); *Oryctolagus cuniculus* chr 8 (NC_013676.1); *Canis familiaris* chr 27 (NC_006609.2); *Monodelphis domestica* chr 8 (NC_008808.1).

4.1.1.2 Differential expression of DYRK4 variants in human tissues

When the expression of *DYRK4* in different human tissues was analyzed by RT-PCR using oligonucleotides matching exons within the catalytic domain, the expression of *DYRK4* mRNA was detected in all the tissues analyzed (Fig. 8*A*). By contrast, *Dyrk4* is predominately expressed in the testis of mouse and rat (Becker et al. 1998; Sacher et al. 2007). The broader tissue distribution of human DYRK4 is also evident through the sources of the ESTs listed in the Unigene database (http://www.ncbi.nlm.nih.gov/unigene), where 9 of the 10 murine ESTs but only 30 of 150 human ESTs are from testis. Interestingly beside testis, murine *Dyrk4* mRNA is only detected in nasopharynx. A microarray expression atlas (ref: Su et al. 2004; accessible at http://genome.ucsc.edu) confirmed the broader distribution of human *DYRK4* (GNF Expression Atlas 2 Data from U133A and GNF1H Chips) and the predominant detection of murine *Dyrk4* (GNF Expression Atlas 2 Data from GNF1M Mouse Chip) in testis and olfactory epithelium. Moreover, *DYRK4* mRNA is detected in human cell lines not derived from testis, such as A549 or HEK293 (Fig. 8*B*), NTERA-2 (Leypoldt et al. 2001) or SH-SY5Y cells (Reimertz et al. 2003) and fibroblasts (Kyng et al. 2003).

PCR reactions with primer pairs specific for transcripts encoding the long or the short N-terminal protein variants highlighted the differentially expression of the corresponding transcripts, with the long isoform present in several tissues and the short isoform predominantly expressed in testis (Fig. 8*A*). The existence of human *DYRK4* transcripts with different 5'-ends was confirmed by RT-PCR and sequencing of the PCR products (Fig. 8*A*). This analysis identified an alternative splicing event that involved the inclusion of an extra exon (exon 6 in humans; exon 3 in mice), which leads to a 9/10 amino acid inclusion in the human/murine DYRK4 proteins (Fig. 7*B* and Fig. 8*A*), and would give rise to a protein isoform of 644/642 amino acids (hDYRK4^{644} and mDYRK4^{642}). In addition to the bands resulting from the inclusion/exclusion of exon 6, the primers also produced longer PCR products in several tissues. Sequencing of these products showed that they are an result of the inclusion of exon 7 (Fig. 8*A*), which would lead to an in-frame premature stop codon.

Notably, the ratio between exon 6+/- or 7+/- isoforms was different when distinct tissues and cell lines were compared (Fig. 8*A*), suggesting that these splicing events are tissue specific and subject to regulation (*see Discussion 5.1.1*).

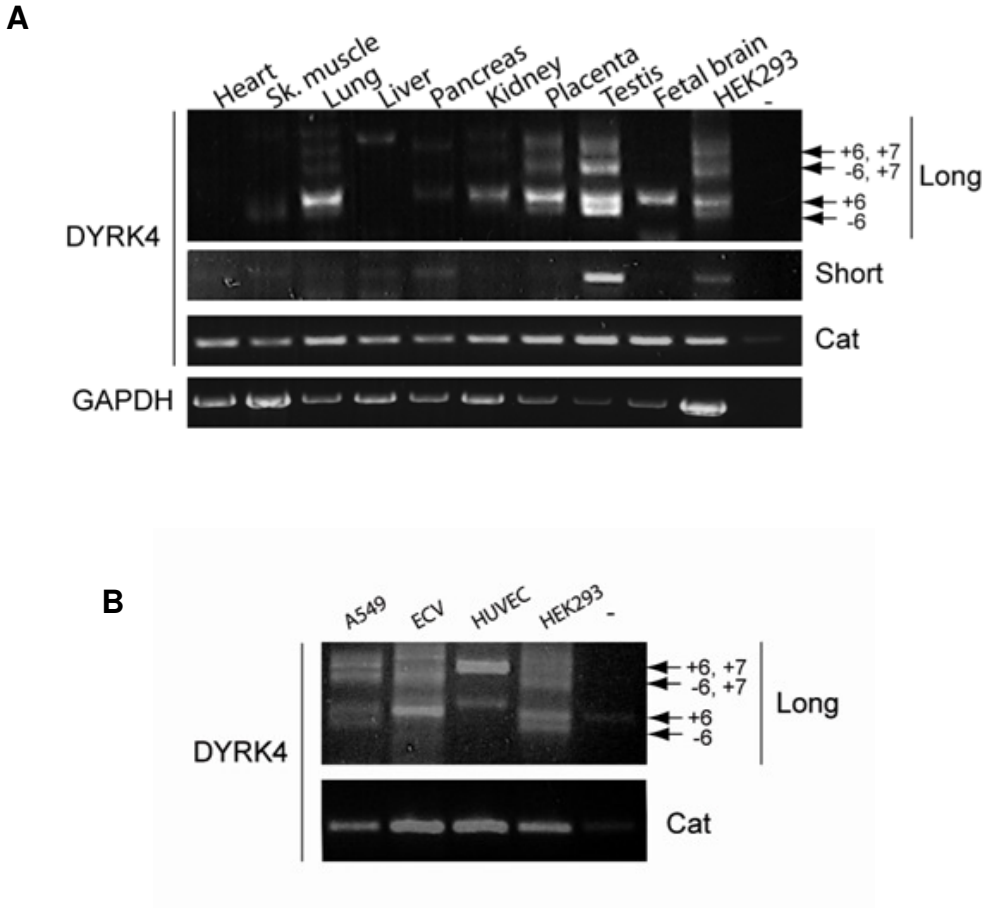

Figure 8: Differential expression of *DYRK4* isoforms.
A. A panel of cDNAs from different human tissues was used for RT-PCR with primer pairs specific for the two main isoforms of human *DYRK4* (shown in Fig. 7*A*). Bands detected with the "long" primers correspond to the inclusion/exclusion of exon 6 and/or exon 7, as confirmed by sequencing of the PCR products from the testis. Total *DYRK4* expression was assessed with primers from the catalytic domain (Cat) and the expression of *GAPDH* was used as a control. **B.** RT-PCR with different oligonucleotide pairs specific for human *DYRK4* and RNA from different cell lines. A549, human carcinoma alveolar basal epithelial cells; ECV, human bladder carcinoma cells; HEK293, human embryonic kidney cells; HUVEC, human umbilical vein endothelial cells. Cat refers to the PCR product obtained with oligonucleotides located in the exons encoding the kinase catalytic domain. DNA sequence of the different PCR products from a representative sample (testis, see Fig. 8*A*) revealed that they correspond to the transcripts with the indicated exon composition.

4.1.1.3 The transcript of the long human DYRK4 isoform is upregulated by tunicamycin in SH-SY5Y cells

Gene expression microarray analysis of human SH-SY5Y neuroblastoma cells had identified *DYRK4* as a tunicamycin-induced gene reaching maximal induction 8 h after treatment (Reimertz et al. 2003). Tunicamycin is an inhibitor of protein glycosylation and induces expression of target genes of the so-called "unfolded protein response (UPR)". Prolonged tunicamycin treatment leads to endoplasmic reticulum (ER) stress and apoptosis.

Using identical conditions, we tested if tunicamycin is able to increase mRNA level of the long and the short isoform of *DYRK4*. As tunicamycin is dissolved in DMSO, we used it as a negative control treatment and normalized relative mRNA level of tunicamycin-treated cells to the mRNA level of DMSO-treated cells. Quantitative real-time reverse transcription PCR (qRT-PCR) using oligonucleotides matching exons within the catalytic domain of DYRK4 confirmed the induction of *DYRK4* mRNA in SH-SY5Y cells treated with tunicamycin (Table 7). Oligonucleotides matching the short isoform of *DYRK4* failed to amplify any product, suggesting that the short isoform of DYRK4 is not expressed in SH-SY5Y or that this pair of oligonucleotides is not suitable for qRT-PCR. In contrast, oligonucleotides matching the long isoform revealed an up-regulation of transcript level by tunicamycin in 4 independent mRNA samples (Table 7). In one of these amplified products the presence of exon 6 was verified by sequencing.

In summary, expression of *hDYRK4*^{644} was detected in SH-SY5Y cells and, although to a variable extent, DYRK4 transcripts were consistently induced by tunicamycin treatment and thus relate DYRK4 to the UPR (*see Discussion 5.1.3*).

Table 7: *DYRK4* mRNA induction by tunicamycin in SH-SY5Y neuroblastoma cells. SH-SY5Y cells were treated for 8 h with 3 µM tunicamycin or vehicle (DMSO) and total RNA was isolated (*see Material and Methods*). Quantitative real-time reverse transcription PCR (qRT-PCR) was performed using oligonucleotides matching the catalytic domain (Cat) or the long isoform (Long) of *DYRK4* (*see Material and Methods*). *DYRK4* mRNA levels were normalized to *GAPDH* and arbitrarily set to 1. qRT-PCRs (1-6) were performed with 4 different RNA samples. nd = not done.

		Long		Cat	
RNA	qRT-PCR	DMSO	Tunicamycin	DMSO	Tunicamycin
A	1	1	437	nd	nd
B	2	1	4.8	nd	nd
C	3	1	0.6	1	1.9
D	4	1	81.3	1	1.8
A	5	nd	nd	1	1.1
B	6	nd	nd	1	1.9

4.1.2 Alternative splicing alters the subcellular localization of DYRK4

4.1.2.1 DYRK4 is mainly localized in the cytosol

The 520 amino acid isoform of human DYRK4 (hDYRK4^{520}) is located in the cytosol of COS-7 cells when expressed exogenously (Sacher et al. 2007). This distribution was confirmed in HeLa cells using wild type hDYRK4^{520} and two kinase deficient mutants* (the KR mutant where Lys133 in the ATP binding site is mutated to Arg, and the YF mutant where Tyr264 in the activation loop is mutated to Phe). The PSORT II algorithm (Nakai and Horton, 2007) predicts the presence of a putative bipartite NLS within the extended N-terminal region, which is conserved in the human and murine long protein variants of DYRK4 (Fig. 7*B* and *C*). Therefore, it has been supposed that the distinct protein isoforms could differ in their subcellular distribution.

To study their subcellular localization, the long variants of human and mouse DYRK4 proteins (hDYRK4^{644} or mDYRK4^{642}), which include the putative NLS, and hDYRK4^{520} or mDYRK4^{594} that do not have the N-terminal extension were fused to GFP. Both, the long and the short variants of human and mouse GFP-tagged DYRK4 were mainly detected in the cytosol when overexpressed in COS-7 cells (Fig. 9*C*, untreated; shown for mouse DYRK4). In some of the cells a significant fraction of both isoforms (long and short, in human and mouse) was also localized in the nucleus.

Experiments performed by our collaborators verified that the NLS of DYRK4 fused to a chimeric GFP-GST protein was able to translocate this cytosolic protein to the nucleus and was interacting with importin α, indicating that DYRK4 contains a *bona fide* NLS. In addition they showed that in SH-SY5Y cells the long variants of human and mouse DYRK4 proteins fused to GFP were localized in the nucleus to a significant extent, whereas GFP-hDYRK4^{520} or GFP-mDYRK4^{594} were mainly detected in the cytosol (published in Papadopoulos et al. 2011). However, both isoforms (long and short, in human and mouse) behaved similarly as in COS-7 cells when overexpressed in HeLa cells.

* Papadopoulos, Chrisovalantis (2007) Functional Characterisation of the Protein Kinase DYRK4, diploma thesis, RWTH Aachen University

Together, these results confirm that different DYRK4 isoforms display distinct subcellular localizations, in a cell type dependent manner. Moreover, these data further suggest that the nuclear accumulation of the long variant of DYRK4 driven by the NLS is partially prevented by a mechanism that remains to be identified (*see Discussion 5.1.4*).

4.1.2.2 CRM1-independent distribution of GFP-mDYRK4

For many proteins, their distribution between the cytoplasm and the nucleus is based on a dynamic equilibrium of nuclear import and nuclear export, with contributions from protein retention in either of these subcellular compartments. The preferential cytoplasmic localization of DYRK4 isoforms in COS-7 cells could result from a strong nuclear export signal (NES)-dependent and CRM1 (exportin-1)-mediated nuclear export that might mask the effect of the NLS in the N-terminal extensions of the long DYRK4 isoforms.

Sequence analysis revealed a putative leucine-rich nuclear export sequence (NES; LX_4LX_2LXL) motif for human and murine DYRK4 present in the long and in the short isoform (Fig. 9*A*). This motif interacts with an exportin which is a member of the importin β family (Ohno et al. 1998). It has been reported that mutation of the two leucines (Fig. 9*A*, asterisks) to alanine destroys NES activity (Feng et al. 1999). Therefore we generated a mutant of GFP-mDYRK4^{642} in which the residues Leu191 and Leu193 were replaced by alanine (GFP-mDYRK4^{642} L191A/L193A). COS-7 cells transiently transfected with GFP-mDYRK4^{642} L191A/L193A did not show any nuclear accumulation of the protein (Fig. 9*B*), indicating that this putative NES motif is not functional or that other NES, not matching this motif, are present in DYRK4.

To further determine the contribution of CRM1-mediated nuclear export to the cytosolic accumulation of DYRK4 and to exclude additional active NES motifs, we exposed cells to an inhibitor of CRM1, leptomycin B. No nuclear accumulation of either isoform was evident after 4 h in the presence of this inhibitor (Fig. 9*C*). The effect of leptomycin B was shown using STAT5A as a positive control.

These results suggest that subcellular localization of the long variant of DYRK4 is modulated due to a strong CRM1-independent NES, an inactivated NLS or an unknown stimulus, which could alter either nuclear export or import.

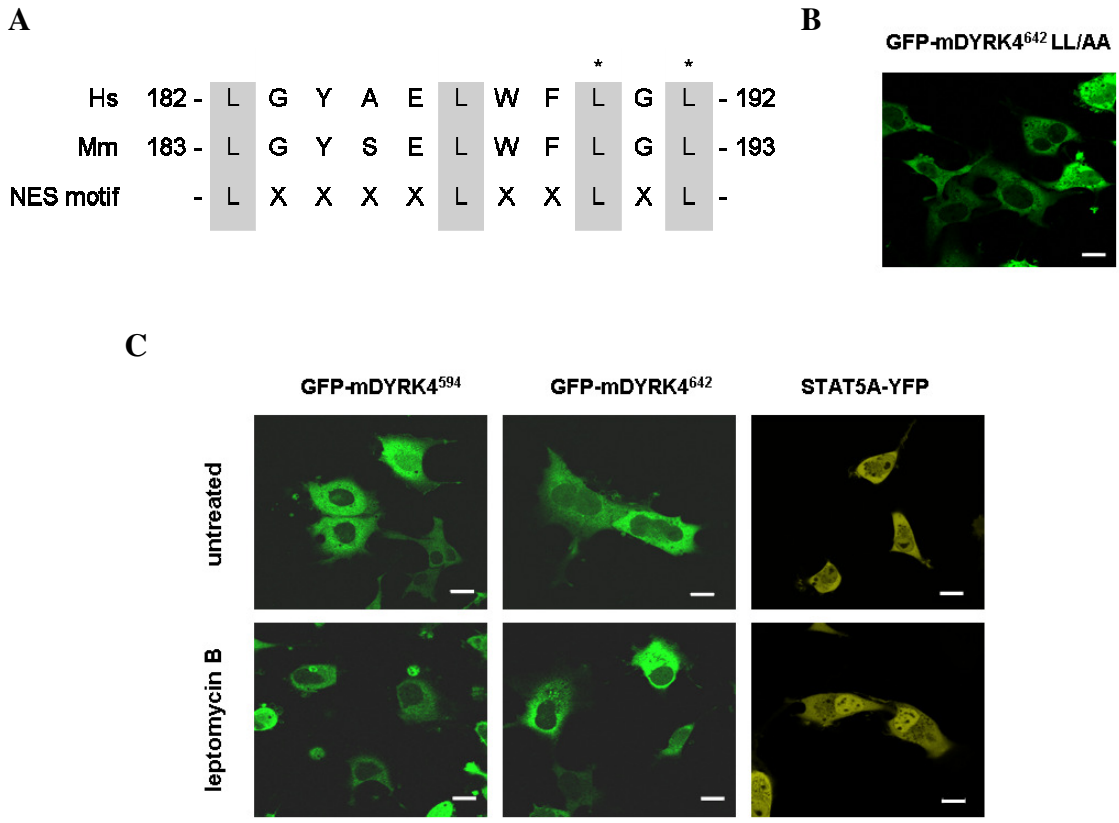

Figure 9: CRM1-independent distribution of GFP-mDYRK4 in COS-7 cells.
A. Sequence and position of the putative nuclear export signal (NES) motif in full-length human (Hs) and murine (Mm) DYRK4 are indicated and compared to the NES consensus sequence. Mutated leucine residues to generate GFP-mDYRK4^{642} L191A/L193A are marked with asterisks. **B**. Subcellular localization of GFP- mDYRK4^{642} L191A/L193A (LL/AA) expressed in COS-7 cells. **C**. Subcellular localization of GFP-mDYRK4^{594} and GFP-mDYRK4^{642} expressed in COS-7 cells was analyzed before (untreated) and 4 h after addition of leptomycin B (10 ng/ml), an inhibitor of CRM1. STAT5A fused to YFP was used as a positive control responding to CRM1 inhibition. Scale bars, 10 µM.

4.1.2.3 Nucleocytoplasmic distribution of DYRK4

The DYRK4 isoforms show a preferential cytoplasmic localization in COS-7 cells. However, low amounts of the proteins are also detectable in the nucleus by confocal microscopy (clearly visible after bleaching of the cytoplasm; see Fig. 10*A*). To answer the question whether the observed subcellular distribution is based on a dynamic equilibrium of constant nuclear export and nuclear import, we analyzed the dynamics of DYRK4 shuttling in single living cells using the fluorescence loss in photobleaching (FLIP) technique (Lippincott-Schwartz et al. 2001). A defined region of interest (ROI) in the cytoplasm was subjected to repeated photobleaching to wipe out the cytoplasmic GFP-fluorescence (Fig. 10*A*, post-bleach (0 min)). Subsequent reduction

in GFP-fluorescence in the nucleus reflects the nucleocytoplasmic shuttling of bleached protein into the nucleus and non-bleached protein out of the nucleus.

The diffusible character of unfused GFP was reflected in its fast nucleocytoplasmic shuttling, which reached equilibrium after 7 min (Fig. 10*A* and *B*). The two isoforms of mDYRK4 displayed distinct nucleocytoplasmic shuttling, with the nucleocytoplasmic exchange of the shorter isoform (mDYRK4^{594}) converging to equilibrium. In comparison with unfused GFP, shuttling of GFP-mDYRK4^{594} was more slowly (Fig. 10*B*, middle panel). Treatment with leptomycin B had no effect on mDYRK4^{594} nucleocytoplasmic shuttling, further supporting that nuclear export was independent of CRM1 (Fig. 10*C*). By contrast, cytoplasmic bleaching of mDYRK4^{642} did not significantly reduce GFP-fluorescence in the nucleus, indicating that this isoform was not able to exit the nucleus (Fig. 10*B*, lower panel). The total loss of GFP-fluorescence in the bleached ROI was obtained faster than for the short variant. The recovery of cytoplasmic GFP-fluorescence, which is not mediated by exit from the nucleus (Fig. 10*B*, lower panel), could be due to cytoplasmic shuttling from cytoplasmic compartments far from the ROI during photobleaching. As expected from the results shown above, the NES mutant of the longer isoform mDYRK4^{642} L191A/L193A, behaved like the wild-type longer isoform (Fig. 10*D*). Similar results were obtained when the corresponding human isoforms (hDYRK4^{520} and hDYRK4^{644}) were assayed (published in Papadopoulos et al. 2011). The static nature of the long DYRK4 isoform could indicate that it is retained in the nucleus by strong interactions with nuclear proteins or chromatin.

In conclusion, these results indicate that the alternatively spliced N-terminal region, common to human and mouse, confers distinct cellular properties to DYRK4.

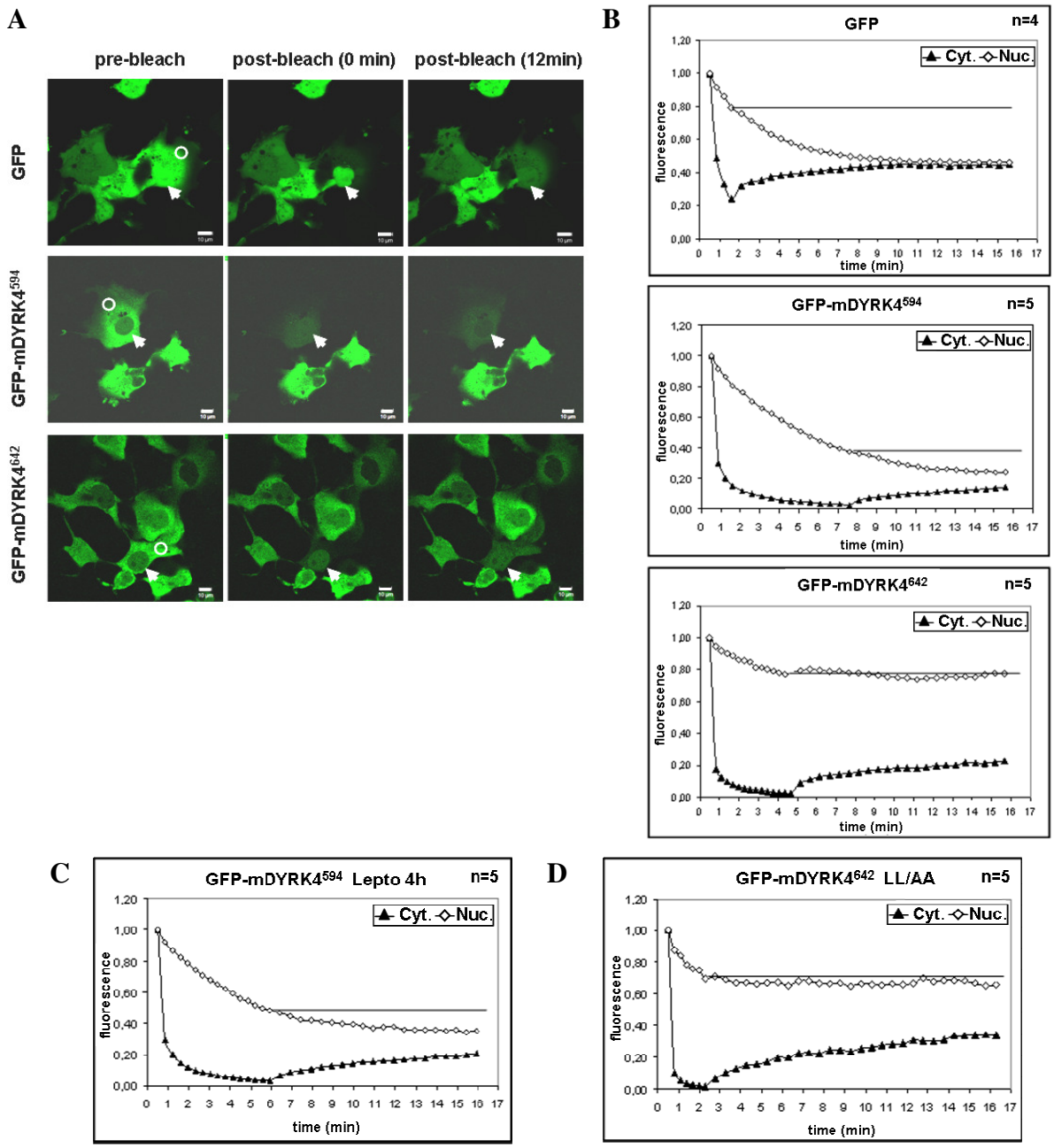

Figure 10: Differences in nucleocytoplasmic shuttling of GFP-DYRK4 isoforms.
A. Cytoplasmic FLIP analysis was performed on GFP, GFP-mDYRK4^{594} or GFP-mDYRK4^{642} expressed in COS-7 cells. The panels show representative images in which the bleached area is indicated by a white circle and the nucleus by an arrow. **B.** Fluorescence was measured in the cytoplasmic and nuclear regions of interest along the time period represented. **C.** Nucleocytoplasmic shuttling of GFP-mDYRK4^{594} in the presence of leptomycin B. The fusion protein was transiently expressed in COS-7 cells and analyzed by FLIP 4 h after addition of leptomycin B (10 ng/ml), an inhibitor of CRM1. **D**. Nucleocytoplasmic shuttling of the NES mutant GFP-mDYRK4^{642} L191A/L193A (LL/AA). This fusion protein was transiently expressed in COS-7 cells and analyzed by FLIP. The diagrams B-D show the normalized averaged fluorescence intensities of n= 4-5 experiments as indicated. Scale bars, 10 µm.

4.1.3 Kinase activity of DYRK4

4.1.3.1 DYRK4 is target of upstream kinases

DYRK4 expressed in mammalian cells migrates as a doublet in SDS gels (Fig. 11). The appearance of the low electrophoretic mobility band does not depend on autophosphorylation, because the band is also present in the two kinase deficient mutants, hDYRK4 YF, where the second tyrosine of the YXY motif (Tyr264) is mutated to Phe (YF) and hDYRK4 KR, where Lys133 in the ATP binding site is mutated to Arg (KR) (Fig. 11). These mutants have previously been described as kinase deficient*. Phosphorylation is a posttranslational modification that can alter electrophoretic mobility. To determine if the doublet occurs due to phosphorylation, wild-type HA-DYRK4 and the two mutants were incubated in the presence or absence of a phosphatase. Treatment of DYRK4 proteins with phosphatase led to the disappearance of the slower migrating band (Fig. 11).

This experiment shows that DYRK4 is phosphorylated by cellular kinases independently of its kinase activity (*see Discussion 5.1.5*).

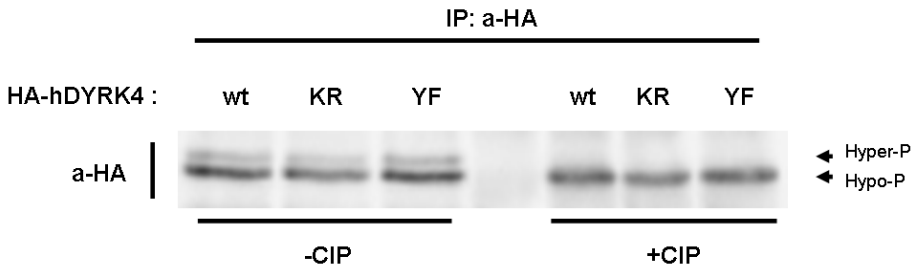

Figure 11: DYRK4 is phosphorylated by cellular kinases.
HeLa cells were transiently transfected with plasmids encoding wild-type HA-hDYRK4^{520} (wt) or its kinase deficient derivatives (KR or YF). HA-tagged proteins were immunoprecipitated with an anti-HA antibody and split in aliquots that were incubated in the absence or presence of calf intestinal phosphatase (CIP). The hyper- and hypophosphorylated forms are indicated by arrows.

* Papadopoulos, Chrisovalantis (2007) Functional Characterisation of the Protein Kinase DYRK4, diploma thesis, RWTH Aachen University

4.1.3.2 Long and short isoform of DYRK4 are catalytically active in vitro

To test if the two isoforms of DYRK4 that differ in subcellular localization are both catalytically active, overexpressed hDYRK4^{520} and hDYRK4^{644} were immunoprecipitated from HeLa or from COS-7 cell extracts and immuno-complexes were subjected to an *in vitro* kinase (IVK) assay with the peptide substrate, DYRKtide. DYRKtide can be used as a non-specific peptide substrate for all kinases of the DYRK family (Himpel et al. 2000). Both isoforms were able to phosphorylate the exogenous peptide (Fig. 12).

Taken together, the alternative use of different 5'-exons does not affect the catalytic domain of DYRK4, and accordingly both the long and short isoforms are catalytically active protein kinases *in vitro*.

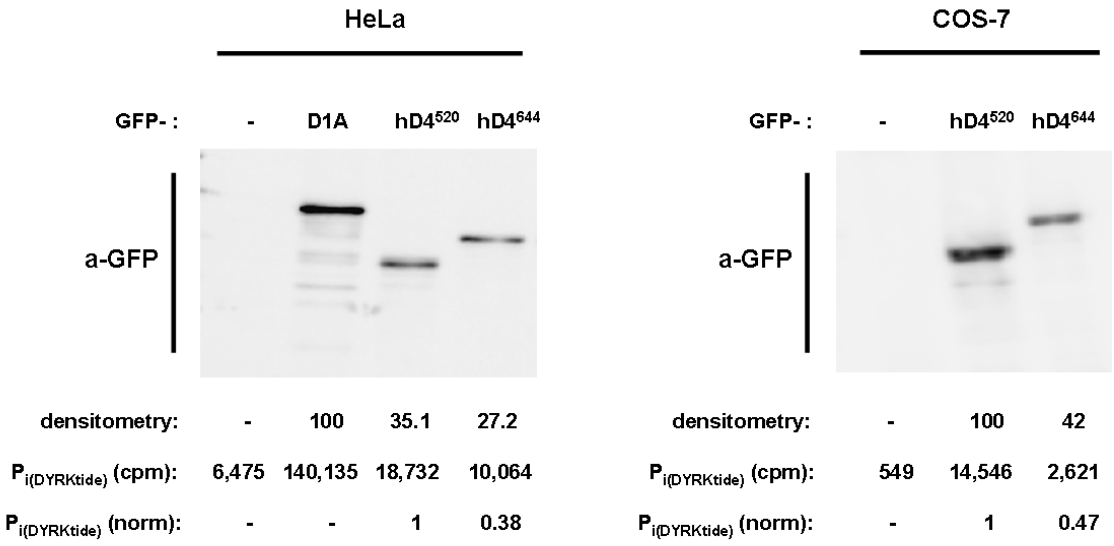

Figure 12: Long and short splicing variants of human DYRK4 are catalytically active protein kinases.
Extracts of HeLa cells or COS-7 cells expressing unfused GFP (-) or GFP-fusion proteins of DYRK1A, hDYRK4^{520} or hDYRK4^{644} were immunoprecipitated with anti-GFP antibody and the immuno-complexes subjected to an IVK assay with DYRKtide. Subsequently, bound proteins were eluted from the resin and analyzed by immunoblotting with anti-GFP antibody. Densitometric evaluation of expression levels and incorporation of labeled phosphate into the peptide (means of triplicate measurement) is indicated below the respective lanes. Cpm, total counts per minute; norm, total cpm normalized to protein expression levels.

4.1.3.3 DYRK4 phosphorylates SF3B1 on Thr434

As no specific substrate for DYRK4 is known and to analyze whether DYRK4 can phosphorylate the same substrates as other DYRKs, one known substrate of DYRK1A, splicing factor 3B 1 (SF3B1) (de Graaf et al. 2006), has been tested for phosphorylation by DYRK4. Therefore, HeLa cells were transfected with GFP-SF3B1-NT (amino acids 1-492) solely or in combination with wild-type HA-hDYRK4 or with the kinase dead mutant HA-hDYRK4 KR. SF3B1 was stronger phosphorylated on Thr434 in cells expressing wild-type DYRK4 (Fig. 13*A*), compared to SF3B1 expressed alone. The kinase deficient mutant failed to enhance Thr434 phosphorylation, suggesting that the active kinase DYRK4 recognizes SF3B1 as a substrate.

As both the long and the short isoforms are catalytically active *in vitro* (Fig. 12), it has been tested whether this is also the case in living cells. HeLa cells were transiently transfected with plasmids expressing GFP-SF3B1 Δ256-382 and GFP-tagged DYRK1A, GFP-hDYRK4^{520}, GFP-hDYRK4^{644} or unfused GFP. GFP-SF3B1 Δ256-382 was used here, because in contrast to HA-tagged hDYRK4^{520}, GFP-tagged hDYRK4^{520} has a similar molecular weight as GFP-SF3B1-NT. Both isoforms, the short and the long one, phosphorylated SF3B1 on Thr434 in HeLa cells (Fig. 13*B*). The difference in phosphorylation level of both isoforms can be explained by the weak expression of the long isoform in this experiment. Notably, phosphorylation of SF3B1 on Thr434 was less efficient than phosphorylation by DYRK1A (Fig. 13*B*). This can be explained by the nuclear subcellular localization of SF3B1 or SF3B1 Δ256-382 (data not shown) and the kinases. DYRK1A was co-localized with SF3B1 in the nucleus when overexpressed, above all in splicing speckles (Alvarez et al. 2003), whereas both isoforms of DYRK4 were only present in a low amount in the nucleus (Fig. 9*C*). Therefore we assume that substrate availability is responsible for the low phosphorylation level of Thr434 by DYRK4.

However, this is the first report showing phosphorylation of a protein by DYRK4 in living cells, confirming that DYRK4 is a catalytically active protein kinase *in vivo*.

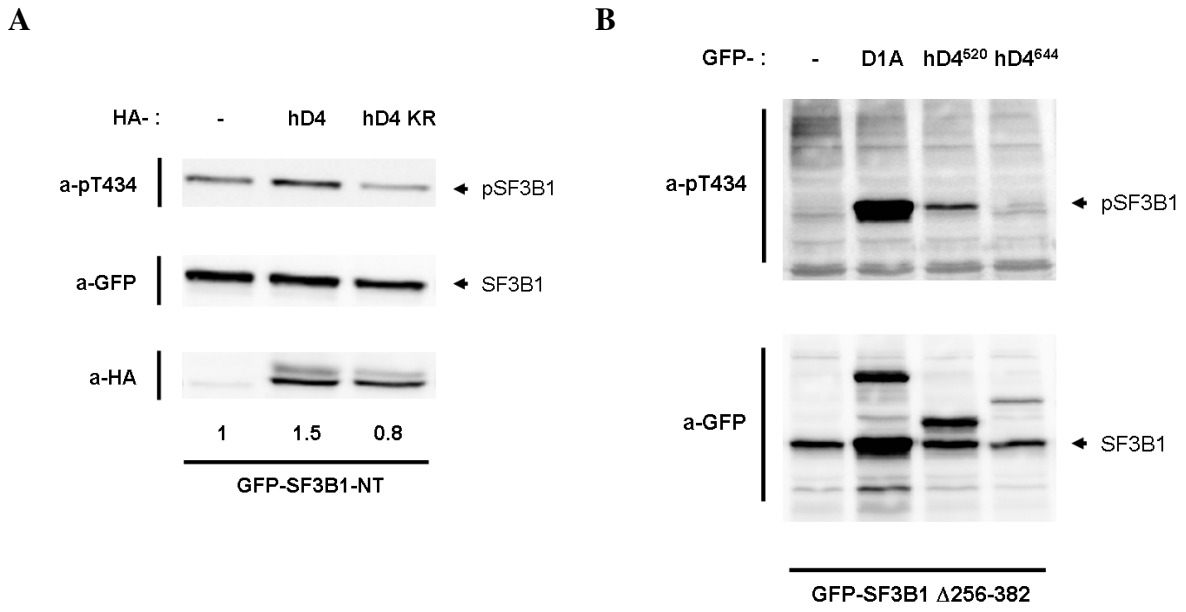

Figure 13: Phosphorylation of SF3B1 by DYRK4.
A. Whole cell lysates of HeLa cells co-expressing wild-type HA-hDYRK4^{520}, the kinase dead mutant HA-hDYRK4 KR or vector control (-) with GFP-SF3B1-NT were analyzed in Western blot. Phosphorylation of SF3B1 was detected using a phosphorylation site-specific antibody (pT434 in SF3B1). Band intensity of pSF3B1 was normalized to intensity of total SF3B1 and the ratio is indicated below the respective lanes. Vector control was arbitrarily set to 1. **B**. Whole cell lysates of HeLa cells co-expressing GFP-SF3B1 Δ256-382 with unfused GFP (-), wild-type GFP-DYRK1A, GFP-hDYRK4^{520} or GFP-hDYRK4^{644} were analyzed in Western blot with indicated antibodies.

4.1.4 Substrate specificity of DYRK4

4.1.4.1 Pep285 is a specific substrate for DYRK4

When characterizing the catalytic activity of DYRK4 it has been found out that the phosphorylation of DYRKtide by DYRK4 was much less efficient than by DYRK1A (Fig. 14*C*). Hence, DYRKtide might not be an optimal substrate for DYRK4 and thus, it has been examined whether DYRK4 exhibited different substrate specificity than other members of the DYRK family. Accordingly, the phosphorylation specificity of DYRK4, or representative mammalian class I and class II DYRKs (DYRK1A and DYRK2, respectively), was studied in phosphosite arrays containing 720 peptides derived from annotated phosphorylation sites in human proteins (Becker, Zerweck, Schutkowski, published in Papadopoulos et al. 2011).

To confirm that substrate specificity of DYRK4 differed from that of DYRK1A, we selected a peptide specifically recognized by DYRK4 for further analysis. Peptide 285 (Pep285) mimics Ser73 in c-Jun (Fig. 14*A*) and was chosen as the top scoring DYRK4 substrate whose phosphorylation by DYRK1A or DYRK2 was sub-threshold in the array experiment. For comparison, DYRKtide was used as non-specific peptide substrate for all kinases of the DYRK family (Himpel et al. 2000). GFP-tagged hDYRK4^{520} and DYRK1A were immunoprecipitated from transiently transfected HeLa cell extracts and immuno-complexes were subjected to an IVK assay with Pep285 and two other DYRK substrates, Pep3 and SAPtide (Fig. 14*A*) as peptide substrates. Pep285 was less efficiently phosphorylated by DYRK4 than DYRKtide, Pep3 and SAPtide (Fig. 14*C*). The amount of kinase used for the different peptides was equal, since the samples were aliquots from a common immunoprecipitation. However, normalization of the data to DYRKtide revealed that Pep285 was significantly better recognized by DYRK4 than by DYRK1A, whereas Pep3 and SAPtide did not show this differences (Fig. 14*B*).

These results are in agreement with the results from the phosphosite array. Pep285 can be used as a specific substrate for DYRK4 in kinase assays. Furthermore, Pep285 was significantly phosphorylated by DYRK4 but not by DYRK1A, and thus supports the proposal that DYRK4 can phosphorylate target sequences not recognized by DYRK1A (*see Discussion 5.1.6*).

A

Name	Sequence	Mimic
Pep285	VGLLKLA**S**PELER	Ser73 c-Jun protein
Pep3	TPGSRSR**T**PSLPT	Thr212 tau protein
SAPtide	RRARKLTA**T**PTPLGG	Thr434 SF3B1 protein
DYRKtide	RRRFRPA**S**PLRGPPK	artificial

B

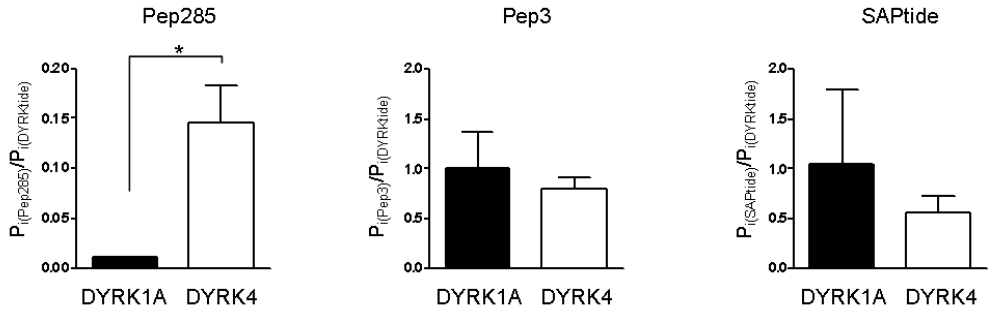

C

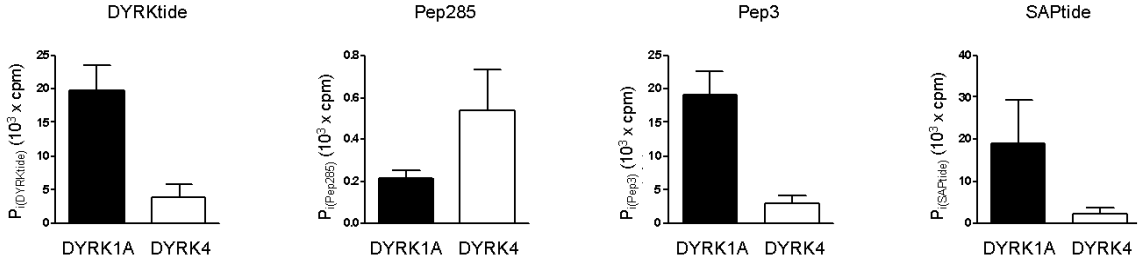

Figure 14: Differential peptide phosphorylation by DYRK4 and DYRK1A.
A. Amino acid sequence of the peptides used in this study. **B.** Peptide selectivity of DYRK4. Anti-GFP immuno-complexes from HeLa cells overexpressing GFP-DYRK1A or GFP-hDYRK4^{520} were assessed in an IVK assay with different peptides as substrates (each at 100 µM). Incorporation of ^{33}P into the indicated peptides was normalized to the phosphate incorporation into DYRKtide. The histogram represents the means ± SD from three independent experiments (*, p=0.0232; paired t test). Raw data corresponding to these experiments are shown in *C*. **C.** Selective phosphorylation of Pep285 by DYRK4. The diagrams show the results of the experiment illustrated in *B* without normalization. Background signal obtained in parallel samples from GFP-transfected HeLa cells was subtracted. Columns represent the amount of radioactive phosphate incorporated into the peptides (means ± SD of three independent experiments).

4.1.4.2 Insertion of the NxGY motif does not significantly alter substrate selectivity of DYRK4

To date only little is known about the structural basis of substrate specificity in the DYRK family of kinases. It has been suggested that the DH-box, a highly conserved motif upstream the kinase subdomain I in all members of the DYRK family, plays a role in the interaction with the substrate (Becker et al. 1999; Kinstrie et al. 2006).

Compared with other members of the DYRK family, mammalian DYRK4 lacks three amino acids (NxG) preceding the DH-box and contain a phenylalanine (F) residue instead of a tyrosine (Y) (Fig. 15*A*). This could be one reason why DYRK4 shows different substrate specificity than DYRK1A (Fig. 14*B* and *C*). To test this hypothesis, it has been determined whether the insertion of the NxGY motif altered the catalytic activity of DYRK4 towards exogenous substrate peptides. A mutant (GFP-hDYRK4^{NLGY}) was generated by inserting the amino acids NLGY into GFP-hDYRK4^{520}. The leucine residue has been chosen, because it is present in dDYRK2 (Fig. 15*A*), which is the closest homologue of DYRK4 in *D. melanogaster* and has been characterized as a catalytically active protein kinase (Lochhead et al. 2003).

GFP-tagged DYRK1A, hDYRK4^{520} or hDYRK4^{NLGY} was immunoprecipitated from transiently transfected HeLa cells. Protein kinases were eluted from immuno-complexes and analyzed by immunoblotting. GFP-hDYRK4^{NLGY} showed no significant difference in tyrosine phosphorylation as detected by a phosphotyrosine-specific antibody or autophosphorylation as detected by autoradiography (Fig. 15*B*). Furthermore, GFP-hDYRK4^{NLGY} migrates as a doublet in SDS gels similar to wild-type GFP-hDYRK4^{520}, indicating that recognition by cellular kinases is not affected by this mutation (Fig. 15*B*). These results suggest that the insertion of the NxGY motif does not interfere with autophosphorylation on tyrosines.

Next, we wanted to determine if the insertion mutant GFP-hDYRK4^{NLGY} is an active serine/threonine kinase and if substrate specificity was altered due to this insertion compared to wild-type GFP-hDYRK4^{520}. Activity was measured in IVK assays with a panel of peptides as substrates as described in 4.1.4.1. The DYRK4^{NLGY} mutant exhibited a largely similar pattern of activity towards the different peptides as wild-type DYRK4 (Fig. 16*A* and *B*). We noticed however that for each peptide the activity of the DYRK4^{NLGY} mutant was between that of wild-type DYRK4 and DYRK1A, suggesting that the insertion of the NLGY motif might shift the target recognition of DYRK4 towards that of DYRK1A. This result may suggest that the absence of the NxGY motif may contribute to the different substrate specificities of DYRK1A and DYRK4. Nevertheless, these experiments revealed no significant differences between wild-type DYRK4 and the insertion mutant DYRK4^{NLGY}.

A

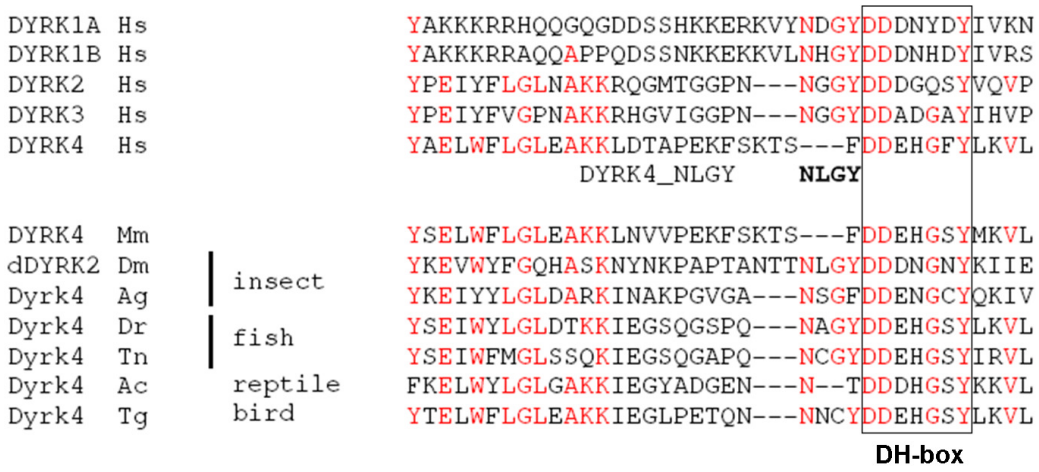

B

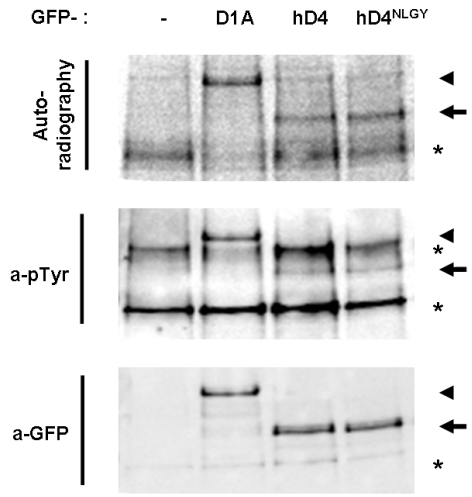

Figure 15: Effect of the NxGY motif on autophosphorylation of DYRK4.
A. Conservation of the NxGY motif located directly N-terminal of the DH-box. Amino acids conserved in the majority of the sequences are marked in red and the integration site of the NxGY motif in human DYRK4^{520} is marked in bold. The DH-box is highlighted by a rectangle. Ac, *Anolis carolinensis* (NM_003845_anoCar1 521 scaffold_55:1366920-1394815+); Ag, *Anopheles gambiae* (XP_317650); Dm, *Drosophila melanogaster* (NP_523564); Dr, *Danio rerio* (XP_693389); Hs, *Homo sapiens* (DYRK1A: AAB18639; DYRK1B: NP_004705; DYRK2: NP_006473; DYRK3: AAG17028; DYRK4: NP_003836); Mm, *Mus musculus* (NP_997093); Tg, *Taeniopygia guttata* (XP_002190423); Tn, *Tetraodon nigroviridis* (CAF98877). **B.** NLGY insertion does not affect autophosphorylation or tyrosine phosphorylation of DYRK4. Extracts of HeLa cells overexpressing GFP-DYRK1A, GFP-hDYRK4^{520}, GFP-hDYRK4^{NLGY} or unfused GFP (-) were immunoprecipitated with an anti-GFP antibody, and analyzed by Western blotting with anti-GFP and anti-phosphotyrosine antibodies as indicated. Autophosphorylation was assessed by autoradiography of nitrocellulose membrane. The arrowhead marks DYRK1A and the arrow the two DYRK4 variants. Asterisks mark unspecific bands.

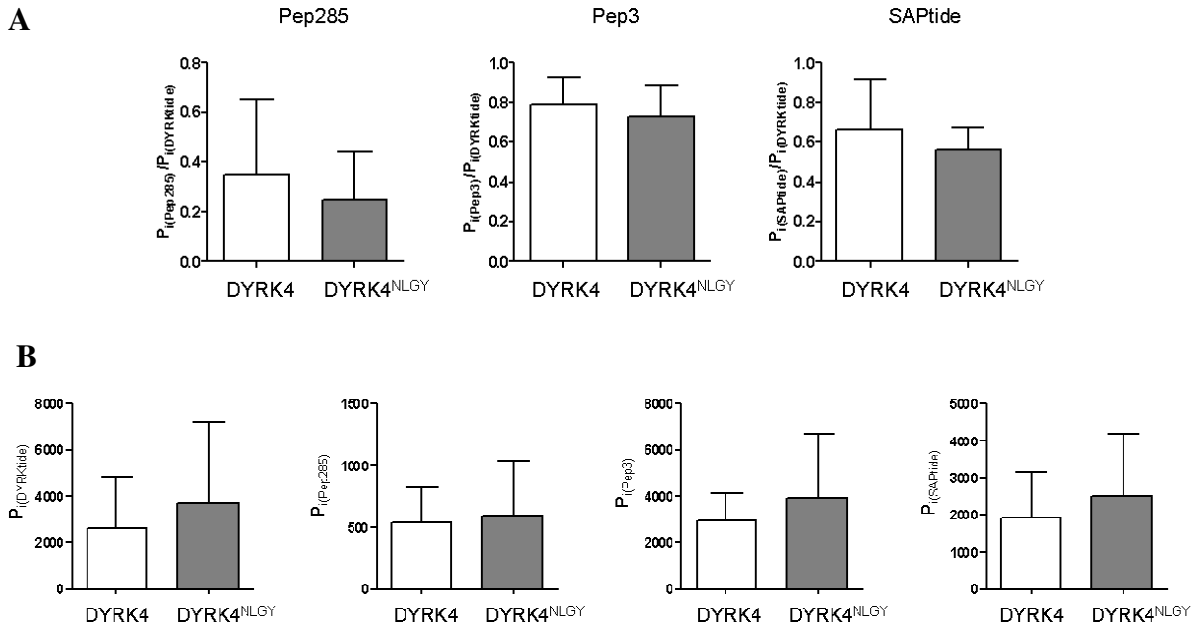

Figure 16: Effect of the NxGY motif on DYRK4 catalytic activity and substrate specificity.
A. GFP-hDYRK4^{520} and GFP-hDYRK4^{NLGY} were immunoprecipitated from extracts of transiently transfected HeLa cells and subjected to an IVK assay with the indicated substrate peptides (Pep285, Pep3, SAPtide and DYRKtide, each at 100 µM). Incorporation of ^{33}P into the indicated peptides was normalized to the phosphate incorporation into DYRKtide. **B.** The diagrams show the results of the experiment illustrated in *A* without normalization. Background signal obtained in parallel samples from GFP-transfected HeLa cells was subtracted. Columns represent the amount of ^{33}P incorporated into the peptides (means ± SD of 3-4 independent experiments).

Finally, to analyze if the DYRK4^{NLGY} mutant can recognize and phosphorylate a substrate protein in living cells, both GFP-tagged proteins were co-expressed with GFP-SF3B1 Δ256-382 in HeLa cells. Both wild-type DYRK4 and the DYRK4^{NLGY} mutant phosphorylated SF3B1 on Thr434 with similar phosphorylation levels (Fig. 17). Consistent with the results shown in Fig. 13, SF3B1 has been confirmed as a substrate for DYRK4.

In summary, insertion of the highly conserved NxGY motif preceding the DH-box into wild-type DYRK4 altered neither tyrosine autophosphorylation nor catalytically activity nor substrate specificity of DYRK4.

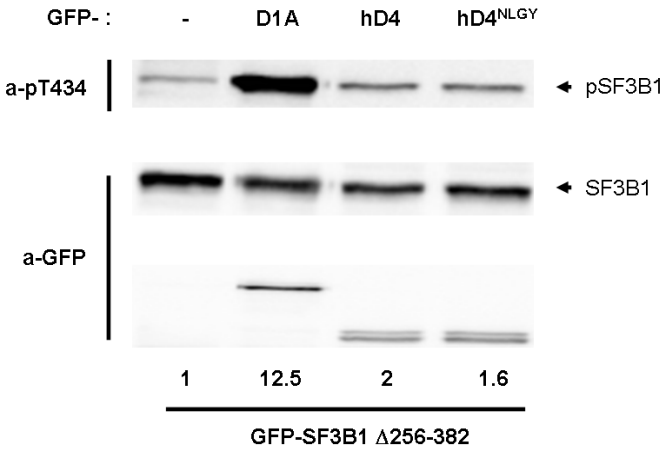

Figure 17: Phosphorylation of SF3B1 by DYRK4^{NLGY}.
Whole cell lysates of HeLa cells co-expressing GFP-DYRK1A, GFP-hDYRK4^{520} or the GFP-hDYRK4^{NLGY} mutant with GFP-SF3B1 Δ256-382 were analyzed by immunoblotting. Phosphorylation of SF3B1 was detected using a phosphorylation site-specific antibody (pT434 in SF3B1). Band intensity of phosphorylated SF3B1 (pSF3B1) was normalized to intensity of total SF3B1 and is indicated below the respective lanes. Ratio of pSF3B1/SF3B1 determined for co-transfection of GFP-SF3B1 Δ256-382 with mock vector (-) was arbitrarily set to 1.

4.2 Posttranslational modifications of DYRK1A during the cell cycle

4.2.1 Harmine inhibits DYRK1A in cell culture

4.2.1.1 Harmine inhibits the phosphorylation of SF3B1

The ß-carboline alkaloid harmine has been found to inhibit DYRK1A *in vitro* (Bain et al. 2007). In this kinase selectivity screen DYRK1A together with two other kinases, among 69 kinases tested, was inhibited by harmine.

Originally harmine has been isolated from *Banisteriopsis caapi*, a South American vine, and has been previously described as a potent inhibitor of monoamine oxidase (MAO) (Kim et al. 1997). To determine if harmine can be used to inhibit DYRK1A in cells, the effect of harmine on a known substrate of DYRK1A, SF3B1, was tested.

SF3B1 is a subunit of the U2 snRNP-associated complex SF3B and was shown to be phosphorylated by DYRK1A on Thr434 (de Graaf et al. 2006). To examine the inhibitory effect of harmine on DYRK1A activity, the stable HEK_GFP-DYRK1A cells were transiently transfected with GFP-SF3B1-NT. This stable cell line overexpresses GFP-tagged wild-type DYRK1A under the control of a

doxycycline-regulatable promoter (Sitz et al. 2008). For comparison, DMAT, a cell-permeable brominated benzimidazolo compound and a well known ATP-competitive inhibitor of Casein Kinase-2 (CK2), that has been reported to be a potent inhibitor of DYRK1A *in vitro* (Pagano et al. 2008), was used. Inhibitors were added 2 h after transfection and 15 min later GFP-DYRK1A expression was induced with doxycycline (2 µg/ml; +dox). As expected, expression of GFP-DYRK1A significantly enhanced the phosphorylation of exogenous GFP-SF3B1-NT and endogenous SF3B1 (Fig. 18, lane 1+5). In contrast, harmine reduced the phosphorylation on Thr434 of GFP-SF3B1-NT in the non-induced HEK_GFP-DYRK1A cells (Fig. 18 lane 1+3+5), but failed to decrease the level of phospho-Thr434 in DYRK1A overexpressing cells (Fig. 18, lane 5+7+8). However, the strong phosphorylation signal of endogenous SF3B1 induced by overexpression of DYRK1A was reduced at a concentration of 5 µM harmine. Treatment with DMAT (5 µM) failed to reduce the level of phospho-Thr434 in overexpressed GFP-SF3B1-NT (Fig. 18, lane 1+2, 5+6), but showed a slight effect on endogenous SF3B1-phosphorylation on Thr434 (lane 5+6).

These results indicate that harmine can be used to inhibit DYRK1A in cultured cells and contributed to the publication of Göckler *et al.* (2009) where harmine has been shown to be a specific inhibitor of DYRK1A.

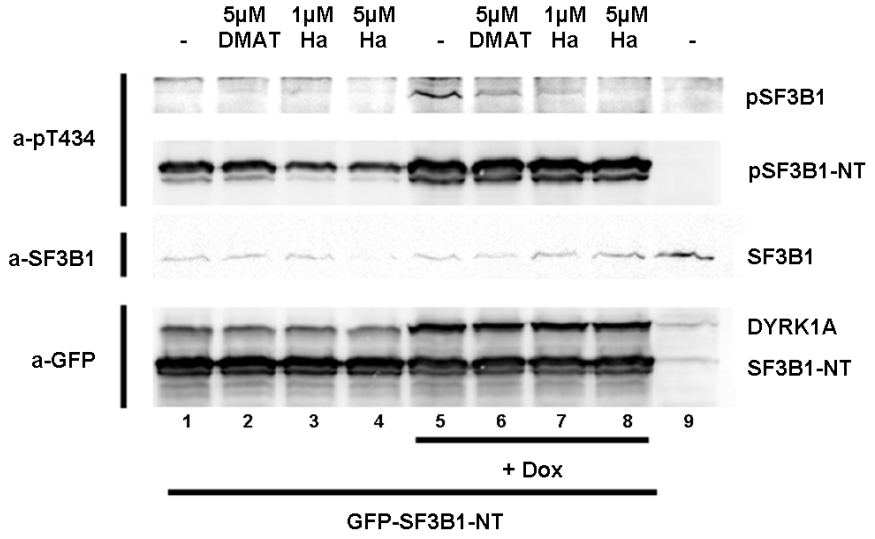

Figure 18: Effect of harmine on phosphorylation of SF3B1 by DYRK1A *in vivo*.
HEK_GFP-DYRK1A cells were transiently transfected with GFP-SF3B1-NT and 2 h post-transfection indicated inhibitors were added as indicated. After 15 min, GFP-DYRK1A expression was induced with doxycycline (2 µg/ml, +Dox) or not. Phosphorylation of GFP-SF3B1-NT and endogenous SF3B1 was determined by immunoblotting with phospho-specific anti-pThr434 antibody. Untransfected cells were used as background control.

4.2.1.2 Harmine inhibits the phosphorylation of Septin4

In a two-hybrid screen for DYRK1A-interacting proteins, Jan Sitz identified a cDNA for Septin4 as a positive clone (2003, Dissertation, LMU München). He has shown that Septin4, a member of the group III septin family of guanosine triphosphate hydrolases (GTPases), specifically interacted with DYRK1A. In collaboration with this group, we wanted to assess whether Septin4 was phosphorylated by DYRK1A in living cells.

When both proteins were co-expressed in cells, Septin4 exhibited a mobility shift in SDS gels. To verify that the mobility shift is due to phosphorylation by DYRK1A and to further characterize the inhibitory effect of harmine on DYRK1A in cell culture, stable HEK293_GFP-DYRK1A ´cells were transiently transfected with FLAG-Septin4. When GFP-DYRK1A expression was induced by doxycycline, FLAG-Septin4 was detected as a double band, where the relative amount of the faster migrating band (black arrowhead) was reduced in comparison to non-induced GFP-DYRK1A overexpression (Fig. 19*A*, lane1+5). Harmine prevented the DYRK1A-dependent mobility shift of FLAG-Septin4 and recovered the intensity of the faster migrating band (Fig. 19*A*, lane 3+4). In contrast, DMAT failed to exhibit an effect on the double band of FLAG-Septin4 (lane 2), suggesting that harmine is a more potent inhibitor of DYRK1A than DMAT. This effect of harmine verified that Septin4 is a substrate of DYRK1A and has been published in a collaborative paper of our groups (Sitz et al. 2008).

Taken together, these results demonstrate that harmine is highly cell-permeant and that it can be used as a specific and potent inhibitor of DYRK1A *in vivo* to verify phosphorylation of presumed DYRK1A substrates.

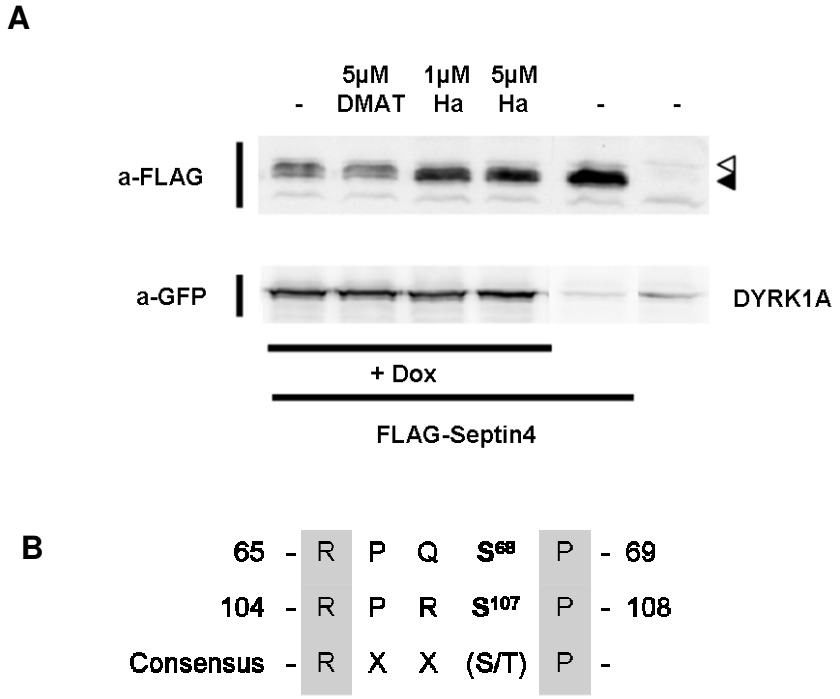

Figure 19: Phosphorylation of Septin4 by DYRK1A.
A. HEK_GFP-DYRK1A cells were transiently transfected with FLAG-Septin4, 2 h post-transfection indicated inhibitors were added and GFP-DYRK1A expression was induced with doxycycline (2 µg/ml, +Dox) additional 15 min later or left untreated and/or non-induced. Effect of harmine on mobility shift due to DYRK1A-dependent phosphorylation of FLAG-Septin4 was analyzed by immunoblotting with anti-FLAG and anti-GFP antibodies. White arrowhead marks the hyperphosphorylated and black arrowhead the hypophosphorylated or unphosphorylated variant of FLAG-Septin4. Untransfected cells were used as background control. **B.** Sequence and position of the presumed DYRK1A phosphorylation site of Septin4, compared to the consensus sequence for DYRK1A substrates. The putative phosphorylated Ser residues are marked in bold.

4.2.2 Phosphorylation of DYRK1A on Serine 748

4.2.2.1 Endogenous DYRK1A is not fully autophosphorylated in cells

To investigate if DYRK1A is completely phosphorylated on its serine, threonine and tyrosine residues in living cells or if DYRK1A is able to autophosphorylate on so far unphosphorylated sites *in vitro*, endogenous DYRK1A from HeLa and PC12 cells was immunoprecipitated. The DYRK1A-specific antibody (anti-D1A), which recognizes a C-terminal epitope of DYRK1A, was able to immunoprecipitate three variants of endogenous DYRK1A (Fig. 20*A*, lane1). Incubation of the immunoprecipitates with ATP revealed slower migrating variants of DYRK1A compared with immunoprecipitates incubated under the same conditions without ATP

(Fig. 20*A* and *B*, lane 1+2, indicated by arrowheads). This demonstrates that DYRK1A is able to incorporate phosphate residues and thereby to cause a mobility shift clearly detectable in SDS gels. These shifted bands show a diffuse pattern, suggesting a heterogeneous phosphorylation on multiple phosphorylation sites during the assay. The three bands of endogenous DYRK1A have also been found with a different C-terminal antibody against DYRK1A (Okui et al. 1999), but to date the origin of the three bands is still unknown. Under the phosphorylation conditions used in this assay, even the fastest-migrating band (Fig. 20*A* and *B*, black arrowhead), which represents either an N-terminal truncated product of DYRK1A (because the anti-D1A antibody recognizes a C-terminal epitope) or an isoform derived from an internal splicing event, is shifted in the gel, suggesting that indeed it is a catalytically active form.

To further examine whether inhibition of DYRK1A autophosphorylation during expression leads to an altered pattern in SDS gels, HeLa cells were treated with two different concentrations of harmine. Harmine treatment did not alter the electrophoretic mobility of DYRK1A (Fig. 20*A*, lane 1+3+5). This suggests that the three variants of DYRK1A are not derived from harmine-inhibitable autophosphorylation events of DYRK1A, but could be due to alternative splicing or phosphorylation by harmine-independent events. Moreover, DYRK1A expressed in the presence of harmine was able to incorporate phosphate residues when incubated with ATP, causing the same band shift detectable in SDS gels like DYRK1A expressed in non-treated cells (Fig. 20*A*, lane 2+4+5 and Fig. 13*B*, lane 2+4). This is consistent with the result that harmine is not an irreversible inhibitor of DYRK1A.

The observation that inhibition of DYRK1A activity does not affect the pattern of bands in SDS gels shows that the autophosphorylation which causes the mobility shift after *in vitro* phosphorylation must either be prevented by unknown mechanisms or counteracted by phosphatases in living cells.

4.2.2.2 Autophosphorylation of exogenous DYRK1A is inducible by Calyculin A

Similar results as for endogenous DYRK1A were obtained with overexpressed DYRK1A fused to GFP (Fig. 21*A*). GFP-DYRK1A was shifted after incubation with ATP (Fig. 21*A*, lane 1+2). Neither treatment with harmine during expression nor presence of harmine in a high concentration (4 µM) during the kinase assay interfered with the autophosphorylation *in vitro* and the resulting mobility shift of

DYRK1A (Fig. 21*A*, lane 2+3 and 5+6). These two approaches, applying harmine during expression or during the assay, strongly support that a) the mature DYRK1A kinase, expressed in the presence of harmine, maintains its ability to autophosphorylate and b) the autophosphorylation on further residues is not inhibited by harmine under the conditions of the *in vitro* assay (*see Discussion 5.2.2*).

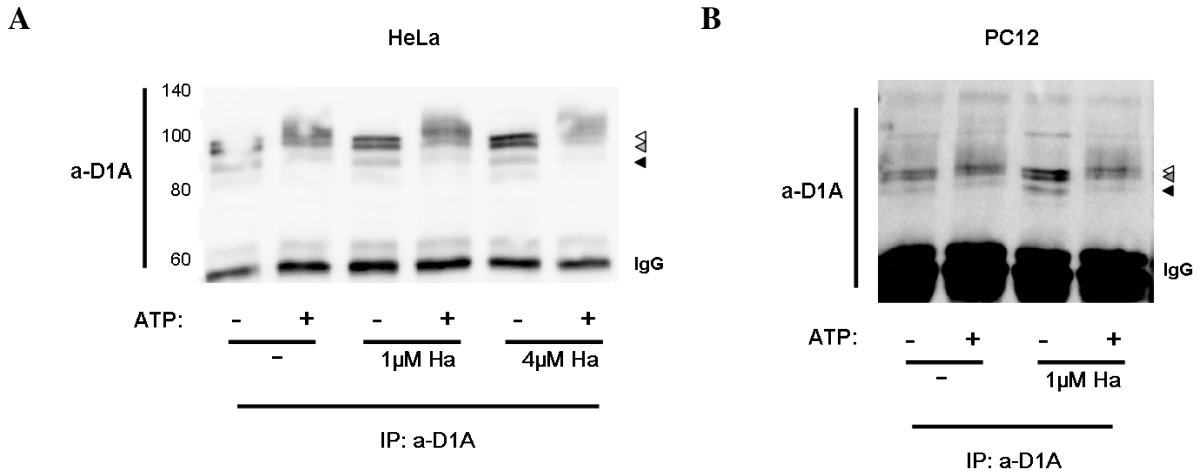

Figure 20: Endogenous DYRK1A is further autophosphorylated *in vitro*.
HeLa cells (**A**) or PC12_GFP-DYRK1A cells induced with doxycycline (2 µg/ml) (**B**) were treated with indicated concentrations of harmine for 2 d or left untreated, lysed and DYRK1A was immunoprecipitated (IP) with anti-DYRK1A antibody. Harmine was washed out and immuno-complexes were split and subjected to a phosphorylation assay in the presence of ATP (+) or mock incubation without ATP (-) (see *Material and Methods*). Proteins were eluted from immuno-complexes by boiling and analyzed by immunoblotting with indicated antibodies. Arrowheads indicate the three variants of endogenous DYRK1A.

Another approach to determine whether the phosphorylation sites within DYRK1A are permanently saturated or are targets of cellular phosphatases, and therefore can be modulated, is the use of Calyculin A, an inhibitor of phosphoprotein phosphatase 1A and 2A (PP1A and PP2A). HeLa cells overexpressing GFP-tagged DYRK1A were treated with Calyculin A for 1 h or left untreated and whole cell lysates were analyzed. GFP-DYRK1A from Calyculin A-treated cells showed a lower electrophoretic mobility compared to GFP-DYRK1A from untreated cells (Fig. 21*B*). This mobility shift is most likely caused by prevention of dephosphorylation of DYRK1A. In parallel, HeLa cells were transfected with the kinase mutants GFP-DYRK1A K188R and GFP-DYRK1A Y321F (*see Introduction 1.2.3*). The K188R mutant failed to exhibit a mobility shift due to Calyculin A treatment (Fig. 21*B*), showing that the hyperphosphorylation of the DYRK1A protein is an autophosphorylation event and is not mediated by an upstream kinase. In contrast,

the Y321F mutant showed a slight mobility shift, thereby suggesting this mutant retains a low activity, what has been previously described (Himpel et al. 2001).

The results indicate that DYRK1A is not fully autophosphorylated in living cells due to activity of phosphatases and/or interaction with other cellular proteins that inhibit autophosphorylation.

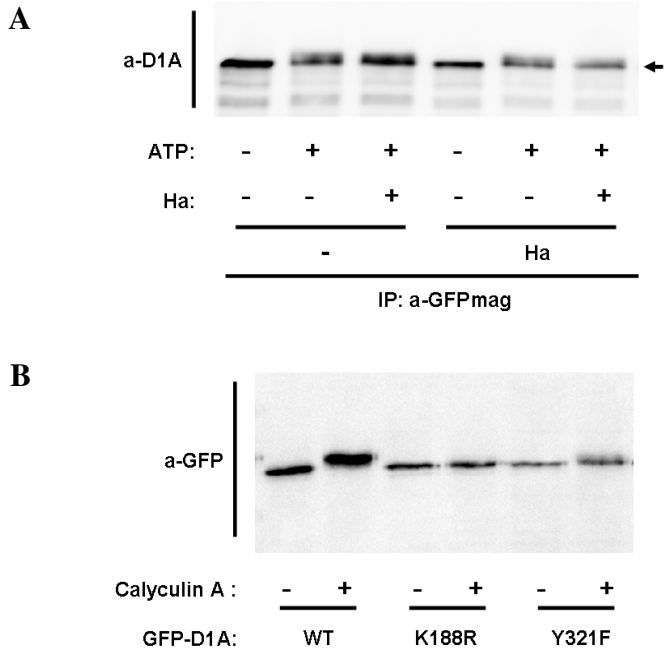

Figure 21: GFP-DYRK1A autophosphorylates *in vitro* and is targeted by phosphatases *in vivo*.
A. HEK_GFP-DYRK1A cells induced with doxycycline (2 µg/ml) were treated with 4 µM harmine for 2 d or left untreated, lysed and immunoprecipitated with a-GFPmag (GFP-Trap coupled to magnetic particles). Harmine was washed out or was present during the assay as indicated. Immunoprecipitates were split and subjected to a phosphorylation assay in the presence of ATP (+) or not (-) (see *Material and Methods*). Immunoprecipitated proteins were analyzed in Western blot. GFP-DYRK1A is marked by a black arrow. **B**. HeLa cells overexpressing wild-type GFP-DYRK1A (WT) or kinase inactive mutants (K188R, Y321F) were treated with 100 nM Calyculin A for 1 h or left untreated. Whole cell lysates were analyzed in Western blot.

4.2.2.3 Generation of a phospho-specific anti-pSer748 antibody

The result that DYRK1A is not fully phosphorylated on its serine, threonine or tyrosine residues and an upregulation of Ser748 phosphorylation in mitotic cells was found by Daub et al. (2008) (*see Introduction 1.3*), suggest that Ser748 phosphorylation levels are regulated .

To characterize the phosphorylation level of Ser748 in asynchronous cells and during the cell cycle, an antibody recognizing the phosphorylated state of this residue

(pSer748) was generated. Further, a GFP-tagged version of DYRK1A in which the Ser748 is mutated to alanine (GFP-D1A S748A) was generated. Two methods were used to test the specificity of the antibody. First we examined the reactivity of overexpressed wild-type GFP-DYRK1A (WT) and GFP-DYRK1A S748A by immunoblotting of whole cell lysates. The anti-pS748 antibody recognized GFP-DYRK1A WT, but not the point mutation version (Fig. 22*A*). Second, GFP-DYRK1A WT was partially purified by IMAC (immobilized-metal affinity chromatography) and incubated with phosphatase. The phospho-specific antibody failed to recognize wild-type GFP-DYRK1A (Fig. 22*B*) after dephosphorylation, demonstrating that the phosphorylation state of the protein is required for detection with this antibody.

Summarized, the generated antibody is specific to detect the phosphorylation on Ser748 and can be used as a valuable tool to examine the phosphorylation state of Ser748.

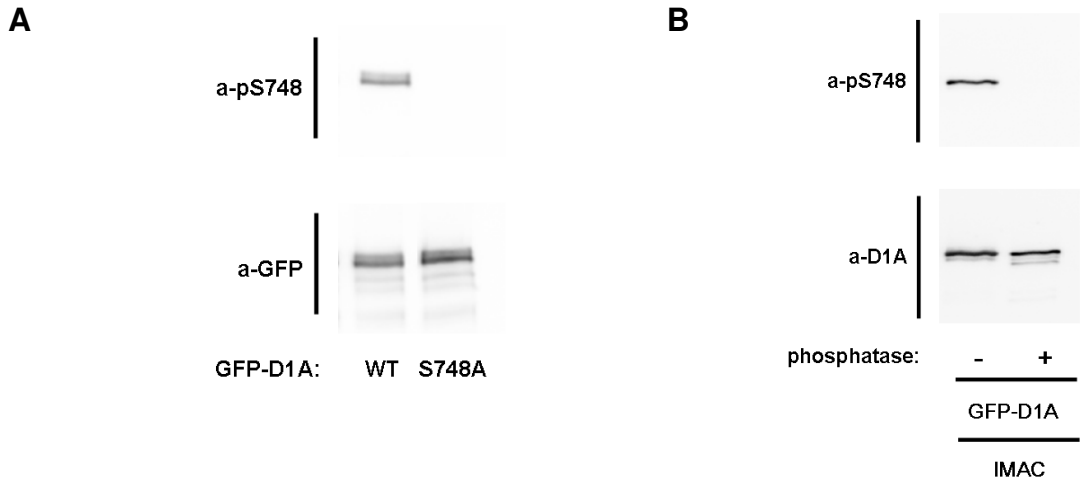

Figure 22: Specificity of the phospho-specific anti-pS748 antibody.
A. Whole cell extracts from HeLa cells overexpressing wild-type GFP-DYRK1A (WT) or GFP-DYRK1A S748A were analyzed in Western blot with anti-pS748 and anti-GFP antibodies. **B**. HEK_GFP-DYRK1A cells were induced with doxycycline (2 µg/ml) for 2 d and GFP-DYRK1A was partially purified by IMAC. Samples were then split and incubated in phosphatase buffer in the absence or presence of calf intestinal phosphatase (CIP). Then samples were analyzed in Western blot with anti-pS748 and anti-DYRK1A antibodies.

4.2.2.4 Phosphorylation on Ser748 is an autophosphorylation event

First, to determine whether DYRK1A autophosphorylates on Ser748, the phosphorylation state of wild-type DYRK1A and the kinase-dead mutant DYRK1A K188R fused to GST and expressed in bacteria was examined. Wild-type DYRK1A (WT) was phosphorylated on Ser748 (Fig. 23*A*). The kinase inactive mutant (KR) showed a very faint reactivity with the phospho-specific anti-pSer748 antibody, consistent with earlier reports that this mutant retains a very low activity (Himpel et al. 2001). Because *E. coli* lacks Ser/Thr phosphatase activity, even a very low degree of autophosphorylation is detectable. Since *E. coli* also lacks endogenous protein kinase, this result indicates that phosphorylation on Ser748 occurs independently of upstream kinases and requires DYRK1A activity.

Next, the ability of DYRK1A to autophosphorylate on Ser748 in living cells was examined. GFP-tagged DYRK1A expressed in HeLa cells was recognized by the phospho-specific anti-pSer748 antibody (Fig. 23*B*), whereas the catalytic inactive mutant (GFP-DYRK1A K188R) was not, what demonstrates that kinase activity of DYRK1A is essential for phosphorylation on Ser748 in mammalian cells. Notably, phosphorylation on Ser748 was not detectable in endogenous DYRK1A (Fig. 23*B*, arrowheads).

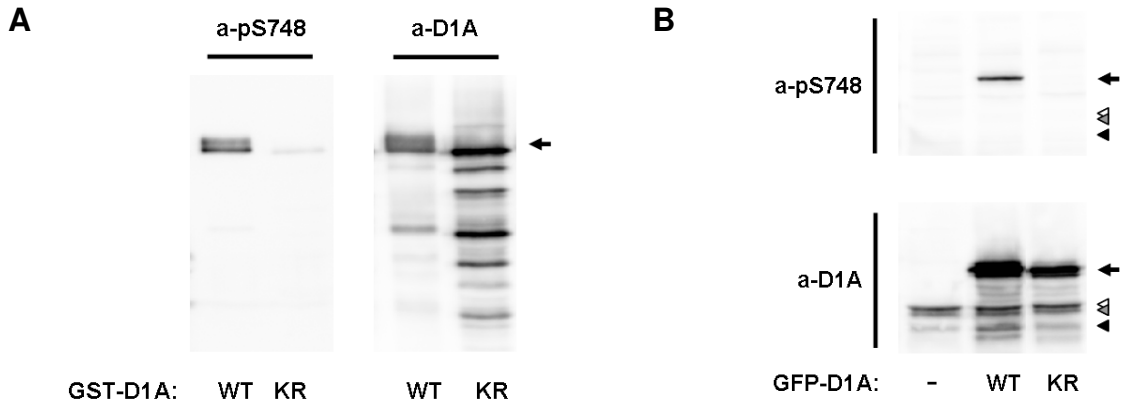

Figure 23: DYRK1A expressed in bacteria and in cells autophosphorylates on Ser748. **A**. Wild-type GST-DYRK1A (WT) or kinase-inactive GST-DYRK1A KR were expressed in *E. coli* and analyzed by immunoblotting with indicated antibodies. Full-length protein is marked by an arrow. **B**. HeLa cells were transiently transfected with wild-type GFP-DYRK1A (WT) or the kinase-inactive mutant GFP-DYRK1A KR and whole cell lysates were analyzed by immunoblotting with indicated antibodies. Recombinant GFP-DYRK1A WT and mutant are marked by an arrow and the three variants of endogenous DYRK1A by arrowheads.

The results in bacteria and mammalian cells indicate that DYRK1A Ser748 phosphorylation is mediated by DYRK1A itself and not by upstream kinases and thus is an autophosphorylation event.

4.2.2.5 DYRK1A autophosphorylation on Ser748 is inhibited by harmine

Recombinant GFP-tagged DYRK1A is autophosphorylated on Ser748, but Ser748 phosphorylation of endogenous DYRK1A could not be detected in whole cell lysates. Therefore endogenous DYRK1A was partially purified from HeLa cells by IMAC. This method is used for purification of histidine-tagged proteins. DYRK1A contains an endogenous histidine repeat (His_{13}-sequence) in the C-terminal region and thus can be partially purified from cell lysates by IMAC.

Endogenous DYRK1A partially purified by IMAC from HeLa or PC12 cells was detected by the phospho-specific anti-pSer748 antibody (Fig. 24*A* and *B*, arrowheads). Treatment of the cells with harmine, an inhibitor of DYRK1A, reduced the detection by the phospho-specific anti-pSer748 antibody compared to the signal of endogenous DYRK1A isolated from non-treated cells (Fig. 24*A* and *B*, arrowheads), suggesting that Ser748 phosphorylation of endogenous DYRK1A is an autophosphorylation event that can be inhibited by harmine.

Next, to elucidate whether phosphorylation of Ser748 interferes with the precipitation method and whether IMAC biased for either the phosphorylated or the non-phosphorylated DYRK1A protein, HeLa cells overexpressing GFP-tagged DYRK1A were lysed and subjected to IMAC. Thereby endogenous and recombinant DYRK1A were partially purified simultaneously from the same cell lysate. This direct comparison showed that endogenous DYRK1A is isolated as efficiently as recombinant GFP-tagged DYRK1A, and that both proteins showed phosphorylation on Ser748 (Fig. 24*A*). In addition, the efficiency of partial purification of DYRK1A by IMAC is not affected by the phosphorylation state of Ser748 (Fig. 24*A*, +/- harmine) and this method can be used as a tool to compare phosphorylation levels of DYRK1A under different conditions.

These results showed that the autophosphorylation on Ser748 in living cells can be inhibited by harmine and most importantly they confirmed the third *in vivo* phosphorylation site in endogenous DYRK1A, in addition to the previously described Tyr321 and Ser529 (Himpel et al. 2001; Alvarez et al. 2007).

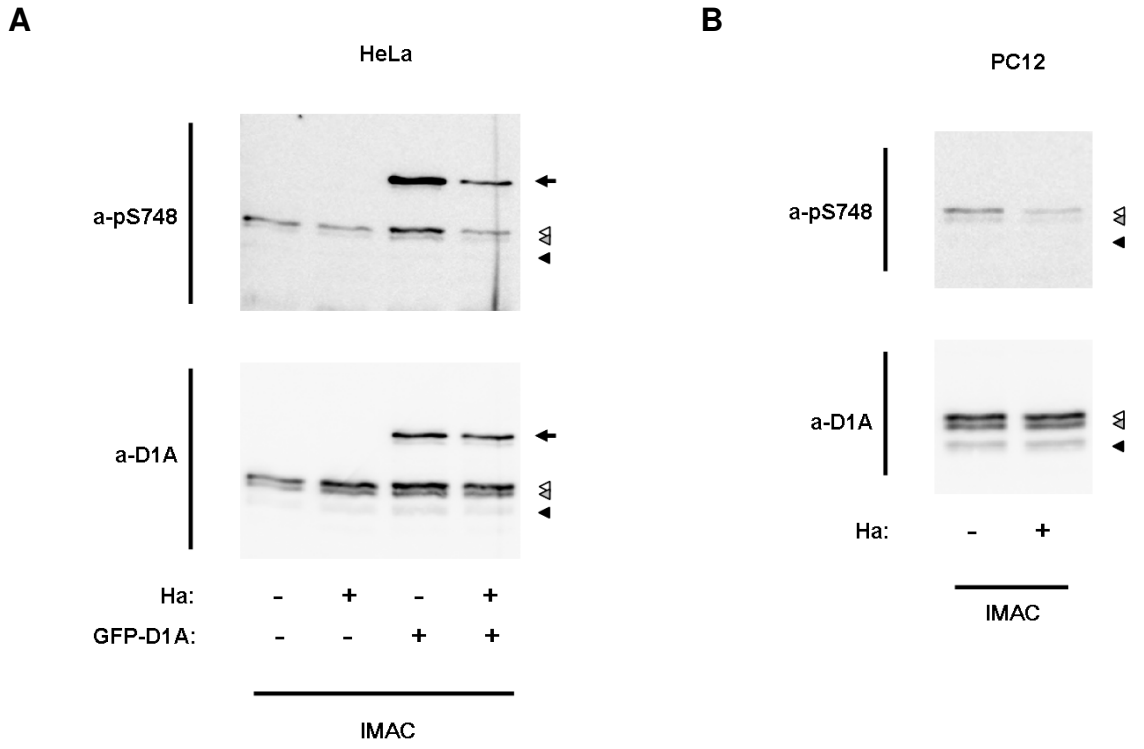

Figure 24: Endogenous DYRK1A is autophosphorylated on Ser748 in living cells.
A. HeLa cells were transiently transfected with GFP-DYRK1A or left untransfected and treated for 1 d with 1 µM harmine (Ha) as indicated. Endogenous DYRK1A and recombinant GFP-DYRK1A were partially purified by IMAC. Samples were analyzed by immunoblotting with anti-pS748 and anti-DYRK1A antibodies. **B.** PC12 cells were treated for 1 d with 1 µM harmine and endogenous DYRK1A was partially purified and subjected to Western blot analysis like in *A*. The arrow marks exogenous GFP-DYRK1A and arrowheads the three variants of endogenous DYRK1A.

4.2.2.6 DYRK1A autophosphorylates on Ser748 in vitro

To test if Ser748 is completely phosphorylated in living cells and if DYRK1A is able to autophosphorylate on Ser748 *in vitro*, the two membranes shown in Fig. 20*A* and Fig. 21*A* were also immunodetected with the phospho-specific anti-pSer748 antibody (anti-pSer748). Endogenous and recombinant DYRK1A purified and subjected to a phosphorylation assay in the presence of ATP showed a stronger signal with anti-pSer748 antibody (Fig. 25*A* and *B*), demonstrating that in untreated cells the phosphorylation on Ser748 is not saturated.

These results provide further evidence that phosphorylation on Ser748 is an autophosphorylation event. Furthermore, the phosphorylation on Ser748 of DYRK1A isolated from untreated cells is elevated when incubated with ATP (Fig. 25*B*, lane1+2+3), indicating that Ser748 is not fully autophosphorylated in living cells.

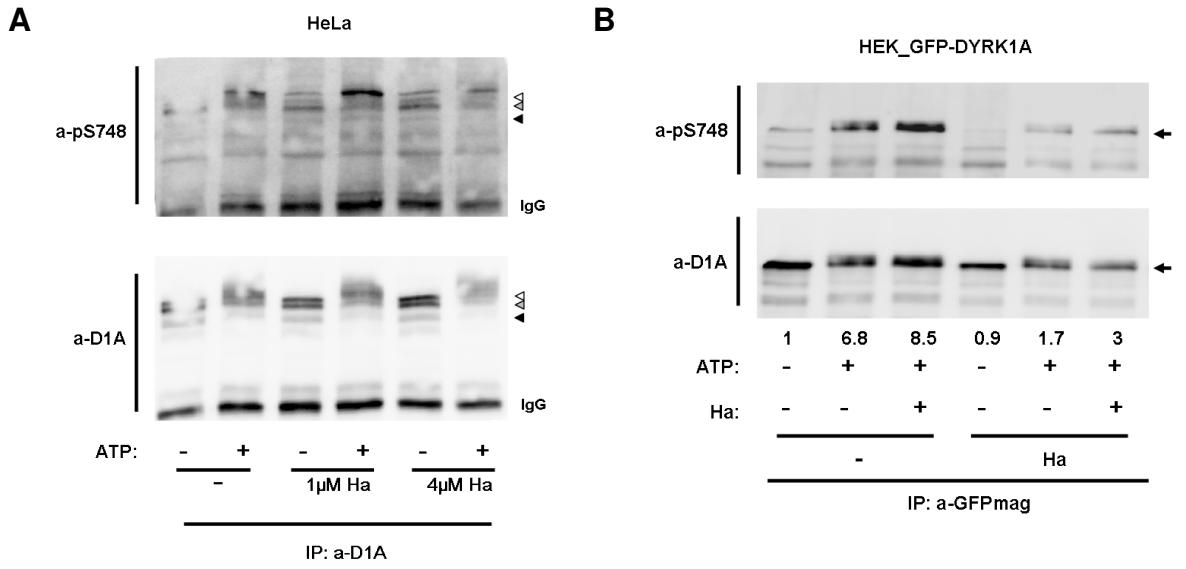

Figure 25: DYRK1A autophosphorylates on Ser748 *in vitro*.
A. HeLa cells were treated with indicated concentrations of harmine for 2 d or left untreated, lysed and DYRK1A was immunoprecipitated (IP) with anti-DYRK1A antibody. Harmine was washed out and immuno-complexes were split and subjected to a phosphorylation assay in the presence of ATP or mock incubation without ATP (see *Material and Methods*). Proteins were eluted from immuno-complexes by boiling and analyzed by immunoblotting with indicated antibodies. Arrowheads indicate the three variants of endogenous DYRK1A. **B**. HEK_GFP-DYRK1A cells induced with doxycycline (2 µg/ml) were treated with 4 µM harmine for two days or left untreated, lysed and immunoprecipitated with a-GFPmag (GFP-Trap coupled to magnetic particles). Harmine was washed out or was present during the assay as indicated. Immunoprecipitates were split and subjected to a phosphorylation assay in the presence of ATP (+) or not (-) (see *Material and Methods*). Immunoprecipitated proteins were analyzed in Western blot. GFP-DYRK1A is marked by a black arrow. The ratio of anti-pSer748 to anti-DYRK1A antibody signal is shown below the respective lanes and was determined using the AIDA software.

Next the question was addressed whether phosphorylation on Ser748 is an one-off reaction that is only catalyzed by a DYRK translational intermediate only present during maturation, as reported for the second tyrosine of the Tyr-X-Tyr motif in the activation loop (Lochhead et al., 2005; *see Introduction 1.2.3*). To prevent autophosphorylation, HeLa cells overexpressing wild-type GFP-DYRK1A were treated with harmine during translation. GFP-DYRK1A was isolated by immunoprecipitation and harmine was removed by washing. Then immuno-complexes were subjected to a phosphorylation assay in the presence or absence of

ATP. Ser748 phosphorylation of GFP-DYRK1A was not detectable in harmine treated cells, but incubation of GFP-DYRK1A, isolated from the same cells, in the presence of ATP during the assay, showed a clearly phosphorylation of Ser748 (Fig. 25*B*, lane 5). Furthermore, recombinant GFP-DYRK1A protein was able to rephosphorylate even when harmine was present in the assay (Fig. 25*B*, lane6), supporting the notion that harmine differentially affects autophosphorylation of Ser748 *in vivo* (in living cells) and *in vitro* (*see Discussion 5.2.2*).

This ability of the mature protein to rephosphorylate *in vitro* demonstrates that the phosphorylation on Ser748 is not an one-off event. In addition, the phosphorylation on Ser748 of DYRK1A isolated from untreated cells is elevated in the presence of ATP (Fig. 25*B*, lane1+2+3), indicating that Ser748 is not fully phosphorylated in asynchronous cells.

4.2.2.7 Calyculin A does not elevate DYRK1A phosphorylation on Ser748

Calyculin A elevates autophosphorylation of DYRK1A (Fig. 21*B*) and DYRK1A is not fully phosphorylated on Ser748 when isolated from cells. Therefore we tested if Calyculin A treatment leads to enhanced level of Ser748 phosphorylation.

HeLa cells overexpressing wild-type GFP-DYRK1A (WT), the mutants with impaired kinase activity (K188R, Y321F) or the point mutant GFP-DYRK1A S748A were treated with Calyculin A. As shown above, treatment with Calyculin A caused a mobility shift of wild-type GFP-DYRK1A due to inhibition of protein phosphatases (Fig. 21*B* and Fig. 26). As expected, the phospho-specific anti-pSer748 antibody failed to recognize the kinase inactive mutant K188R of DYRK1A in cells treated with Calyculin A, supporting once more that Ser748 phosphorylation occurs due to autophosphorylation and is not mediated by upstream kinases. The kinase deficient mutant Y321F is weakly phosphorylated on Ser748, consistent with the reported low activity of this DYRK1A variant. Finally, the point mutant S748A exhibited the same pattern as the wild-type GFP-DYRK1A protein, indicating that the mobility shift is not caused only by enhanced phosphorylation level on this residue. Furthermore, the quantification of several independent experiments (n= 5) revealed that the phosphorylation level of Ser748 is not upregulated by Calyculin A (ratio of phospho-specific pSer748 antibody to total amount of protein anti-GFP in Calyculin A-treated and untreated cells; 1.092 ± 0.1446).

Taken together, exposure of cells to Calyculin A induces a mobility shift of catalytically active DYRK1A, but had no effect on phosphorylation level on Ser748. This suggests that exogenous GFP-tagged DYRK1A either a) is a target of phosphatases other than PP1A or PP2A or b) interacts with yet unknown cellular proteins that regulate the phosphorylation level of Ser748.

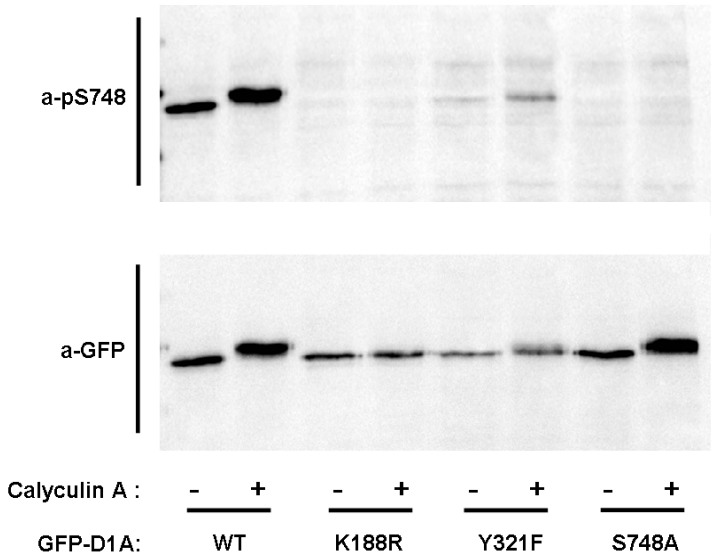

Figure 26: Effect of Calyculin A on DYRK1A Ser748 phosphorylation.
HeLa cells transiently transfected with wild-type GFP-DYRK1A (WT), the kinase deficient mutants (K188R, Y321F) or the point mutant S748A were treated with 100 nM Calyculin A for 1 h before lysis and whole cell extracts were analyzed by immunoblotting with anti-pSer748 antibody. Total amount of protein was verified using anti-GFP antibody. Whole cell extracts from cells overexpressing GFP-DYRK1A WT and the kinase deficient mutants (K188R, Y321F) were used also in the experiment shown in Fig. 21*B*.

4.2.2.8 Ser748 autophosphorylation occurs via an intermolecular mechanism

A closer look on the sequence of DYRK1A around Ser748 reveals the presence of a proline in the P+1 position and an arginine at P-3 and therefore this sequence matches perfectly the consensus target sequence (RXXp(S/T)P) for DYRK1A substrates (Fig. 27*A*) defined based on intermolecular phosphorylation of peptides (Himpel et al. 2000).

To test whether the autophosphorylation on Ser748 is an intermolecular event, wild-type GFP-DYRK1A (WT) and the kinase inactive HA-tagged DYRK1A KR were co-expressed in HeLa cells. Due to the tags the proteins have different molecular masses and can be easily distinguished on SDS gels. As shown above, the kinase inactive mutant (HA-DYRK1A KR) is not phosphorylated on Ser748 when expressed alone in HeLa cells (Fig. 27*B*, lane2). When co-expressed with active wild-type GFP-DYRK1A, the kinase inactive mutant is detected by the phospho-specific anti-pS748 antibody (Fig. 27*B*, lane3). Activity of endogenous DYRK1A was apparently to low to generate detectable levels of intermolecular phosphorylation when HA-DYRK1A KR was expressed alone.

This result demonstrates that phosphorylation of Ser748 can be an intermolecular (*trans*) autophosphorylation event, where the C-terminal tail harbouring Ser748 is recognized by the catalytic domain as a substrate, but phosphorylation in *cis* can not be excluded (*see Discussion 5.2.3*).

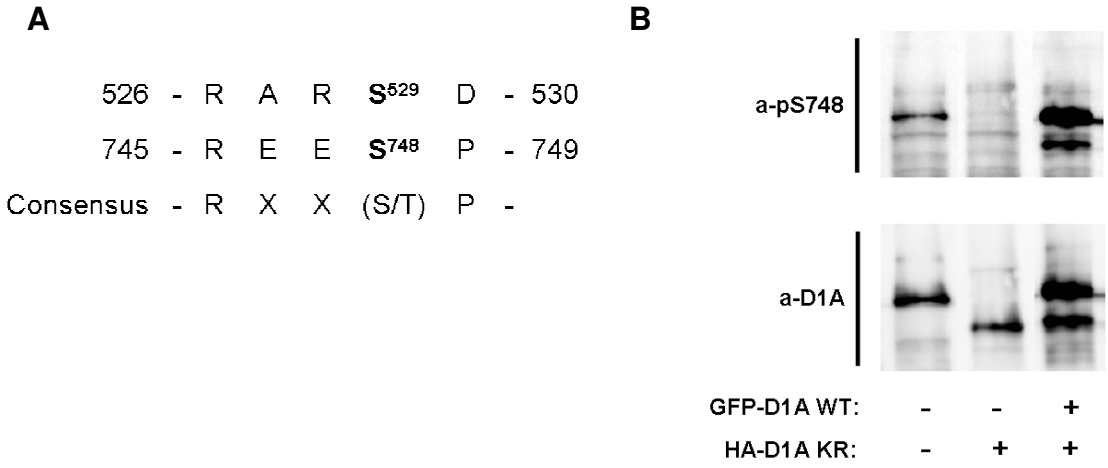

Figure 27: DYRK1A autophosphorylates on Ser748 via an intermolecular mechanism.
A. Alignment of the sequence surrounding Ser748 is compared to the known Ser529 autophosphorylation site of DYRK1A (Alvarez et al. 2007) and the consensus sequence for DYRK1A substrates. The phosphorylated Ser residues are marked in bold. **B.** HeLa cells were transiently transfected with wild-type GFP-DYRK1A (WT), the kinase-inactive mutant HA-DYRK1A K188R (KR) or both as indicated. Whole cell extracts were analyzed by immunoblotting with indicated antibodies.

4.2.2.9 Ser748 phosphorylation alters DYRK1A activity

The phosphorylation of a kinase can modulate its activity e.g. by conformational changes or by altering its interaction with other proteins. A dynamic phosphorylation can thereby regulate the activity of a kinase. Up to date, it has been reported for DYRK1A that the autophosphorylation on Ser529 regulates the interaction with a protein which enhances DYRK1A activity (Alvarez et al. 2007) (*see Discussion 5.2.4*).

To analyze if phosphorylation on Ser748 alters DYRK1A activity, we generated a point mutant of GFP-DYRK1A by glutamic acid substitution of Ser748 (GFP-DYRK1A S748E). Furthermore, the residue Thr751 located close to the Ser748 (Fig. 28*C*) could, in principle, also be phosphorylated and thereby interfere with Ser748 phosphorylation. In addition, Ser758, which has been found to be upregulated in mitotic cells like Ser748 (Daub et al. 2008), could interfere with Ser748 phosphorylation or detection by anti-pS748 antibody. To exclude involvement of Thr751 and Ser758 phosphorylation the double mutants GFP-DYRK1A T751A/S758A (TA/SA), GFP-DYRK1A S748E/S758E (EE) and S748E/S758A (EA) have been also generated. The substitution of serine residues by glutamic acid generates a phosphorylation-mimetic mutant, and the substitution by alanine a phosphorylation-deficient one. Additionally, a C-terminal truncated mutant of DYRK1A lacking the last 19 amino acids was generated (GFP-DYRK1A ΔC19) (Fig. 28*C*). HeLa cells were transiently transfected with the GFP-DYRK1A constructs. GFP-tagged proteins were immunoprecipitated either using an agarose-coupled (Fig. 28*A*) or a magnetic-coupled anti-GFP antibody (Fig. 28*B*) and subjected to an *in vitro* kinase assay with DYRKtide as exogenous peptide substrate.

Substitution of Ser748 with alanine (S748A) and thereby prevention of its phosphorylation reduced the phosphorylation of DYRKtide in two independent experiments (Fig. 28*A*, P_i (norm)= 0.66; data not shown, P_i (norm)= 0.5). The phosphorylation-mimetic mutants, GFP-DYRK1A S748E/S758E (EE) and S748E/ S758A (EA), showed an increase of activity (Fig. 28*A* and *B*). The EA mutant phosphorylated DYRKtide stronger than the EE indicating that the phosphorylation of Ser758 is not the one mediating this increment. Even the GFP-DYRK1A T751A/S758A (TA/SA) mutant showed an increased activity in comparison with wild-type GFP-DYRK1A, suggesting that these residues could influence Ser748 phosphorylation when they are available for phosphorylation, and indicating that the increased activity of DYRK1A is mediated independently of these residues.

In contrast, deletion of the last 19 amino acids of DYRK1A (GFP-D1A ΔC19) resulted in an increase of activity (Fig. 28*A*, and two further independent experiments, data not shown), suggesting the involvement of an inhibitory protein (*see Discussion 5.2.4*)

Taken together, these results suggest that Ser748 phosphorylation leads to an increase of DYRK1A activity.

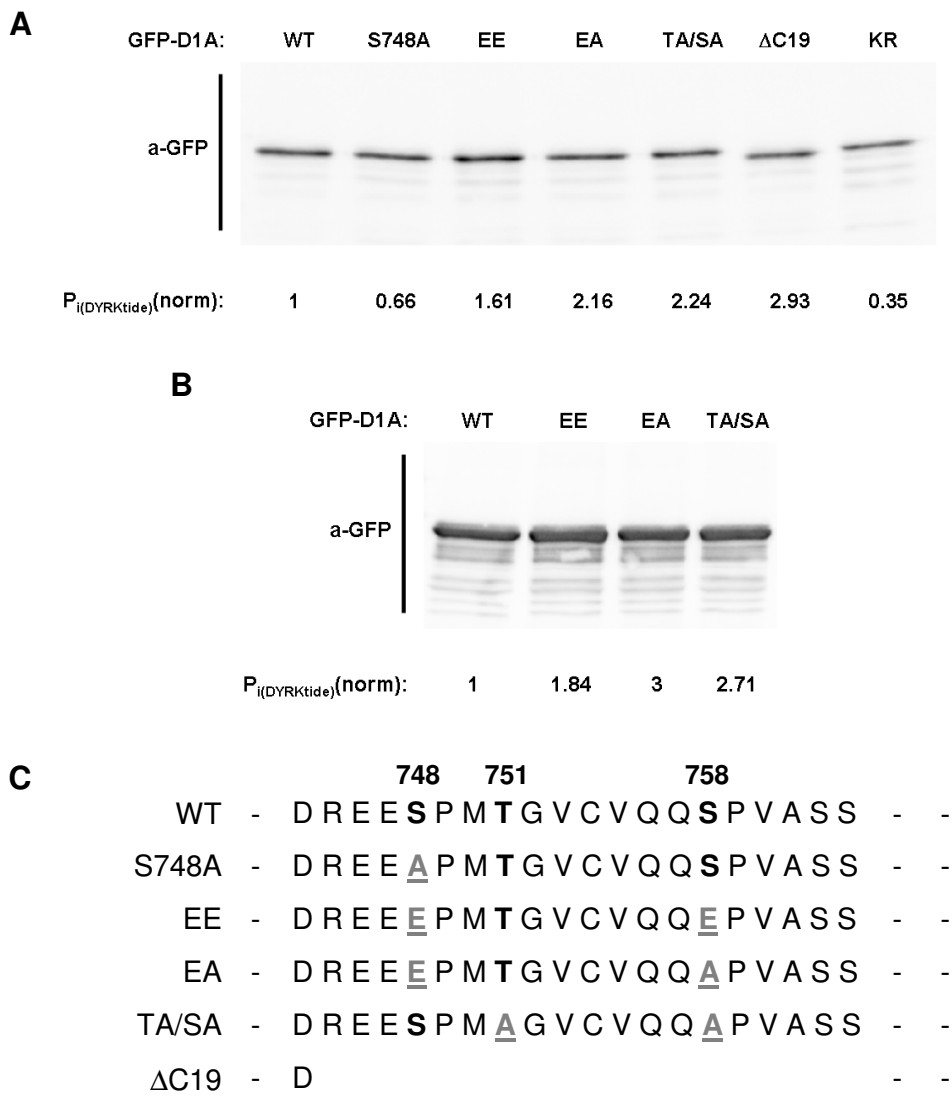

Figure 28: Influence of Ser748 phosphorylation on catalytic activity of DYRK1A. Extracts of HeLa cells transiently transfected with indicated wild-type GFP-DYRK1A or mutants were immunoprecipitated with GFP-mag (**A**) or anti-GFP antibody (**B**) and subjected to an IVK assay with DYRKtide. Subsequently, bound proteins were eluted and analyzed by immunoblotting with anti-GFP (**A, B**). Incorporation of labeled phosphate into DYRKtide normalized to densitometric evaluation of expression levels is indicated below the respective lanes. The phosphorylation of DYRKtide by wild-type GFP-DYRK1A (WT) was arbitrarily set as 1. **C**. The sequence of the last 20 amino acids of DYRK1A is shown. Residues considered as putative phosphosites are marked in bold and numbered. Mutated residues are marked in grey, bold and underlined.

4.2.2.10 Ser748 phosphorylation of DYRK1A in mitotic cells

As DYRK1A isolated from asynchronous cells is not fully phosphorylated, we tested if DYRK1A immunoprecipitated from mitotic cells is also able to further phosphorylate on its serine, threonine or tyrosine residues *in vitro*.

Therefore GFP-DYRK1A protein isolated from asynchronous HeLa cells and from cells synchronized with nocodazole, a specific inhibitor of microtubule formation that reversibly arrests cells at metaphase (Zieve et al. 1980; Hamilton and Snyder, 1982), was analyzed in an *in vitro* phosphorylation assay as described before (Fig. 29). GFP-DYRK1A expressed in the presence of harmine in asynchronous HeLa cells was used as a control. Surprisingly, DYRK1A from mitotic cells exhibited retarded bands on SDS gel similar to these of DYRK1A expressed in harmine treated cells when incubated in the presence of ATP (Fig. 29). At least two clear bands of GFP-DYRK1A were detectable by immunoblotting, when ATP was added to the phosphorylation assay. Unfortunately, in this particular experiment GFP-DYRK1A isolated from untreated asynchronous cells failed to show a mobility shift (in contrast to a series of experiments performed the same way; as in Fig. 25*B*).

Nevertheless, this experiment shows that DYRK1A is not completely phosphorylated on its serine, threonine or tyrosine residues in mitotic arrested cells.

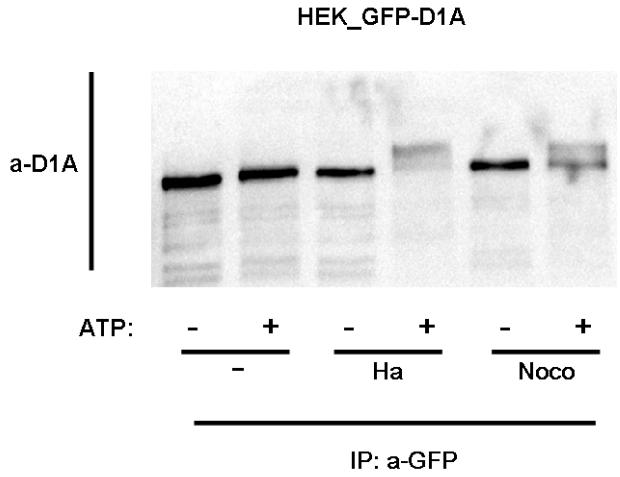

Figure 29: DYRK1A is not fully phosphorylated in mitotic cells.
HEK_GFP-DYRK1A cells induced with doxycycline (2 µg/ml) were treated with 4 µM harmine (Ha) for two days or with nocodazole (50 ng/ml; Noco) for 16 h or left untreated (-). GFP-DYRK1A was immunoprecipitated with anti-GFP antibody, split and subjected to a kinase assay in the presence of ATP (+) or not (-) (see *Material and Methods*). After the reaction, GFP-DYRK1A was eluted by boiling and analyzed in Western blot with the indicated antibody.

To analyze if phosphorylation on Ser748 is upregulated during mitosis we transfected HeLa cells with wild-type GFP- DYRK1A (WT) and treated the cells with nocodazole. GFP-DYRK1A WT showed no detectable increased phosphorylation level of Ser748 in mitotic cells (Fig. 30*A*, lane 2+3). To confirm the effect of nocodazole on the cell cycle, the same membrane was incubated with an anti-pThr434 antibody, which recognizes the phosphorylated Thr434 residue of SF3B1 (Fig. 30*A*, pSF3B1). Treatment with nocodazole increased the reactivity of the anti-pThr434 antibody with endogenous SF3B1, consistent with the reports that SF3B1 is hyperphosphorylated in mitotic cells (Boudrez et al. 2002).

Next, to determine whether nocodazole treatment a) induces Ser748 phosphorylation of DYRK1A in a cell type specific manner and b) generates variants of DYRK1A with different electrophoretic mobility, GFP-DYRK1A was partially purified by IMAC from HEK_GFP-DYRK1A cells that were treated with nocodazole or left untreated. Three different migrating bands were detected for GFP-DYRK1A, with the middle one giving the strongest signal with the anti-DYRK1A antibody (Fig. 30*B*, indicated by the grey arrow). We suggest that this represents the main variant of GFP-DYRK1A in cells. As the mRNA of GFP-DYRK1A is not spliced, these variants derive from posttranslational modifications. Quantification of the Ser748 phosphorylation level of all three variants together, by determination of the ratio signal of phospho-specific anti-pSer748 antibody to signal of total DYRK1A, showed that Ser748 phosphorylation is not upregulated in mitotic cells compared to asynchronous cells (Fig. 30*B*). However, the slowest migrating band (white arrow) appeared to show a stronger phosphorylation on Ser748 in mitotic cells.

These results show that upregulation of Ser748 phosphorylation took place only in a minor part of overexpressed GFP-DYRK1A and thereby suggest that our experimental settings are not suitable to detect mitosis-dependent changes in phosphorylation (*see Discussion 5.2.1*).

Finally, to investigate if fast dephosphorylation during mitosis is the reason why no upregulation on Ser748 phosphorylation can be observed, asynchronous and mitotic HeLa cells overexpressing GFP-DYRK1A were treated with increasing amounts of Calyculin A. As shown above, nocodazole treatment showed neither an affect on Ser748 phosphorylation (Fig. 31, lane 1+2) nor generated a mobility shift of GFP-DYRK1A in total cell lysates. GFP-DYRK1A from Calyculin A-treated asynchronous cells showed a clear shift with all three concentrations of Calyculin A.

A shift appeared also for unspecific bands, but taken this shift as a baseline the shift for GFP-DYRK1A is still noticeable. The same pattern was received for GFP-DYRK1A from Calyculin A-treated mitotic cells. As expected from the results shown above (*see Results 4.2.2.7*), Calyculin A-treatment failed to enhance Ser748 phosphorylation in asynchronous and in mitotic cells (Fig. 31, ratio indicated below respective lane).

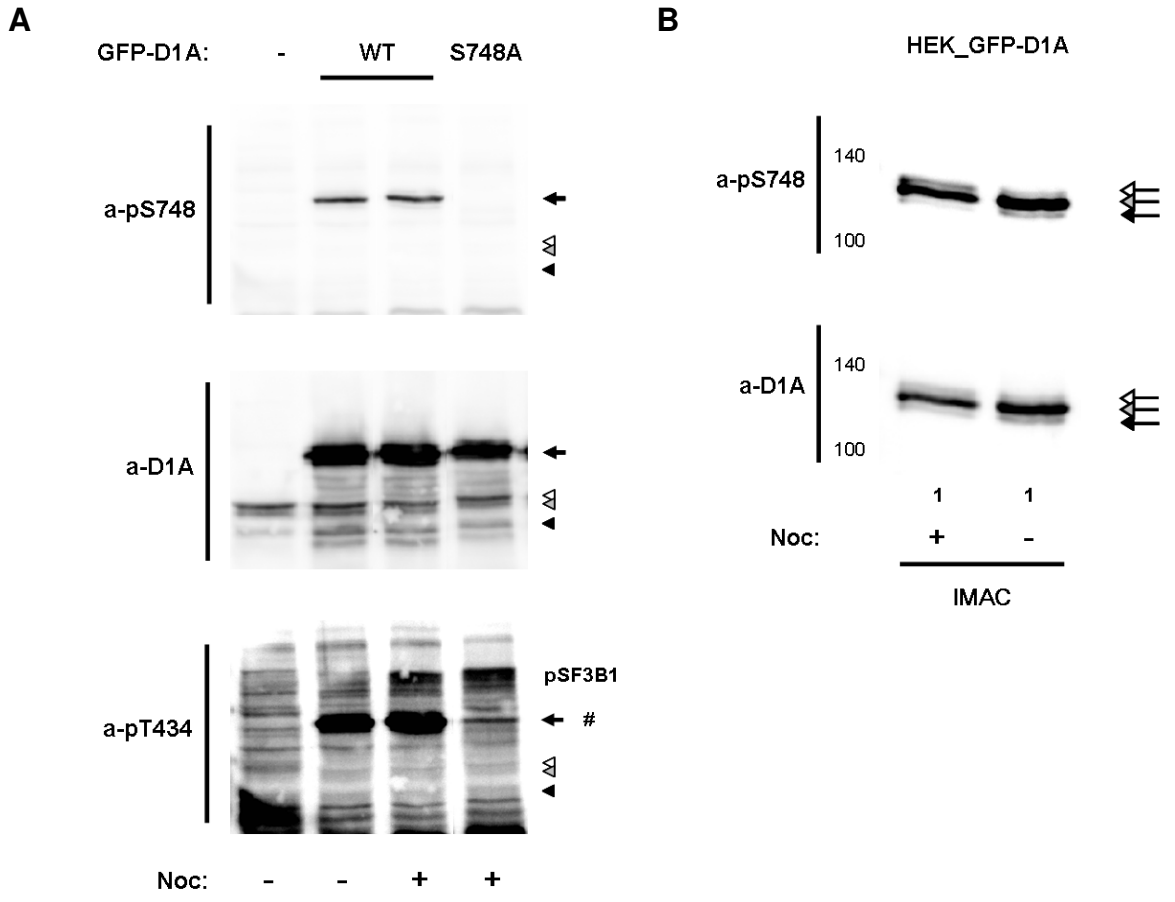

Figure 30: Effect of nocodazole on DYRK1A Ser748 phosphorylation.
A. HeLa cells were transiently transfected with wild-type GFP-DYRK1A (WT) or GFP-DYRK1A S748A and cells were treated with nocodazole (50 ng/ml; Noc) for 16 h or left untreated as indicated. Whole cell extracts were analyzed by immunoblotting with phospho-specific anti-pSer748 and anti-DYRK1A antibodies. Mitotic arrest by nocodazole treatment was determined by detecting the highly phosphorylated endogenous SF3B1 protein (pSF3B1) using anti-pThr434 antibody. Black arrow marks GFP-DYRK1A, arrowheads mark the three variants of endogenous DYRK1A and # the background signal of anti-pSer748 due to the use of the same secondary antibody. **B**. HEK_GFP-DYRK1A cells induced with doxycycline (2 µg/ml) for 2 d were treated with nocodazole (100 ng/ml; Noc) for 16 h or left untreated. GFP-DYRK1A was partially purified by IMAC and analyzed by immunoblotting with anti-pS748 and anti-DYRK1A antibodies. The ratio of anti-pSer748 to anti-DYRK1A antibody is shown below the respective lanes and was determined by densitometry using the AIDA software. The position of marker proteins (in kilodaltons) is indicated. Arrows mark the three variants of GFP-DYRK1A.

In the experiments shown above, endogenous DYRK1A was not recognized at detectable levels by the phospho-specific anti-pSer748 antibody (Fig. 31, arrowheads). However, detecting endogenous DYRK1A with the anti-DYRK1A antibody revealed a shift of the bands when treated with 20 nM of Calyculin A (Fig. 31, lane 3+6). With higher concentrations of Calyculin A, the recognition by the anti-DYRK1A antibody was lower, suggesting that the endogenous protein is phosphorylated on different sites and thereby many different variants of DYRK1A are generated with different phosphorylation levels and different molecular masses. This would lead to a diffuse and weak signal.

In summary, GFP-DYRK1A from mitotic cells behaves like in asynchronous cells. Prevention of dephosphorylation also results in a mobility shift of GFP-DYRK1A in mitotic cells. However, upregulation of Ser748 phosphorylation was not detectable in mitotic cells treated with Calyculin A, suggesting that fast dephosphorylation by PP1A and PP2A is not responsible for this event.

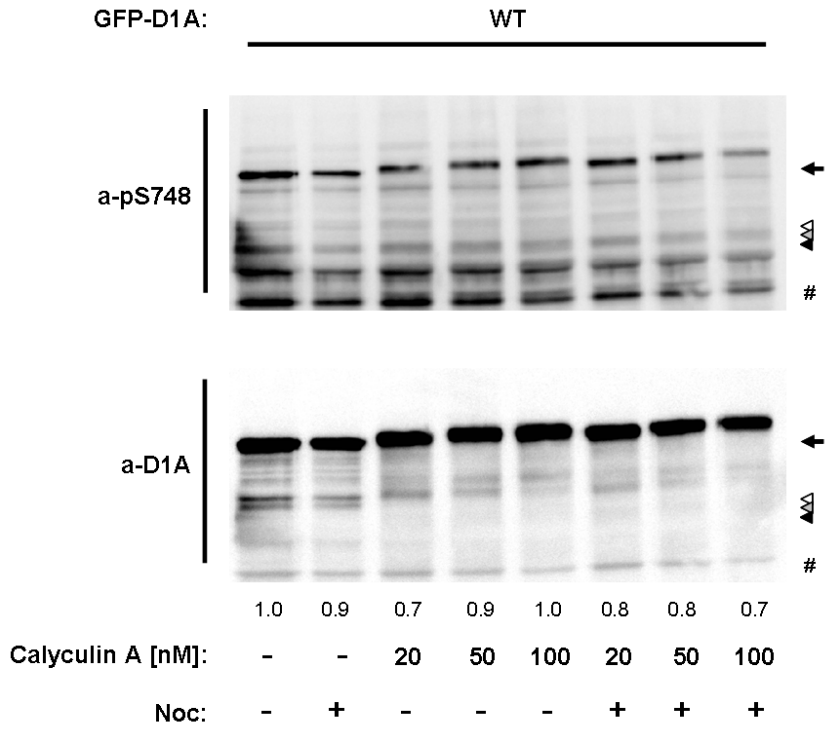

Figure 31: Effect of Calyculin A on DYRK1A Ser748 phosphorylation in mitotic cells. HeLa cells transiently transfected with wild-type GFP-DYRK1A (WT) were treated with nocodazole (50 ng/ml; Noc) for 16 h or left untreated as indicated. Different concentrations of Calyculin A were added 1 h before lysis and whole cell extracts were analyzed by immunoblotting with anti-pSer748 and anti-DYRK1A antibodies. The ratio of anti-pSer748 to anti-DYRK1A antibody signal is shown below the respective lanes and was determined by densitometry using the AIDA software. Black arrow marks GFP-DYRK1A, arrowheads mark the three variants of endogenous DYRK1A and # an unspecific signal.

4.2.3 Posttranslational modifications of DYRK1A during mitotic exit

4.2.3.1 Establishment of cell cycle synchronization

To investigate posttranslational modifications of DYRK1A during the cell cycle, a protocol for synchronization had to be established and verified. Two methods for synchronization were chosen a) the double thymidine block (early S phase block) and b) the thymidine-nocodazole block (mitotic block) (ref: www.sbcellcycle.org; State-of-the-art in human cell synchronization; DIAMONDS Deliverable 1-D1.1.3). For cell cycle analysis, two cell lines were examined:

a) The HeLa cell line which is a well-characterized cell line in cell cycle research and is simple to transfect even during synchronization. Furthermore, the Ser748 phosphorylation was originally identified in HeLa cells (Daub et al. 2008).

b) The PC12_GFP-DYRK1A cell line which overexpresses GFP-DYRK1A under the control of a doxycycline-inducible promoter at endogenous level and thereby transfection of the cells can be avoided. In addition, PC12 is a neuronal cell line and serves to determine if findings in HeLa are cell type specific. Further, neuronal cells are able to exit the cell cycle and differentiate, and a role of DYRK1A in premature neuronal differentiation has been reported (Yabut et al. 2010).

Cells were released from cell cycle arrest by washing out of thymidine or nocodazole respectively and then collected at indicated time points. To verify cell cycle transition and to assign the time points to the phases of cell cycle, cell synchrony was monitored by flow cytometry (FACS) of propidium iodide-stained cells (Fig. 32*A* and *C*). 56.6 % of thymidine-released cells reached G_2/M phase after 6 h and 9 h after thymidine release 61.8 % of the cells exit mitosis while still 28.3 % remained in G_2/M phase, as estimated from the flow cytometry data (Fig. 32*A* and *B*). Nocodazole-induced arrest in G_2/M phase is more efficient (Fig. 32*C* and *D*). Synchronization was also monitored by immunoblotting with antibodies against a) Cyclin D1, which is downregulated in S phase (*see Introduction 1.3.1.2*), b) histone H3 phosphorylation on Ser10 as marker of mitosis (Hendzel et al. 1997) and c) retinoblastoma protein (RB) phosphorylation on Ser807/Ser811, which is dephosphorylated at mitotic exit up to early G_1 phase (*see Introduction 1.3.1.1*).

Arrest by double thymidine or nocodazole block efficiently synchronizes cells in early S phase or M phase, respectively (Fig. 32*B* and *D*) and release from such an arrest is an adequate method to analyze cell cycle dependent events.

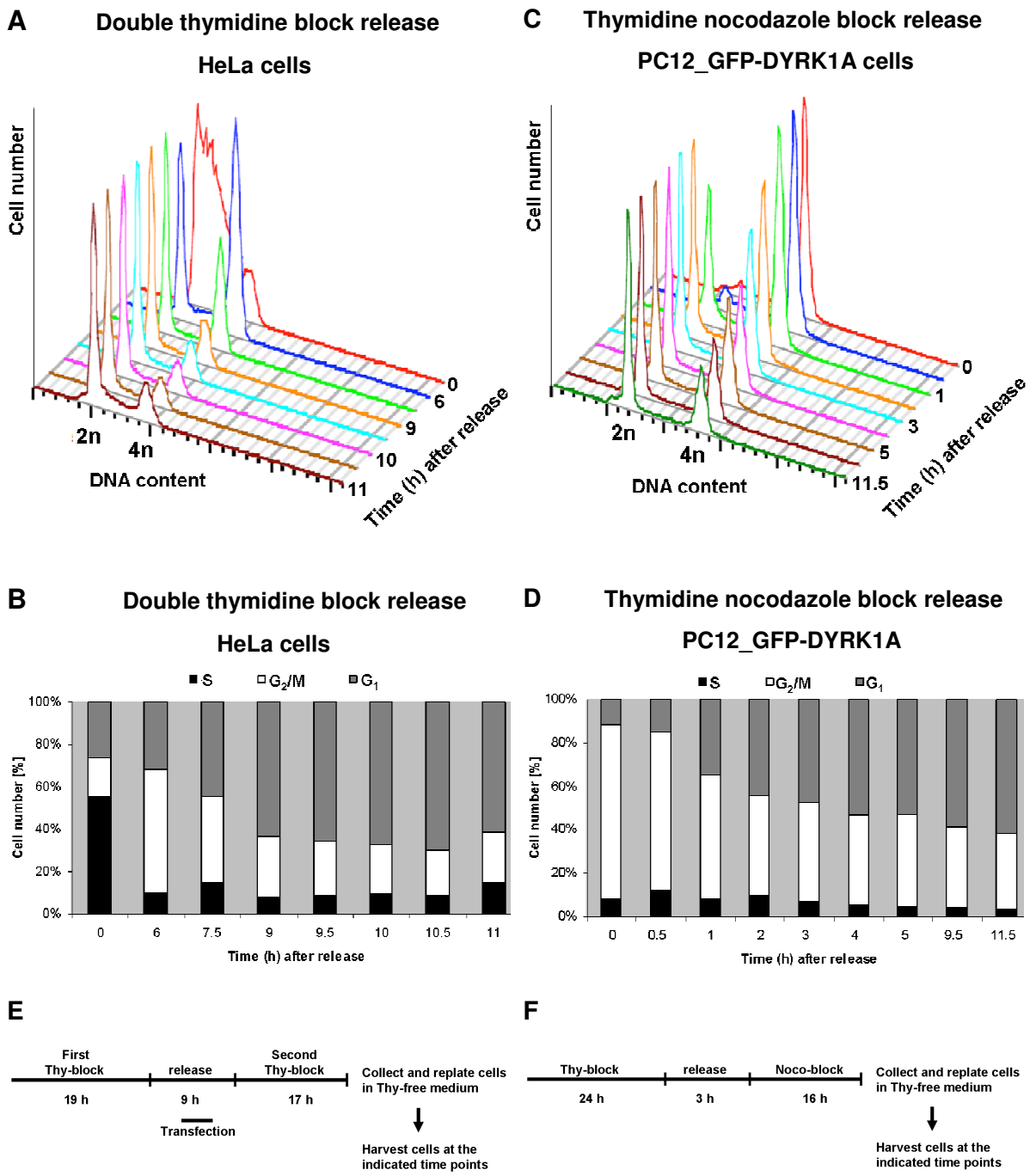

Figure 32: Cell cycle synchronization.
A. Synchronization at the G_1/S transition by a double thymidine block. HeLa cells were treated with 2 mM thymidine for 19 h, released in fresh medium for 9 h and then treated again with 2 mM thymidine for 17 h. Cells were collected at the indicated time points (0, 6, 7.5, 9, 9.5, 10, 10.5, 11 h) after release from the second thymidine block. Cells were fixed and stained with propidium iodide and the DNA content (2n, diploid; 4n, tetraploid) was analyzed by flow cytometry (FACS). **B.** FACS profile of the double thymidine block-released cells shown in *A*. **C.** G_2/M arrest by thymidine nocodazole treatment. PC12_GFP-DYRK1A cells were treated with 2 mM thymidine for 24 h, released in fresh medium for 3 h and treated with nocodazole (100 ng/ml) for 16 h. Cells were collected at the indicated time points (0, 0.5, 1, 2, 3, 4, 5, 9.5, 11.5 h) after release from the nocodazole block. Cells were fixed, stained and analyzed like in *A*. **D.** FACS profile of the thymidine nocodazole block-released cells shown in *C*. **E and F.** Scheme of treatment. Thy, thymidine; Noco, nocodazole.

4.2.3.2 Ser748 phosphorylation of DYRK1A during the cell cycle

As no upregulation on Ser748 phosphorylation of DYRK1A was observed in cells arrested in G_2/M phase, the phosphorylation on Ser748 was further analyzed during the cell cycle. Previous results (Fig. 30*A*) showed that endogenous DYRK1A Ser748 phosphorylation was not detectable in whole cell lysates, therefore the stable cell line PC12_GFP-DYRK1A which expresses GFP-DYRK1A under the control of a doxycycline-inducible promoter, was used to avoid transient transfection or purification of endogenous DYRK1A.

PC12_GFP-DYRK1A cells induced with doxycycline and synchronized by double thymidine block were released and harvested at indicated time points for Western blot analysis. By monitoring the phosphorylation state of histone H3, the M phase was revealed to take place around 7.5 to 10.5 h after thymidine block release (Fig. 33*A* and *C*). The phosphorylation of Ser748 in GFP-DYRK1A (Fig. 33*B* and *D*, arrow) did not change significantly during progressing through the cell cycle. Strikingly, the protein levels of GFP-DYRK1A and endogenous DYRK1A were quite similar, but the phospho-specific anti-pSer748 antibody failed to detect the endogenous DYRK1A. Nevertheless, the phospho-specific anti-pSer748 antibody was used in the following experiments.

Together with the previous results, these data indicate that Ser748 phosphorylation of GFP-DYRK1A does not alter during the cell cycle.

4.2.3.3 Degradation of DYRK1A during mitotic exit

Unexpectedly, the cell cycle experiments revealed a variability of DYRK1A protein level at different stages of the cell cycle (Fig. 33*B*, time points 0, 9.5, 10 and 11 h). Therefore all independent experiments have been compared and it has been decided to focus on the time points where downregulation of DYRK1A protein level was consistently observed (Fig. 33*B* and *D*, time points 9, 9.5, 10 h). These time points correspond to late M phase or mitotic exit (*see Results 4.2.3.1 and 4.2.3.2*).

Notably, GFP-DYRK1A was degraded at the same time points as endogenous DYRK1A (Fig. 33*B* and *D*, arrow and arrowheads*)*. As expression of exogenous GFP-DYRK1A is not modulated by the endogenous DYRK1A promoter, the downregulation of DYRK1A protein level does not take place at a transcriptional level, but rather indicates degradation of the DYRK1A protein during mitotic exit.

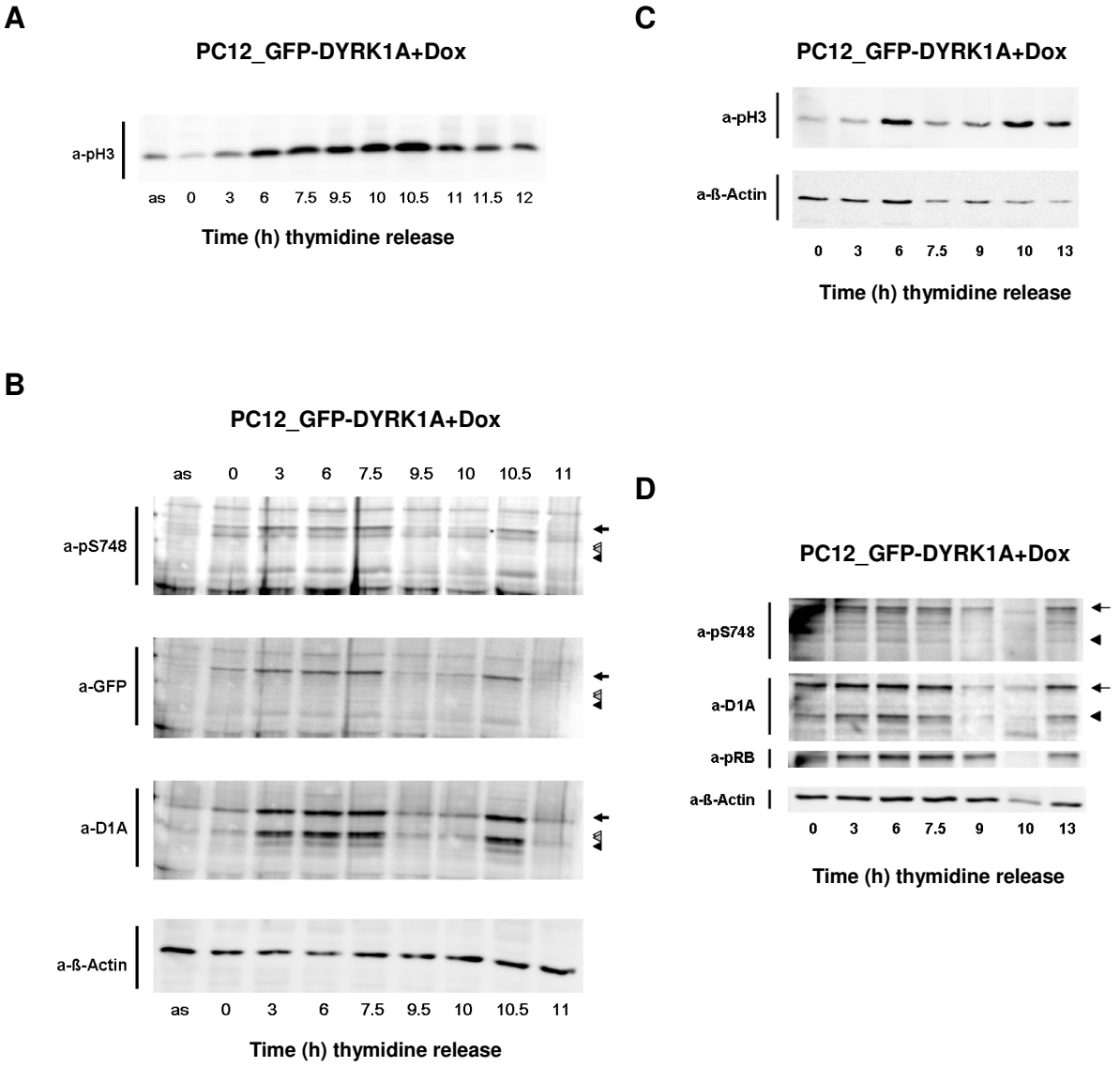

Figure 33: DYRK1A is degraded during M/G_1 transition.
PC12_GFP-DYRK1A cells were induced with doxycycline (2 µg/ml, +Dox) and synchronized at the G_1/S transition by a double thymidine block or left untreated (as, asynchronous). Cells were collected at the indicated time points after release from the second thymidine block. Whole cell lysates were subjected to a 15% (***A*** and ***C***) or 10% (***B*** and ***D***) SDS gel and analyzed in Western blot with indicated antibodies (with β-Actin as a loading control). Arrow marks exogenous GFP-DYRK1A and arrowheads mark endogenous DYRK1A. Two independent experiments are shown, were *A* + *B* and *C* + *D* show samples from the same whole cell lysates.

To confirm that the degradation of DYRK1A in late mitosis is not an artifact caused by the thymidine treatment and is not a PC12 cell specific event, HeLa cells were synchronized in parallel with PC12_GFP-DYRK1A at G_2/M using nocodazole.

Synchronization was verified by the phospho-specific anti-pRB antibody (*see Introduction 1.3.1.1*). RB was dephosphorylated 2 h after release from nocodazole block and rephosphorylated after 5 h, indicating that cells exit mitosis between these time points (Fig. 34). This is consistent with a previous report that Ser807 of RB is dephosphorylated at mitotic exit (Rubin et al. 2001). Further, SF3B1 exhibits a slower migrating variant on SDS gels during mitosis (Fig. 34, upper arrow) what supports the determination of the mitotic exit between 2 and 5 h after nocodazole-release. Degradation of DYRK1A was detectable in both cell lines and at the same time points (Fig. 34, arrowhead), and again exogenous GFP-DYRK1A (asterisk) shows the same pattern as endogenous DYRK1A. As described above, GFP-DYRK1A in PC12 cells show much higher levels of Ser748 phosphorylation than the endogenous DYRK1A, but no change of phosphorylation level was observed during the cell cycle.

As a conclusion, these results support that downregulation of DYRK1A occurs by degradation specifically during late mitosis and is cell type independent.

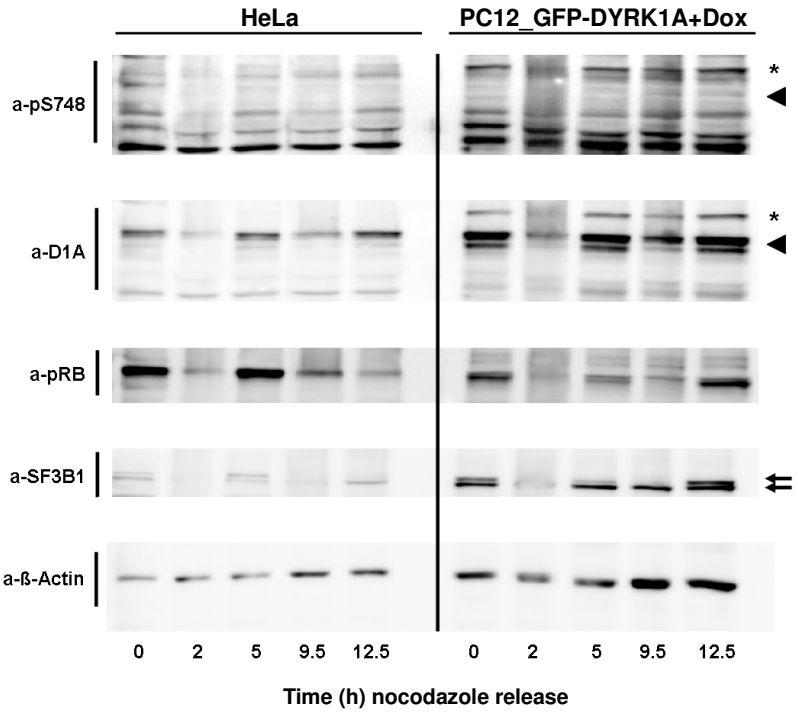

Figure 34: DYRK1A degradation during mitotic exit.
HeLa or PC12_GFP-DYRK1A cells induced with doxycycline (2 µg/ml, +Dox) were synchronized at the G_2/M phase by nocodazole block. Cells were collected at the indicated time points after release from the cell cycle block. Whole cell lysates were analyzed in Western blot with indicated antibodies (with β-Actin as a loading control). Asterisk marks exogenous GFP-DYRK1A, arrowhead endogenous DYRK1A and arrows the two variants of SF3B1.

4.2.3.4 Degradation of DYRK1A during mitotic exit is inhibited by MG132

The anaphase-promoting complex or cyclosome (APC/C) is an E3 ubiquitin ligase which targets substrate proteins for destruction by the 26S proteasome and is active during mitosis and in the G_1 phase (Peters et al. 2006). As protein levels of DYRK1A were decreased at mitotic exit, we addressed the question if the APC/C-26S proteasome system is involved in DYRK1A degradation.

PC12_GFP-DYRK1A induced with doxycycline were synchronized at G_2/M with nocodazole and released into fresh medium containing MG132, a specific proteasome inhibitor, or left untreated. As expected, cells released from nocodazole block in the absence of MG132 showed decreased levels of DYRK1A at mitotic exit (Fig. 35*A*, 0.5, 1, 2 h), but cells treated with MG132 failed to show DYRK1A degradation (Fig. 35*A*). Strikingly, MG132-treatment also affected dephosphorylation of RB (Fig. 35*A*, grey arrow), dephosphorylation of histone H3 (Fig. 35*B*) and the disappearance of the slow migrating variant of SF3B1 (Fig. 35*A*, black arrows), indicating that exit from mitosis is retarded or partially inhibited.

This experiment suggests that DYRK1A degradation could be mediated by the proteasome and the time points imply the involvement of the ubiquitin ligase APC/C (*see Discussion 5.2.6*).

4.2.3.5 Degradation of overexpressed DYRK1A is independent of its kinase activity

To analyze if kinase activity of DYRK1A is required for its degradation at mitotic exit, HeLa cells overexpressing wild-type GFP-DYRK1A or the kinase deficient DYRK1A K188R mutant were synchronized by double thymidine block. Both GFP-DYRK1A variants showed a decrease of protein level 10 h after release from thymidine block (Fig. 36*A* and *C*). The same is observed for endogenous DYRK1A (Fig. 36*A* and *C*, arrowhead). Again, no changes in Ser748 phosphorylation levels for wild-type GFP-DYRK1A was detectable (Fig. 36*A*). Antibodies against Cyclin D1, downregulated during S phase, and histone H3 phosphorylation determine the time point of degradation to the late mitosis (Fig. 36*B* and *D*). Detection with the anti-GFP antibody, which recognizes the N-terminal GFP-tag of DYRK1A, revealed a stepwise C-terminal degradation of the protein (Fig. 36*A* and *C*, dots). These fragments are not detectable with the anti-DYRK1A antibody that is directed against the last 90 amino acids in the C-terminal region of DYRK1A. As the anti-DYRK1A antibody is able to

detect the GFP-DYRK1A ΔC19 mutant (Fig. 37*A*) the longest fragment must be truncated in the C-terminal region between amino acid 674 and 744.

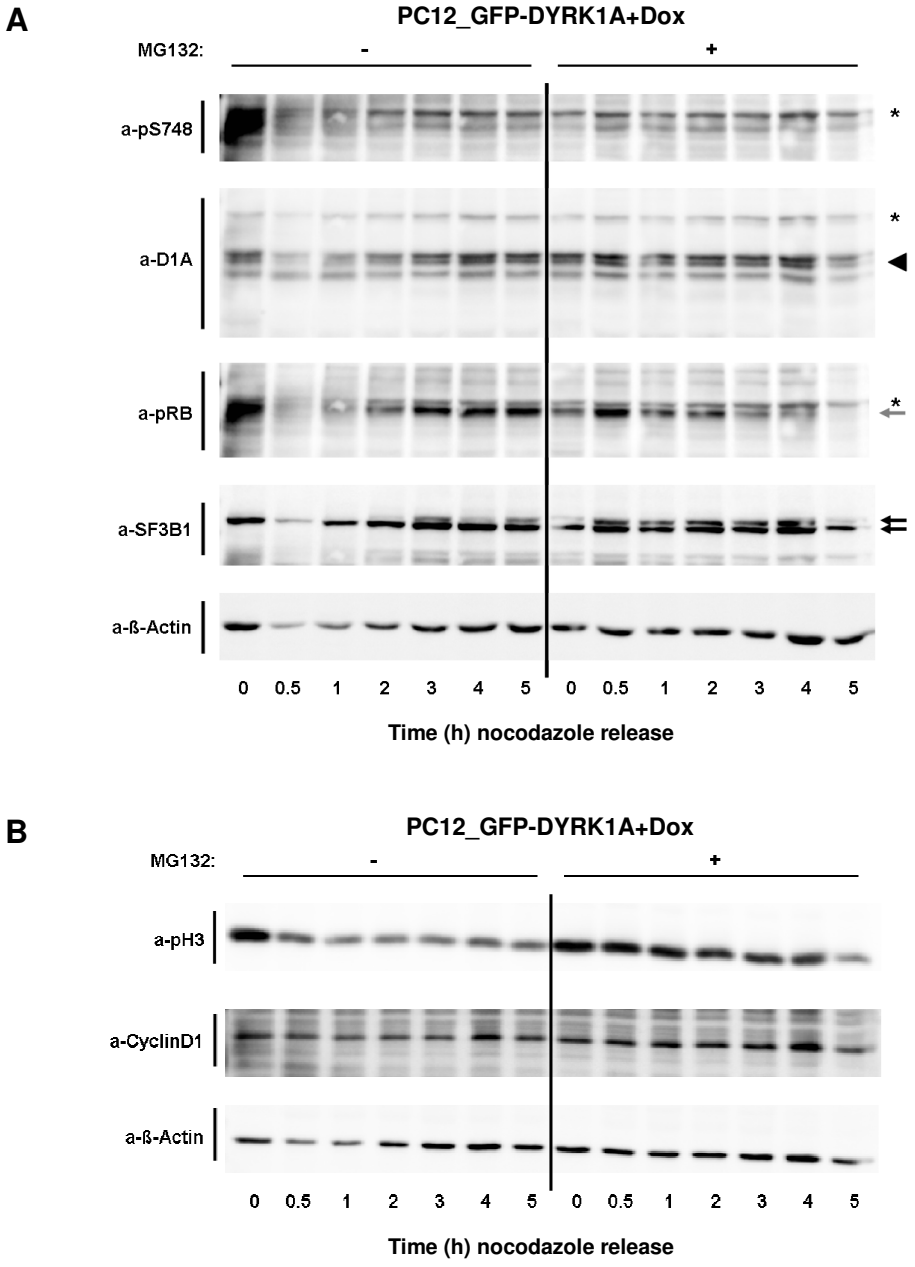

Figure 35: DYRK1A degradation is inhibited by MG132.
A. and **B**. PC12_GFP-DYRK1A cells induced with doxycycline (2 µg/ml, +Dox) were arrested at the G_2/M by nocodazole treatment and then released into fresh medium in the presence or absence of 20 µM MG132, a 26S proteasome inhibitor. At the indicated time points after release from the cell cycle block cells were collected and whole cell lysates were subjected to a 10% (***A***) or 15% (***B***) SDS gel and analyzed in Western blot with indicated antibodies. Asterisk marks exogenous GFP-DYRK1A, arrowhead endogenous DYRK1A, black arrows the two variants of SF3B1 and grey arrow phosphorylated retinoblastoma protein (RB).

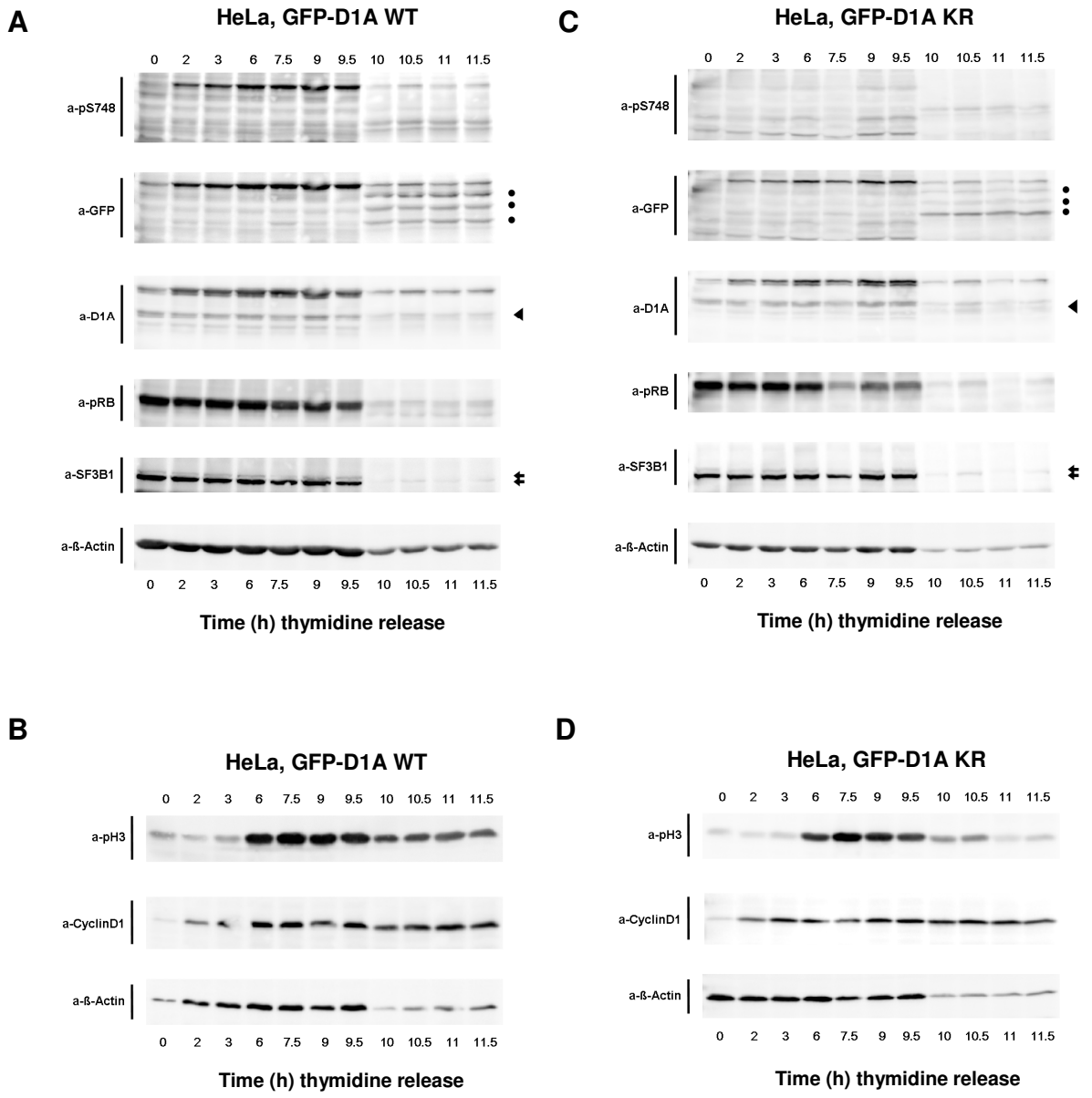

Figure 36: DYRK1A is degraded at mitotic exit independently of its kinase activity. HeLa cells were transiently transfected with plasmids expressing wild-type GFP-DYRK1A (WT) or the kinase dead mutant GFP-DYRK1A K188R (KR) 2 h after release from the first thymidine block. 2 h post-transfection cells were washed and 5 h later the second thymidine block was performed (see Fig. 32*E*). G_1/S synchronized cells were collected at the indicated time points after release from the second thymidine block. Whole cell lysates were subjected to a 10% (***A*** and ***C***) or 15% (***B*** and ***D***) SDS gel and analyzed in Western blot with indicated antibodies (with β-Actin as a loading control). Arrowhead marks endogenous DYRK1A, dots the truncated variants of GFP-DYRK1A WT or KR and arrows mark the two variants of SF3B1. *A* + *B* and *C* + *D* show samples from the same whole cell lysates.

Notably, the degradation of β-Actin, which was thought to serve as a loading control (Fig. 36*A*-*D*), suggests that all proteins undergo degradation 9.5 h after thymidine block release. But Cyclin D1 protein levels remained stable (Fig. 36*B*

and *D*). In addition, Coomassie staining of an independent gel, using the protein lysates of wild-type GFP-DYRK1A overexpressing cells, confirmed that not all proteins were degraded unspecifically (data not shown).

As β-Actin is a target of caspases (Mashima et al. 1995), the C-terminal truncation pattern of DYRK1A is similar to patterns obtained by caspase cleavage and the point that Cyclin D1 levels (degradation via ubiquitinylation) are not affected suggest that degradation observed in this overexpression experiments may rather be triggered by caspase cleavage than proteasomal destruction (*see Discussion 5.2.6*).

These data demonstrate a C-terminal degradation of overexpressed GFP-DYRK1A during mitotic exit, which is independent of its kinase activity.

4.2.3.6 Catalytically active DYRK1A interferes with RB dephosphorylation

The phosphorylation status of RB is a crucial regulation mechanism for cell cycle control (*see Introduction 1.3.1.1*). As RB is sequentially phosphorylated at multiple Ser/Thr residues, dephosphorylation occurs also sequentially and is temporally regulated (Rubin et al. 2001). Phosphoprotein phosphatase 1 (PP1) dephosphorylates RB at mitotic exit. In our study we used a phospho-specific anti-pRB antibody that recognizes the phosphorylated residues Ser807/811. As reported, Ser807 is dephosphorylated 30 min after mitotic release (Rubin et al. 2001).

The pattern of phosphorylated RB differed markedly between HeLa cells overexpressing wild-type GFP-DYRK1A or kinase inactive GFP-DYRK1A KR after release from double thymidine block. The phosphorylation level of RB declined rapidly 7.5 h after thymidine release and remained at low level (Fig. 36*C*, 7.5-9.5 h) when the cells overexpressed the kinase dead mutant of DYRK1A (KR). In contrast, this dephosphorylation was not observed in cells overexpressing wild-type GFP-DYRK1A (Fig. 36*A*, 7.5-9.5 h). Following the histone H3 phosphorylation, which reached its maximum around 7.5 h after thymidine release, cells can be considered to be in M phase (Fig. 36*B* and *D*). Furthermore, phosphorylation level of histone H3 after 10 h of thymidine block release did not decrease obviously in HeLa cells overexpressing wild-type GFP-DYRK1A, compared to cells overexpressing GFP-DYRK1A KR (Fig. 36*B* and *D*, 10-11.5 h).

The experiment was also performed with HeLa cells overexpressing GFP-DYRK1A ΔC19 or unfused GFP. GFP-DYRK1A ΔC19 (Fig. 30*A*) showed the same degradation pattern as wild-type and the kinase dead mutant of GFP-DYRK1A

(Fig. 36*A* and *C*). Unfused GFP was not degraded at mitotic exit, confirming that not all proteins were degraded unspecifically. Consistent with the results for wild-type GFP-DYRK1A, the catalytically active GFP-DYRK1A ΔC19 mutant prevented the dephosphorylation of RB (Fig. 37*A*, 7.5-9.5 h). But, the effect on histone H3 dephosphorylation was not as strong for GFP-DYRK1A ΔC19 (Fig. 37*B*) as for wild-type GFP-DYRK1A (Fig. 36*B*). Overexpression of unfused GFP did not affect dephosphorylation of RB (Fig. 37*C*, 10-11.5 h) or histone H3 (Fig. 37*C*, 10-11.5 h).

To summarize this data, it appears that RB dephosphorylation is prevented at mitotic exit when catalytic active GFP-DYRK1A is overexpressed.

4.2.3.7 The C-terminus of DYRK1A is essential for interference with RB and histone H3 dephosphorylation

Considering that GFP-DYRK1A underwent cleavage at sites in the C-terminal domain at mitotic exit and that the GFP-DYRK1A ΔC19 mutant lacking the Ser748 showed similar behavior towards the dephosphorylation of RB like wild-type GFP-DYRK1A, the question was addressed whether the regions outside the catalytic domain are crucial for the interference with RB dephosphorylation.

Therefore deletion mutants of GFP-DYRK1A were generated (Fig. 38*A*). As catalytic activity of DYRK1A is necessary for interference with RB dephosphorylation (*see Results 4.2.3.6*), the catalytic activity of the three deletion mutants was investigated. First, the three deletion mutants, immunoprecipitated with anti-GFP antibody, phosphorylated the peptide substrate DYRKtide in an IVK assay (data not shown). Second, GFP-SF3B1 Δ256-382 was phosphorylated on Thr434 by all three deletion mutants when co-expressed in HeLa cells (data not shown).

Summarized, GFP-DYRK1A ΔC, GFP-DYRK1A ΔN and GFP-DYRK1A ΔCΔN are enzymatically active kinases *in vitro* and in living cells.

In order to study the impact of the C-terminal region of DYRK1A on RB dephosphorylation at mitotic exit, HeLa cells overexpressing wild-type GFP-DYRK1A, the deletion mutants or unfused GFP were released from double thymidine block and harvested at indicated time points (Fig. 38*B-F*) similar to the experiment shown in Fig. 35 and Fig. 36.

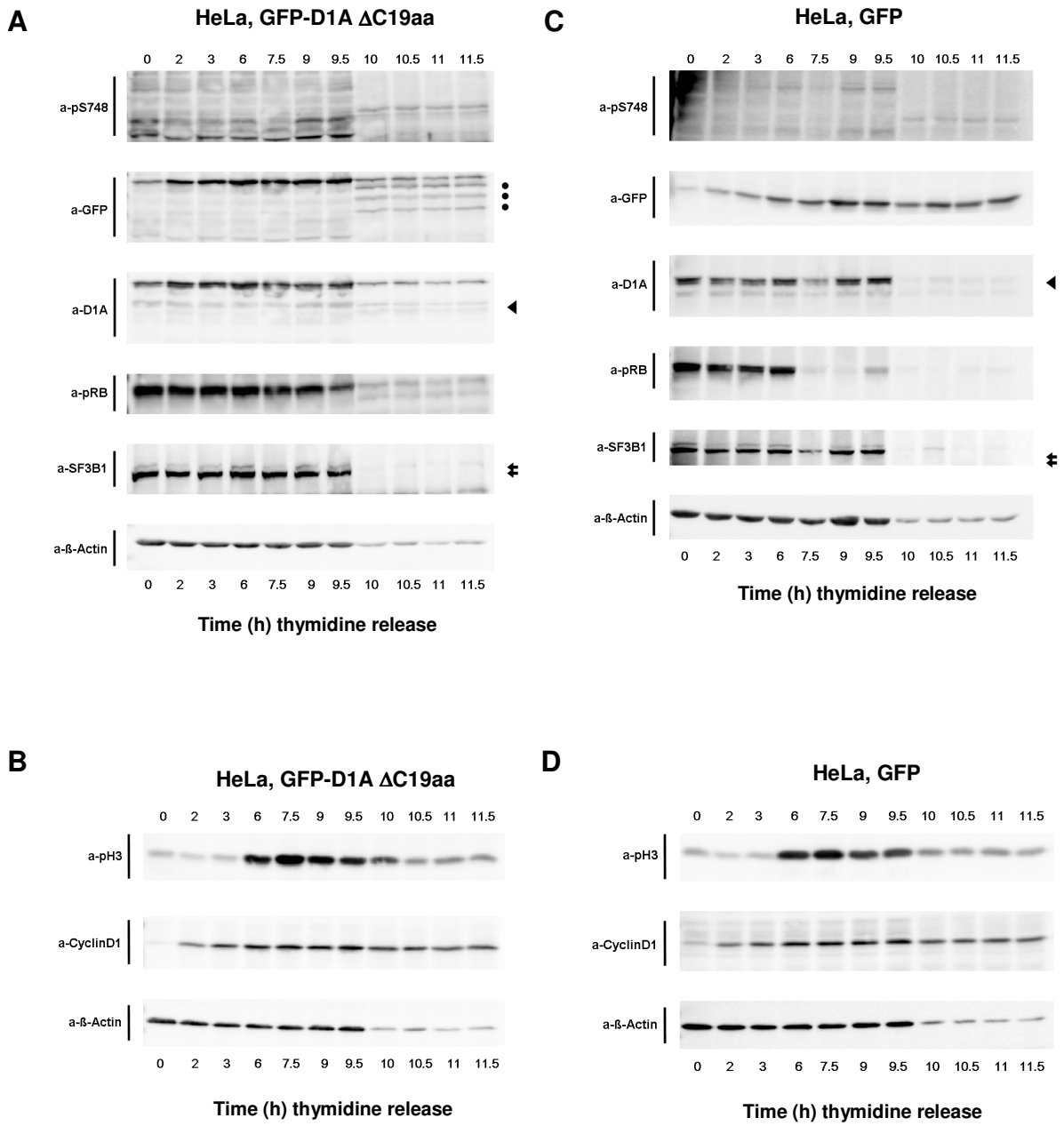

Figure 37: DYRK1A interferes with RB dephosphorylation.
HeLa cells were transiently transfected with plasmids expressing GFP-DYRK1A ΔC19aa or unfused GFP 2 h after release from the first thymidine block. 2 h post-transfection cells were washed and 5 h later the second thymidine block was performed (see Fig. 32*E*). G_1/S synchronized cells were collected at the indicated time points after release from the second thymidine block. Whole cell lysates were subjected to a 10% (***A*** and ***C***) or 15% (***B*** and ***D***) SDS gel and analyzed in Western blot with indicated antibodies (with β-Actin as a loading control). Arrowhead marks endogenous DYRK1A, dots the truncated variants of GFP-DYRK1A ΔC19 and arrows mark the two variants of SF3B1. *A* + *B* and *C* + *D* show samples from the same whole cell lysates.

In contrast to the previous experiment, dephosphorylation of RB occurred 3 h after thymidine release (Fig. 38*C* and *E-F*) and not 7.5 h (Fig. 36*C* and Fig. 37*C*). Analysis using the histone H3 phosphorylation antibody revealed that this time point

corresponds to mitosis (Fig. 39*A*-*E*). Histone H3 phosphorylation was upregulated 6 h after thymidine release and Cyclin D1 was downregulated at time point 0 h and present at time point 3 h. Therefore cells harvested at time point 3 h after thymidine release, correspond to G_2 phase. RB dephosphorylation 3 h after thymidine release did not occur in HeLa cells overexpressing wild-type GFP-DYRK1A (Fig. 38*B*, time point 3 h), whereas in cells expressing unfused GFP, RB is dephosphorylated (Fig. 38*F*). Overexpressing the catalytic domain of DYRK1A, as represented in GFP-DYRK1A ΔCΔN, did not interfere with dephosphorylation of RB (Fig. 38*C*, time point 3 h). The N-terminal deleted fusion protein (Fig. 38*D*, time point 3 h) showed the same RB phosphorylation state as wild-type GFP-DYRK1A suggesting that the deletion of this region is not essential for the interference. In contrast, deletion of the C-terminal region of DYRK1A eliminated the ability of DYRK1A to affect RB dephosphorylation (Fig. 38*E*).

These results suggest that the C-terminal region is required for the effect of DYRK1A on RB phosphorylation level in G_2 phase.

Following the phosphorylation of RB in HeLa cells expressing unfused GFP and released from thymidine block, the expected dephosphorylation of RB occurred at time point 11 h (Fig. 38*F*). Compared to the histone H3 phosphorylation (Fig. 39*E*), this time point can be determined to mitotic exit or early G_1 phase. Consistent with the pattern obtained at time point 3 h, N-terminally deleted fusion protein of DYRK1A behaved like wild-type GFP-DYRK1A and showed a dephosphorylation of RB (Fig. 38*B* and *D*) and of Histone H3 (Fig. 39*A* and *C*), suggesting exit from mitosis. In contrast, in cells expressing the catalytic domain or the C-terminal deletion mutant of DYRK1A the dephosphorylation of RB (Fig. 38*C* and *E*), the dephosphorylation of histone H3 (Fig. 39*B* and *D*) and thus exit from mitosis was prevented.

In summary, these experiments suggest that DYRK1A might interfere with crucial mechanisms of cell cycle control, such as the dephosphorylation of RB (directly or indirectly) and that DYRK1A degradation at mitotic exit could be an essential event to enter the next stage of the cell cycle. However, more experiments are required to elucidate the role of DYRK1A and the role of the C-terminal region of DYRK1A in cell cycle and above all at mitotic exit.

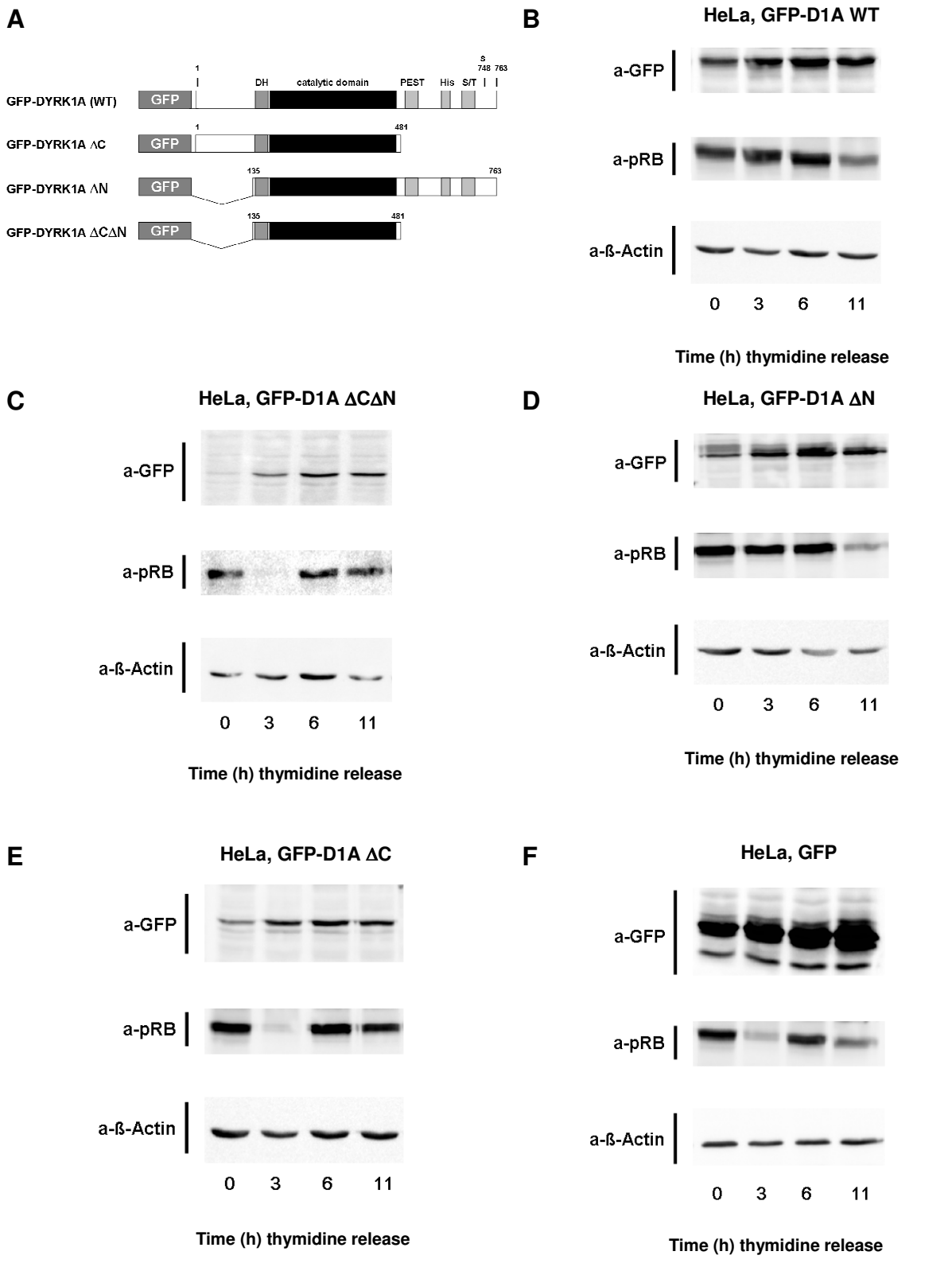

Figure 38: C-terminal deletion of DYRK1A interferes with RB dephosphorylation.
A. Schematic illustration of the deletion constructs of GFP-DYRK1A. **B.-F.** HeLa cells were transiently transfected with plasmids expressing wild-type GFP-DYRK1A (***B***), indicated GFP-DYRK1A deletion mutants (***C-E***) or unfused GFP (***F***) during double thymidine block (see Fig. 32*E*). G_1/S synchronized cells were collected at the indicated time points after release from the second thymidine block. Whole cell lysates were analyzed in Western blot with indicated antibodies (with β-Actin as a loading control).

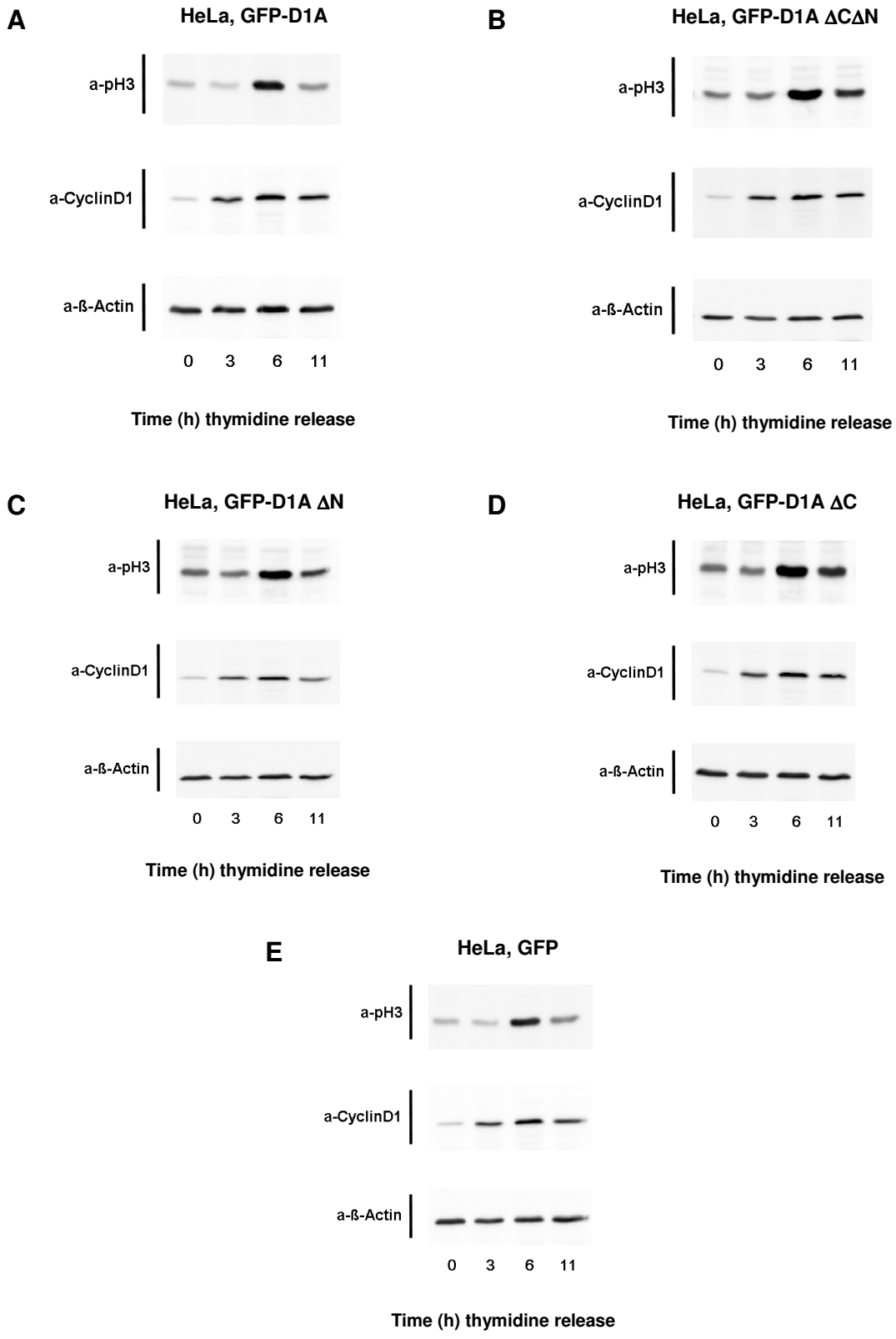

Figure 39: C-terminal deletion of DYRK1A alters dephosphorylation of Histone H3.
A-E. HeLa cells were transiently transfected with plasmids expressing wild-type GFP-DYRK1A (***A***), indicated GFP-DYRK1A deletion mutants (***B-D***) or unfused GFP (***E***) during double thymidine block (see Fig. 32*E*). G_1/S synchronized cells were collected at the indicated time points after release from the second thymidine block. Whole cell lysates were analyzed in Western blot with indicated antibodies (with β-Actin as a loading control).

5. Discussion

5.1 DYRK4

The mammalian DYRK family consists of 5 members, of which DYRK1A, DYRK1B, DYRK2 and DYRK3 have been extensively studied due to their roles in cell differentiation and survival, and their critical participation in processes such as neurogenesis or cancer (Aranda et al. 2010). By contrast, very little is known about the fifth member of the family, DYRK4. This study revealed several features of mammalian DYRK4 that are common to DYRK kinases, such as the mode of activation or the subcellular distribution as a regulatory mechanism. Furthermore, different substrate specificity characterized during this work could be important for establishing functional differences between DYRK family members.

5.1.1 Alternative promoter use and alternative splicing of DYRK4

Several different transcripts of human and mouse *DYRK4* are expressed, each encoding distinct protein products, due to alternative promoter use and first exon choice, as evident for other mammalian *DYRK* genes (reviewed in Aranda et al. 2010).

In this study, the genomic structure of human DYRK4 was defined and a new isoform (hDYRK4^{644}) was identified which has a different 5'-terminal sequence containing at least one motif (Fig. 7*B*) which is not present in the short variant previously described (hDYRK4^{520}). The new splicing variant of DYRK4 is present in mouse and human (Fig. 7*A*-*C*). Tissue distribution of the long isoform differs from the short one, with the long isoform present in several human tissues and the short isoform predominantly expressed in testis (Fig. 8*A*). Further, as the additional N-terminal sequence is conserved in mammals (Fig. 7*C*) the longer isoform can be considered as the reference sequence for DYRK4. Use of alternative promoters probably underlies the differential expression pattern of the two *DYRK4* 5' variants in human tissues.

By distinct alternative splicing events, further variants are generated, some of which lead to small in-frame deletions/insertions while others give rise to aberrant protein products. Exon 6 can be alternatively spliced out in-frame, generating a deletion of 9 amino acids in the N-terminal domain similar to a variant of DYRK1A (reviewed in Aranda et al. 2010). The ratio of these two splice variants, with or

without exon 6, differs in tissues and in cell lines (Fig. 8*A* and *B*). This suggests the existence of a regulatory mechanism for this alternative splicing event and the possibility that each protein isoform fulfils a distinct functional role. The presence of exon 7 differs also in tissues and in cell lines (Fig. 8*A* and *B*). Insertion of exon 7 leads to the appearance of an in-frame stop codon and the generation of a short truncated protein. However, if the ATG in exon 8 is used as the initiator codon, a 571 amino acid protein may be produced. These upstream open reading frames (uORFs) are not unusual in human genes and can cause a reduction of protein expression (Calvo et al. 2009).

5.1.2 DYRK4 gene expression

DYRK4 gene expression has been reported to be restricted to the testis in rodents (Becker and Joost, 1999; Sacher et al. 2007), but the expression of human *DYRK4* mRNA was detected in all the tissues analyzed (Fig. 8*A*). Further, it should be noted that human *DYRK4* has also been described to be expressed in NTera, a human neuronal precursor cell line, where it is upregulated during retinoic acid induced differentiation (Leypoldt et al. 2001), in SH-SY5Y neuroblastoma cells, where *DYRK4* is upregulated by tunicamycin-induced ER stress (Reimertz et al. 2003), in MCF-7 breast cancer cells, where it is upregulated by XBP1 (X-box binding protein-1) overexpression (Gomez et al. 2007), but downregulated by tanshinone IIa (Wang et al. 2005) and in Jurkat cells (T cell lymphoblast-like cells) (Gwack et al. 2006).

Bringing these findings together with the results of this study, human *DYRK4* shows a broad pattern of expression in various tissues and cell lines (Fig. 8*A* and *B*) that suggests a functional discrepancy between mouse and humans, and which severely limits the value of mouse models for the functional analysis of human DYRK4. The unusually low degree of sequence conservation between human and mouse DYRK4 (93% of amino acid identity in the catalytic domain; 63% in the N-terminal and 47% in the C-terminal region) when compared with other orthologous DYRK pairs (e.g. human and rat DYRK1A: 3 of 763 amino acids differ) propose that DYRK4 has acquired different functions during evolution. Therefore the described *Dyrk4* deficient mice which are vital and fertile (Sacher et al. 2007) may not display a valid model to elucidate the role of DYRK4 in humans.

5.1.3 A putative role of DYRK4 in the unfolded protein response

In this study, the mRNA of the newly identified long DYRK4 isoform (hDYRK4^{644}) has been observed to be strongly upregulated by tunicamycin treatment in SH-SY5Y cells, but in contrast DYRK4 in general (using oligonucleotides matching the catalytic domain) showed only a twofold induction (Table 7).

Tunicamycin induces unfolded protein response (UPR), a cellular stress response conserved between all mammalian species, including yeast and worm. Inhibition of protein glycosylation by tunicamycin leads to accumulation of unfolded proteins in the ER lumen. This so-called ER stress has been suggested to play a role in the pathogenesis of neurodegenerative disorders such as Alzheimer's disease (Sherman and Goldberg, 2001). Proteins upregulated by ER stress have been classified with respect to their expression kinetics. Early response proteins include molecular chaperones aiming to alleviate ER stress and late response proteins trigger an evolutionary conserved caspase-dependent apoptosis (Perez-Sala and Mollinedo, 1995). *DYRK4* has been found to be an intermediate tunicamycin-induced response gene (Reimertz et al. 2003). Using the same cell line and conditions, the effect of tunicamycin on *DYRK4* has been verified in this study. A second hint that DYRK4 may play a role in the UPR is the report that it is upregulated by XBP1 overexpression (Gomez et al. 2007). Human XBP1 is a transcription factor that participates in the UPR and is persistently activated due to tunicamycin treatment (Reimertz et al. 2003).

Taken together, these findings strongly suggest a role of DYRK4 in the UPR, but further studies are required to elucidate whether DYRK4 is involved in the early response pathway, supporting survival of the cell, or in the late response pathway, initiating apoptosis.

5.1.4 The subcellular localization of DYRK4 could represent a regulatory mechanism

Several mechanisms including active nuclear import, active nuclear export, and nuclear or cytosolic retention regulate the subcellular localization of proteins larger than 45 kDa (exclusion size of the nuclear pore), such as DYRK4. The results of this study show that all these mechanisms could act on DYRK4 and they might indeed modulate the biological activity of DYRK4 by altering the accessibility of substrates or modulators in particular subcellular compartments.

The short isoform of human DYRK4, GFP-DYRK4^{520}, was localized in the cytosol of COS-7 cells (Sacher et al. 2007). Subcellular localization of the newly identified long DYRK4 isoform (hDYRK4^{644} or mDYRK4^{642}) is different. Its extended N-terminal region, which is highly conserved (Fig. 7C), accounts for this difference. Our collaborators showed that the N-terminal extension harbours a classic NLS based on the binding to importin α, and on the nuclear import of a heterologous protein when fused to it (Papadopoulos et al. 2011). In addition, the extended N-terminal region mediates the nuclear retention of the long isoform (hDYRK4^{644} or mDYRK4^{642}), as suggested by the lack of nucleocytoplasmic shuttling in FLIP experiments (Fig. 10*A* and *B*). Detectable amounts of hDYRK4^{520} and mDYRK4^{594}, which lack the conserved N-terminal NLS, were found in the nucleus, which suggests that a second NLS could exist in DYRK4, such as that described between the kinase subdomains X and XI in DYRK1A (Alvarez et al. 2003). The DYRK4 long isoform was only partially localized in the nucleus suggesting that full nuclear accumulation was prevented by mechanisms such as strong CRM1-independent nuclear export, NLS masking or an interaction with cytosolic proteins. Further research will help uncovering the signals that modulate the subcellular localization of DYRK4. Regulated nuclear translocation has been demonstrated for DYRK2 or yeast Yak1p in response to extracellular signals (Moriya et al. 2001; Taira et al. 2007) (*see Introduction 1.2.5*). This could be a common feature of the DYRK family of kinases.

Summarized, and given that NLSs have been identified in DYRK4 (this study) and DYRK2 (Taira et al. 2007), and that DYRK3 is also at least partially localized in the nucleus (Lord et al. 2000; Guo et al. 2010), the distinction of “cytosolic” class II DYRKs from the “nuclear” class I DYRKs must be regarded as an oversimplification of the complex behaviour of these kinases.

5.1.5 DYRK4 is phosphorylated by cellular kinases

The characteristic migration of DYRK4 as a doublet in SDS gels, where the slower migrating band disappeared after phosphatase treatment (Fig. 11), show similarity to the fly orthologue of DYRK4, dDYRK2, which is the only DYRK protein migrating as a doublet due to phosphorylation in non-treated cells reported so far (Lochhead et al. 2003). Strikingly, for dDYRK2 the appearance of the doublet depends on autophosphorylation, but in case of DYRK4 catalytic activity is not required as the

kinase inactive version shows the same doublet as wild-type DYRK4 (Fig. 11). Furthermore, our collaborators identified phosphorylated residues outside the catalytic domain in both wild-type and kinase inactive hDYRK4^{520} using mass spectrometry analysis (Papadopoulos et al. 2011).

Phosphorylation of the second tyrosine residue within the activation loop (Tyr-X-Tyr motif) appears to be necessary for full activity of DYRK4, like in other DYRK kinases (reviewed in Aranda et al. 2010). Once expressed, DYRK kinases are constitutively active, but the activity of some DYRKs can be modulated post-translationally by phosphorylation on serine/threonine residues.

Regulatory phosphorylation of other DYRK kinases by upstream kinases has been reported recently, as in the case of yeast Yak1 by PKA (protein kinase A), worm MBK-2 by CDK-1 (cyclin-dependent kinase 1), mammalian DYRK2 by MAP3K10 (mitogen-activated protein kinase kinase kinase 10) or ATM (ataxia telangiectasia mutated) (Lee et al. 2011; Cheng et al. 2009; Varjosalo et al. 2008; Taira et al. 2010).

In conclusion, human DYRK4 is phosphorylated by cellular kinases and this phosphorylation could affect its subcellular localization, kinase activity or interaction with other proteins.

5.1.6 Substrate specificity of DYRK4

The new identified peptide substrate Pep285 is significantly phosphorylated by DYRK4 but not by DYRK1A (Fig. 14*B* and *C*). As no substrate for DYRK4 is known, this peptide can be used to analyze the specificity of DYRK inhibitors *in vitro* and their effect on their family members.

Up to now, substrate specificity of DYRK kinases has been little explored, although DYRK1A, DYRK2 and DYRK3 have previously been reported to differ in their specificities towards protein and peptide substrates (Becker et al. 1998; Campbell and Proud et al. 2002). However, only a few substrates were compared in these studies since the experiments were directed towards systematically analyzing the importance of specific residues in a given peptide on substrate recognition.

The experimental set-up employed by our collaborators offers a broader view by using an array with peptides that reflect known human phosphorylation sites (Papadopoulos et al. 2011). The validity of the assay was not only supported by the identification of two known DYRK1A phosphorylation sites but also, by the fact

that the majority of the peptides phosphorylated by DYRK1A match its consensus target sequence, with a proline at P+1 and an arginine at P-3 (Himpel et al. 2000).

The new identified peptide substrate Pep285 does not contain an arginine at P-3 or P-2 (Fig. 14*A*). However, the relatively high number of DYRK substrates that do not contain an arginine residue at P-3 or P-2 contrasts with the almost absolute requirement for the arginine observed elsewhere (Campbell and Proud et al. 2002), where DYRKs were considered as arginine-directed protein kinases. This difference is most likely due to the fact that in the previous study, the importance of the arginine was only tested in the context of one specific DYRK target site (Ser539 in eukaryotic initiation factor 2Bε), whereas the phosphosite array contains a large selection of diverse peptides. One example of an arginine-independent target site of DYRK1A is Thr434 in SF3B1 (de Graaf et al. 2006), which is mimicked by the peptide SAPtide, a peptide that is phosphorylated with a similar efficiency as DYRKtide by both DYRK1A and DYRK4 (Fig. 14*B* and *C*).

Given that human DYRKs appear to be co-expressed in some tissues and that they could be localized in the same subcellular compartments, substrate specificity may represent a critical factor that governs biological specificity among this family of protein kinases. Further research will be necessary to exactly define the structural determinants that distinguish target site recognition by DYRK4 from that of the other members of the DYRK family. Finally, Pep285 sequence could help to identify possible target sequences and substrates of DYRK4.

5.2 DYRK1A

As DYRK1A is a constitutively active protein kinase, which do not require an activating kinase, other control mechanisms may regulate the biological activity of DYRK1A. Posttranslational modification of DYRK1A can be such a mechanism that modulates its activity. Thus, targeting posttranslational modification of DYRK1A could be a tool to decrease the activity of DYRK1A.

This study revealed Ser748 as an autophosphorylation site in DYRK1A which phosphorylation increases DYRK1A activity. The inhibitor harmine is able to block Ser748 autophosphorylation. Another mechanism to downregulate DYRK1A activity is its degradation. This is the first study showing regulated degradation of DYRK1A and suggesting its involvement in mitotic exit. Understanding the regulation of Ser748

autophosphorylation and the mechanism which prime DYRK1A for degradation could be important for the development of drug targets which could then interfere with these mechanisms to decrease DYRK1A activity.

5.2.1 Different phosphorylation level of endogenous DYRK1A and GFP-DYRK1A

Partially purified endogenous and exogenous (GFP-tagged) DYRK1A are both phosphorylated on Ser748 (Fig. 24). However, Ser748 phosphorylation of endogenous DYRK1A could not be detected in whole cell lysates. A reason for this might be that protein level of endogenous DYRK1A is not sufficient to allow detection by the phospho-specific antibody. The stable PC12_GFP-DYRK1A cell line shows an expression level of GFP-DYRK1A similar to endogenous DYRK1A, but still the phospho-specific antibody only recognizes exogenous DYRK1A in whole cell lysates (Fig. 34).

A possible explanation would be that the GFP protein fused N-terminally directly interfere with Ser748 phosphorylation of DYRK1A by altering the conformation of DYRK1A and thereby indirectly changing its subcellular localization or interaction with cellular proteins.

Differential subcellular localization of endogenous DYRK1A and GFP-DYRK1A could display different phosphorylation levels. This could be due to either a) increased autophosphorylation activity of DYRK1A when localized in the nucleus or b) interaction with nuclear or cytosolic proteins, which block or promote Ser748 phosphorylation or c) the presence of nuclear or cytosolic phosphatases. Overexpressed GFP-DYRK1A accumulates in the nucleus of HeLa and in neuronal cells, but endogenous DYRK1A is detected in both the nucleus and the cytosol (Aranda et al. 2010; *see Introduction 1.2.5*). Similar localization has been observed with exogenous GFP-DYRK1A when expressed at low levels in the stable PC12_GFP-DYRK1A cell line (Fig. 4). Distribution between both compartments seems to be different for endogenous DYRK1A and GFP-DYRK1A and even from cell to cell as observed for exogenous GFP-DYRK1A (Fig. 4).

As a conclusion, differences on Ser748 phosphorylation levels of endogenous DYRK1A and GFP-DYRK1A observed in this study, suggest that GFP affects the function of DYRK1A in living cells.

5.2.2 Harmine and the Ser748 autophosphorylation of DYRK1A

Harmine does not inhibit tyrosine autophosphorylation of GFP-DYRK1A in HEK293 cells, and GFP-DYRK1A isolated from harmine-treated cells has similar catalytic activity as that purified from untreated cells (Göckler et al. 2009). Otherwise, harmine inhibits substrate phosphorylation potently (Fig. 18 and Fig. 19). It has therefore been postulated that harmine differentially affects tyrosine autophosphorylation by the translational intermediate of DYRK1A and substrate phosphorylation by the mature DYRK1A.

The autophosphorylation at Ser748 is inhibited by harmine in cells (Fig. 24*A*, *B* and Fig. 25*A*, *B*). Strikingly, harmine was not capable to inhibit autophosphorylation of Ser748 *in vitro* (Fig. 25*B*), at least not at a detectable level. *In vitro*, DYRK1A is able to autophosphorylate Ser748 even in the presence of high concentrations of harmine (Fig. 25*B*). In living cells harmine inhibits Ser748 autophosphorylation almost completely, which could be explained by the presence of cellular phosphatases. Ser748 autophosphorylation could reflect a balance between autophosphorylation and dephosphorylation in living cells (Fig. 40). Harmine inhibits the autophosphorylation and thereby would shift this balance. Even if DYRK1A autophosphorylation occurs in the presence of harmine at low levels, the strong dephosphorylation by phosphatases predominates (Fig. 40) and therefore phosphorylated Ser748 is not detectable. *In vitro*, phosphatases are missing and the balance is not given. Even low levels of rephosphorylation on Ser748 would lead to a measurable signal.

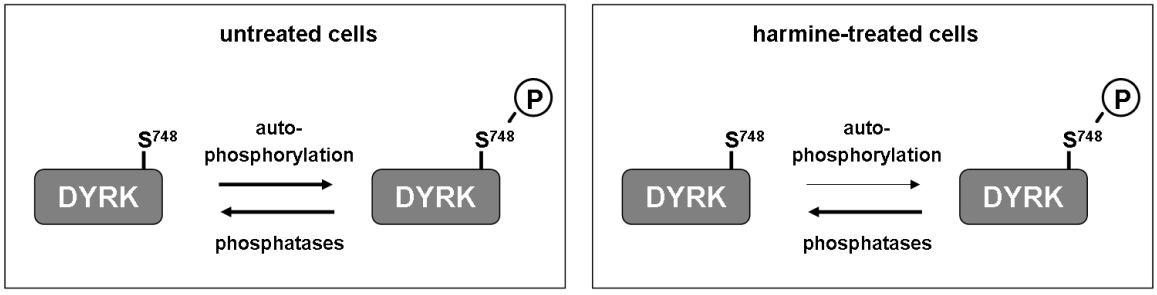

Figure 40: Autophosphorylation balance of DYRK1A.
Schematic presentation of reversible serine autophosphorylation of DYRK1A. In untreated cells there is a balance between autophosphorylation and dephosphorylation by phosphatases. Treatment with harmine inhibits autophosphorylation and thereby shifts the balance to unphosphorylated Ser748.

Taken together, the finding that harmine inhibits autophosphorylation at Ser529 in HEK293 cells (Alvarez et al. 2007) and at Ser748 in HeLa, PC12 and HEK_GFP-DYRK1A cells (this study) lead to the hypothesis that harmine inhibits both substrate phosphorylation and serine autophosphorylation of mature DYRK1A, but not tyrosine autophosphorylation of the translational intermediate.

5.2.3 Inter- and intramolecular autophosphorylation of DYRK1A

In general, phosphorylation in *cis* (intramolecular) occurs if phosphorylation of a protein kinase by itself can be validated, and the active kinase is not capable to phosphorylate its kinase inactive version. Phosphorylation in *trans* (intermolecular, phosphorylation of one protein kinase molecule by another one) takes place when the kinase inactive mutant is phosphorylated by its wild-type active version.

The third Ser/Thr autophosphorylation site for DYRKs which is characterized in this study, Ser748 of mammalian DYRK1A, shows both features of autophosphorylation (Fig. 23*A*, *B* and Fig. 27*B*). The kinase active DYRK1A version is phosphorylated on Ser748 and the kinase inactive is not when expressed in *E. coli*. Ser748 phosphorylation is an autophosphorylation event and kinase activity is essential. The kinase inactive DYRK1A expressed in living cells does not show any Ser748 phosphorylation, therefore no upstream kinase is capable to phosphorylate Ser748. Co-expression of both (the active and the inactive version) in living cells leads to Ser748 phosphorylation of the kinase inactive version by the active version of DYRK1A (Fig. 27*B*) and thus phosphorylation of Ser748 in *trans* is validated.

Further methods to distinguish *cis* and *trans* are either a) using a peptide, which contains the Ser/Thr or Tyr residue of interest, or a truncated domain of the protein containing the Ser/Thr or Tyr residue of interest, as an exogenous substrate (*trans*) in an IVK assay or immunoblotting with the phospho-specific antibody at the corresponding residue, respectively or b) measuring if the rate of phosphorylation increases as the concentration of protein kinase molecules increases (titration), what would provide evidence for *trans* and not *cis* phosphorylation.

Up to date two Ser/Thr autophosphorylation sites for DYRKs are known, Thr335 of yeast Yak1 and Ser529 of mammalian DYRK1A. Both autophosphorylations occur via an intramolecular phosphorylation event as the kinase inactive mutants of Yak1 or DYRK1A cannot be phosphorylated by their equivalent wild-type kinases (Lee et al. 2011; Alvarez et al. 2007). In principle, Yak1

is able to recognize this residue as a substrate phosphorylation site and to phosphorylate Thr335 in *trans*, when the truncated N-terminal domain of Yak1, containing Thr335, serves as exogenous substrate (Lee et al. 2011). It seems that Thr335 is only accessible for phosphorylation in *cis* in full-length Yak1, probably due to its conformation. It has not been tested, if mammalian DYRK1A is able to phosphorylate a peptide or the truncated C-terminal domain containing Ser529. In contrast to Ser748 which sequence matches perfectly the consensus target sequence ($RX_{1-2}p(S/T)P$) for DYRK1A substrates, Ser 529 does not contain a proline at P+1 (Fig. 27*A*).

Summarizing, the three Ser/Thr autophosphorylation sites for DYRK identified so far show different mechanisms of autophosphorylation. The two autophosphorylation sites published to date are intramolecular events and this study reports an autophosphorylation that can occur by an intermolecular mechanism.

5.2.4 Ser748 phosphorylation of DYRK1A may modulate its activity

Tyrosine autophosphorylation of the YXY-motif is essential for kinase activity of DYRKs (Himpel et al. 2001). Once expressed DYRK1A is a constitutively active kinase.

The autophosphorylation of DYRK1A on Ser748 seems to be involved in increasing of DYRK1A kinase activity. Substitution of Ser748 with alanine (S748A) showed a reduction in kinase activity. GFP-DYRK1A S748A maintained only ~60% of the activity of wild-type GFP-DYRK1A (Fig. 28*A*). As the GFP-DYRK1A ΔC19 mutant showed an increase of activity similar to the phosphorylation-mimetic mutants, GFP-DYRK1A S748E/S758E (EE) and S748E/S758A (EA) (Fig. 28*A* and *B*), autophosphorylation on Ser748 seems not to be directly involved, but rather suggests that an inhibitory protein is implicated. As the IVK assays have been performed with GFP-DYRK1A immunoprecipitated from cells, it is possible that regulatory proteins have been co-immunoprecipitated and were present in the reaction. One possible mechanism (Fig. 41) would be that DYRK1A binds to an inhibitory protein, when Ser748 is unphosphorylated and thus kinase activity of DYRK1A is reduced. Phosphorylation on Ser748 would disrupt this binding and increase the kinase activity. Binding of the inhibitory protein could be mediated by the last 19 amino acids, because they seem to be essential as their deletion leads to an increase of kinase activity.

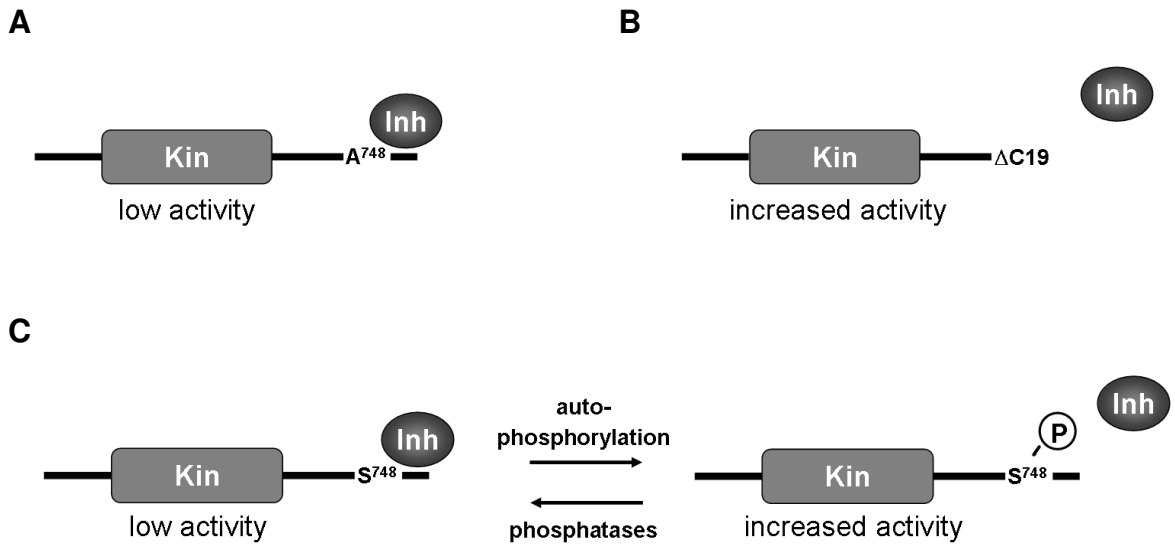

Figure 41: Model for regulation of DYRK1A kinase activity via Ser748 phosphorylation.
A. Substitution of Ser748 by Ala and thereby prevention of autophosphorylation on Ser748 leads to a reduced activity of DYRK1A (Fig. 28*A*) by binding of an yet unidentified inhibitory protein (Inh). **B.** Deletion of the 19 C-terminal amino acids leads to an increase of DYRK1A activity (Fig. 28*A*). **C.** Autophosphorylation on Ser748 of wild-type DYRK1A would disrupt the binding of an inhibitory protein (Inh) and enhance DYRK1A kinase activity. Dephosphorylation by phosphatases would keep a balance. A putative enhanced phosphorylation on Ser748 induced by an unknown mechanism or a putative downregulation of the specific phosphatases would regulate DYRK1A kinase activity.

Another possible explanation could be that no inhibitory protein is involved, but that the last 19 amino acids directly interact with a yet unknown binding site within DYRK1A itself and thereby alter its conformation or prevent the access to the ATP-binding pocket or the catalytic center, as Ser748 is also phosphorylated in *trans*.

The known autophosphorylation site of DYRK1A, Ser529, is involved in the regulation of kinase activity. The DYRK1A S529A mutant maintained only ~50% of wild-type DYRK1A activity when immunoprecipitated from living cells and subjected to IVK assay with DYRKtide peptide as substrate (Alvarez et al. 2007). Autophosphorylation on Ser529 of DYRK1A seems not to be directly affecting kinase activity, but rather regulates the binding of 14-3-3 to this autophosphorylated Ser529 residue. Binding of 14-3-3 increases DYRK1A kinase activity (Alvarez et al. 2007). Thus, autophosphorylation on Ser/Thr residues and thereby modulation of kinase activity could be a general mechanism for DYRKs. A recent study showed that yeast Yak1 autophosphorylates on at least four Ser/Thr residues resulting in full kinase

activity (Lee et al. 2011). Further, Bmh1, a yeast 14-3-3 protein, binds to autophosphorylated sites of Yak1 (with Thr335 as primary binding site) and inhibits its kinase activity. Therefore 14-3-3 is a good example that protein interaction facilitated by autophosphorylation on Ser/Thr residues, can trigger opposite (increasing or inhibiting) effects on kinase activity of DYRK family members, even if the interaction is taking place with same protein (Alvarez et al. 2007; Lee et al. 2011).

As a conclusion, the results suggest that Ser748 phosphorylation leads to an increase of DYRK1A activity. This is probably mediated by the interaction with a regulatory protein as this feature is already reported for other Ser/Thr autophosphorylation sites of DYRK kinases. As mutation of both Ser529 or Ser748 leads to an ~50-60% reduction of catalytic activity of DYRK1A, targeting one of those or both sites could trigger important effects, as *DYRK1A* heterozygous mice exhibit clear phenotopic alterations (Fotaki et al. 2002).

5.2.5 Ser748 phosphorylation of DYRK1A during mitosis

A two-fold increase in Ser748 phosphorylation of DYRK1A has been reported in mitotic cells (Daub et al. 2008).

In this study, the same cell line (HeLa cells) and the same synchronization protocols has been used. As Ser748 phosphorylation is present in both S phase and in M phase at least on a basal level (Fig. 33*D* and Fig. 36*A*), slight changes in phosphorylation levels can be difficult to distinguish. Ser748 phosphorylation during the release from S phase arrest did not reveal any differences in phosphorylation levels of GFP-DYRK1A in HeLa cells or PC12_GFP-DYRK1A cells. The synchronization was controlled by detecting changes in histone H3 phosphorylation levels (Fig. 36*A* and *B*) and by FACS analysis (Fig. 32*A* and *B*). A reason why slight changes cannot be detectable could be the resolution of GFP-DYRK1A on a SDS gel. In this study conventional one-dimensional gel electrophoresis has been used. Partially purified GFP-DYRK1A showed three different migrating bands which differed in their Ser748 phosphorylation level (Fig. 30*B*). Therefore, it is possible that alteration of the phosphorylation status of each band cannot be detected and two-dimensional gel electrophoresis would be an option to make slight changes in phosphorylation levels between different GFP-DYRK1A variants detectable.

Another reason why an upregulation of Ser748 phosphorylation during mitosis was not observed could be the different behaviour of endogenous and GFP-tagged

DYRK1A (*see Discussion 5.2.1*). The hypothesis that Ser748 phosphorylation of DYRK1A is regulated like in the model suggested in Fig. 41 could explain why overexpressed GFP-DYRK1A shows a stronger detectable phosphorylation compared to endogenous one. Either a) the amount of phosphatases dephosphorylating Ser748 of DYRK1A could be limited or b) the nuclear localization of GFP-DYRK1A prevents dephosphorylation by cytosolic phosphatases. Nevertheless, as in mitosis the nuclear membrane disappears and GFP-DYRK1A would be available to dephosphorylation by cytosolic phosphatases another hypothesis could be that phosphatases dephosphorylating Ser748 are slightly downregulated in mitosis. Thereby the two-fold upregulation of Ser748 phosphorylation found by Daub et al. (2008) could be explained for endogenous DYRK1A which was probably located in the cytosol.

Finally, the mass spectrometry analysis from Daub et al. (2008) reports two M phase-induced phosphorylation sites for DYRK1A, Ser748 and Ser758. This serine also has a proline at P+1 position but not an arginine at P-3 and thus does not match as perfect as Ser748 the consensus target sequence for DYRK1A substrates. Therefore it is possible that Ser758 could be also an autophosphorylation site of DYRK1A and could be the one which shows a stronger regulation of phosphorylation level during mitosis. The Phosida database (http://www.phosida.com) assigns both Ser748 and Ser758 the same p-value score. However, the IVK assays using the GFP-DYRK1A S748E/S758A (EA) mutant suggests that phosphorylation of Ser748 could be the functional one.

In summary, using a phospho-specific antibody against Ser748 did not reveal any modulation in phosphorylation of this residue in the stages of the cell cycle.

5.2.6 Degradation of DYRK1A during mitotic exit

Downregulation of DYRK1A activity cannot only be regulated by inhibiting kinase activity, but also by degradation of the protein.

This is the first study showing that DYRK1A is degraded during mitotic exit. The simultaneous disappearance of endogenous DYRK1A and exogenous GFP-DYRK1A during mitotic exit (Fig. 33*B* and *D*) indicates that downregulation of DYRK1A is regulated on protein level and thus occurs via degradation, because the two proteins are expressed under the control of different promoters. This event is a) not cell type dependent as it has been observed in HeLa and

PC12_GFP-DYRK1A cells and b) not dependent on the synchronization methods as it occurs when cells were released from both S phase and M phase (Fig. 33*B*, *D* and Fig. 34).

Treatment with the specific and potent proteasome inhibitor, MG132, prevents the degradation of DYRK1A (Fig. 35*A*) suggesting that the 26S proteasome system may mediate this degradation. Using MG132 is a common method to validate whether the 26S proteasome is involved in degradation during mitotic exit (e.g. Tang et al. 2009). The reappearance of DYRK1A after entry of G_1 phase correlates with the anaphase promoting complex/cyclosome (APC/C) inactivation and thus suggests that DYRK1A is targeted by the APC/C. The APC/C is an E3 ubiquitin ligase, which is active during mitosis and in the G_1 phase. The APC/C targets cell cycle proteins for degradation by the 26S proteasome by tagging them with ubiquitin (reviewed in Peters, 2006). Two known recognition amino acid sequences for APC/C recognition are the destruction-box (D-box; consensus RXXLXXXN) and the KEN-Box (consensus KEN). Both are not present in DYRK1A. Thus, it might be also possible that MG132 is preventing the proteasomal degradation of a protein that protects DYRK1A against degradation.

In contrast, the degradation pattern of overexpressed GFP-DYRK1A during mitotic exit might also suggest a caspase-mediated cleavage event (Fig. 36*A*, *B* and Fig. 37*A*). The finding that an antibody detecting the N-terminal part of GFP-DYRK1A (anti-GFP) is recognizing different fragments and another antibody detecting the C-terminal part (anti-DYRK1A) strongly indicates that the degradation occurs in the C-terminal region domain. Sequence analysis of the C-terminal domain of DYRK1A did not reveal any known cleavage sites for caspases. It should be considered that cleavage by caspases does not necessarily lead to degradation of a protein in general, but can also give rise to a truncated variant which exhibits different properties than the full-length protein, such as higher or lower kinase activity. The finding that β-Actin is also degraded in this experiments (Fig. 36*A-D* and Fig. 37*A-D*) suggests that in this experiment a caspase-mediated pathway could have been induced.

Taken together, the two different degradation patterns of a) endogenous DYRK1A and low level GFP-DYRK1A and b) overexpressed GFP-DYRK1A obtained during mitotic exit should be analyzed separately. Endogenous and lowly overexpressed GFP-DYRK1A degradation during mitotic exit might be regulated by

ubiquitinylation and subsequent proteasomal destruction and highly overexpressed DYRK1A may cause activation of and cleavage by caspases.

5.2.7 The effect of overexpressed DYRK1A on cell cycle proteins

5.2.7.1 The retinoblastoma protein (RB)

As expected, dephosphorylation of RB occurs at mitotic exit (Fig. 35*A*, without MG132) (*see Introduction 1.3.1.1*) and phosphorylation returns about 3 h after nocodazole release. Degradation of DYRK1A correlates with dephosphorylation of RB in HeLa and PC12_GFP-DYRK1A cells (Fig. 32*D*, Fig. 33 and Fig. 34). It has not been analyzed if DYRK1A is able to phosphorylate RB directly on these residues which are followed by a proline. It is more likely that DYRK1A interferes indirectly with RB phosphorylation, as overexpression of DYRK1A altered Cyclin B protein level (Branchi et al. 2004) (*see Introduction 1.3.2*). High levels of Cyclin B in transgenic mice overexpressing DYRK1A suggest that DYRK1A might stabilize this protein. The degradation of DYRK1A observed in this work, may cause destabilization of Cyclin B and thereby could explain the dephosphorylation of RB, whose hyperphosphorylated state is maintained by Cyclin B during mitosis (*see Introduction 1.3.1.1*). Vice versa, overexpression of active DYRK1A prevented dephosphorylation of RB at mitotic exit (Fig. 36*A* and Fig. 38*B*). This could be due to stabilization of Cyclin B by DYRK1A which then maintains RB phosphorylation. The kinase inactive version of DYRK1A did not interfere with RB phosphorylation and showed similar RB phosphorylation like in cells transiently transfected with unfused GFP (Fig. 36*B* and Fig. 37*B*). Human Cyclin B contains three serine and one threonine residues followed by a proline, but all lack an arginine at P-2 or P-3 position. Nevertheless, Cyclin L2 is reported to be a substrate of DYRK1A and three serine residues have been found to be phosphorylated by DYRK1A *in vitro*, all followed by a proline but without an arginine at P-2 or P-3 position (de Graaf et al. 2004).

RB is dephosphorylated by phosphoprotein phosphatase 1 (PP1) during mitotic exit (*see Introduction 1.3.1.1*). The results of this study cannot exclude that the effect of DYRK1A on RB phosphorylation is caused by interference between DYRK1A and PP1.

Summing up, the effect of altering DYRK1A protein level on RB phosphorylation at Ser807/811 suggests that DYRK1A might play a role in the cell cycle specific phosphorylation of RB.

5.2.7.2 Protein level of Cyclin D1

The degradation of Cyclin D1 is regulated by phosphorylation (*see Introduction 1.3.1.2*). It has been found that DYRK1B phosphorylates Cyclin D1 at Thr288 and thereby causes its degradation (Zou et al. 2004). In a recent publication was shown that overexpression of DYRK1A can also induce Cyclin D1 degradation (Yabut et al. 2010) (Table 1).

When cells were released from thymidine block, overexpression of DYRK1A in HeLa cells failed to cause a detectable effect on Cyclin D1 protein levels compared to cells overexpressing unfused GFP (Fig. 36*B*, Fig. 37*D*, Fig. 39*A*-*E*). Therefore this effect of DYRK1A on Cyclin D1 may occur in a cell type dependent manner. The constant protein levels of Cyclin D1 exclude the possibility that all proteins unspecifically undergo degradation 10 h after thymidine release under the used experimental conditions (Fig. 36*B*, *D* and Fig. 37*B*, *D*).

5.2.7.3 Phosphorylation level of histone H3

Dephosphorylation of histone H3 on Ser10 correlates with mitotic exit (*see Introduction 1.3.1.3*), similar to dephosphorylation of RB at Ser807/811. Overexpression of DYRK1A seems to influence both dephosphorylation levels, but the effect on histone H3 Ser10 phosphorylation is not as impressive as for RB (Fig. 38*B*-*F* and Fig. 39*A*-*E*). Considering the hypothesis that overexpression of DYRK1A stabilizes Cyclin B and thus dephosphorylation of RB is prevented, overexpressed DYRK1A would cause an altered mitotic exit. A delayed histone H3 dephosphorylation can be observed when active GFP-DYRK1A is overexpressed (Fig. 36*B* and *D*). Anyway, in the second experiment the effect of full-length DYRK1A and its deletion mutants was not consistent regarding the correlation between RB and histone H3 phosphorylation (Fig. 38*B*-*F* and Fig. 39*A*-*E*).

Nevertheless, an alteration on Ser10 dephosphorylation of histone H3 can be observed when active GFP-DYRK1A is overexpressed, thus further investigation has to be performed to elucidate if this alteration is caused directly by DYRK1A or is a side effect of cell cycle arrest.

6. Summary

Members of the dual-specificity tyrosine(Y)-phosphorylation regulated kinase (DYRK) family play key roles in the regulation of cell differentiation, proliferation and survival with DYRK1A being the best characterized member due to its gene location within the Down syndrome critical region (DSCR) on chromosome 21 in humans. DYRK1A is a candidate target for drug development, as it is overexpressed in Down syndrome individuals. The roles of DYRK1A in cell differentiation and apoptosis have been extensively characterized, but recent reports have implicated DYRK1A also in cell cycle control. For example, an upregulation of DYRK1A Ser748 phosphorylation was observed in a screening of mitotic cells compared to asynchronous cells. In contrast, investigation of DYRK4 has been neglected so far. This dissertation aims to address these open questions by providing a comprehensively molecular analysis of DYRK4 and a characterization of DYRK1A during the cell cycle.

This study revealed the subcellular localization, substrate specificity and tissue distribution of DYRK4. The here discovered long DYRK4 splice variant (human DYRK4^{644}) showed a broader tissue distribution compared to the already described short isoform (human DYRK4^{520}) and an induction of transcript levels in the human SH-SY5Y neuroblastoma cell line in response to endoplasmic reticulum stress. Moreover, the longer isoform contains a functional nuclear localization signal and displayed distinct nucleocytoplasmic mobility compared to the shorter isoform in live cell imaging experiments. A fusion protein of green fluorescent protein (GFP) and the long isoform did not exit the nucleus, whereas GFP fluorescence in the nucleus significantly decreased in the case of the short isoform in fluorescence loss in photobleaching experiments. Furthermore, it was shown here that DYRK4 is phosphorylated by other kinases independently of its kinase activity and can phosphorylate a known substrate of DYRK1A in living cells. Finally, it was confirmed that the substrate specificity of DYRK4 differed from that of DYRK1A and a peptide was identified which is specifically recognized by DYRK4.

To elucidate the phosphorylation state of DYRK1A it was shown that DYRK1A autophosphorylation in living cells is inducible by a phosphatase inhibitor and that DYRK1A autophosphorylates *in vitro*. A phospho-specific antibody was generated to study the phosphorylation of DYRK1A at Ser748. Using a kinase inactive mutant of DYRK1A, Ser748 phosphorylation was found to be an autophosphorylation event

that can occur in *trans* (intermolecular event). Furthermore, mimicking Ser748 phosphorylation by substitution of the serine with a glutamic acid residue enhanced DYRK1A activity towards a substrate peptide. However, no modulation of Ser748 phosphorylation levels during the phases of cell cycle was detectable.

In these cell cycle experiments, a degradation of endogenous DYRK1A and GFP-DYRK1A during mitotic exit was observed in two different cell lines (rat neuronal PC12 and human cervix carcinoma HeLa) and using two different synchronization methods. This degradation was inhibited in the presence of the proteasome inhibitor, MG132, suggesting a role of the anaphase-promoting complex or cyclosome (APC/C) that mediates proteasomal destruction of proteins during mitotic exit. Degradation of GFP-DYRK1A was also found in overexpression experiments independently of the kinase activity of DYRK1A. Furthermore, overexpression of wild-type GFP-DYRK1A interfered with dephosphorylation of the retinoblastoma protein during mitotic exit whereas the kinase inactive mutant or a mutant lacking the C-terminus of DYRK1A did not show this effect.

In summary, this study 1) provides a characterization of the newly discovered long splice variant of DYRK4 as well as differences in substrate specificity of DYRK4 towards DYRK1A and 2) characterizes the role of DYRK1A during the cell cycle and the autophosphorylation on Ser748.

7. Zusammenfassung

Mitglieder der *dual-specificity tyrosine(Y)-phosphorylation regulated kinase* (DYRK) Familie haben Schlüsselfunktionen bei der Regulation von Differenzierung, Proliferation und des programmierten Zelltods. DYRK1A ist auf Grund seiner Genlokalisation innerhalb der *Down syndrome critical region* auf Chromosom 21 beim Menschen die am Besten charakterisierte Proteinkinase dieser Familie. Da DYRK1A bei Down-Syndrom überexprimiert ist, stellt es ein mögliches Ziel für eine pharmakologische Therapie dar. Die Rolle von DYRK1A in Zelldifferenzierung und in der Apoptose wurde umfangreich charakterisiert, wohingegen neueste Publikationen zusätzlich einen Einfluss von DYRK1A auf den Zellzyklus implizieren. Kürzlich wurde zum Beispiel in einem Screening eine Hochregulation der Phosphorylierung von DYRK1A an Ser748 in mitotischen Zellen gefunden. Im Gegensatz zu DYRK1A wurde DYRK4 bisher kaum erforscht. Die vorliegende Dissertation geht diesen offenen Fragestellungen durch eine umfassende molekulare Analyse von DYRK4 und der Charakterisierung von DYRK1A im Zellzyklus nach.

In dieser Arbeit wurden die subzelluläre Lokalisation, die Substratspezifität und die Gewebsverteilung von DYRK4 aufgeklärt. Die hier entdeckte lange DYRK4 Spleißvariante (human DYRK4^{644}) zeigte verglichen mit der schon beschriebenen kurzen Variante (human DYRK4^{520}) eine breitere Gewebsverteilung sowie eine Induktion als Stressantwort des endoplasmatische Reticulum in der menschlichen SH-SY5Y Neuroblastomazelllinie. Des Weiteren besitzt die lange Isoform ein funktionelles nukleäres Lokalisationssignal und verfügte in Lebendzell-Experimenten über eine unterschiedliche nukleozytoplasmatische Mobilität im Vergleich zur kurzen Isoform. In *fluorescence-loss-in-photobleaching*-Versuchen verblieb ein Fusionsprotein aus dem grün-fluoreszierenden Protein (GFP) und der langen Isoform im Zellkern, wohingegen im Falle der kurzen Isoform die GFP-Fluoreszenz im Zellkern signifikant sank. Außerdem wurde hier gezeigt, dass DYRK4 durch andere Kinasen unabhängig von seiner Kinaseaktivität phosphoryliert wurde und dass DYRK4 ein für DYRK1A bekanntes Substrat in Lebendzellen phosphorylieren konnte. Schließlich wurde bestätigt, dass die Substratspezifität von DYRK4 und DYRK1A unterschiedlich ist und ein Peptid identifiziert, welches spezifisch von DYRK4 erkannt wird.

Durch die Behandlung mit einem Phosphataseinhibitor wurde belegt, dass die Autophosphorylierung von DYRK1A in HeLa-Zellen induzierbar ist und dass

DYRK1A sich auch *in vitro* autophosphorylierte. Um die Phosphorylierung von DYRK1A an Ser748 zu untersuchen, wurde ein phospho-spezifischer Antikörper gegen das Ser748 generiert. Mittels der kinase-inaktiven Mutanten von DYRK1A wurde gezeigt, dass an Ser748 eine Autophosphorylierung in *trans* (intermolekular) erfolgt. Die Imitation der Phosphorylierung an Ser748 durch Austausch des Serinrestes mit Glutaminsäure erhöhte die Aktivität von DYRK1A gegenüber einem Peptidsubstrat. Jedoch wurden keine Veränderungen des Ser748-Phosphorylierungslevels während der Phasen des Zellzyklus detektiert.

In den Zellzyklusversuchen wurde der Abbau von endogenem DYRK1A und GFP-DYRK1A während des Austritts aus der Mitose in zwei verschiedenen Zelllinien (neuronale PC12-Zellen aus der Ratte und menschliche Zervixkarzinom HeLa-Zellen) und mittels zwei unterschiedlicher Synchronisationsmethoden beobachtet. Dieser Abbau wurde bei Behandlung mit dem Proteasominhibitor MG132 inhibiert, was eine Rolle des Anaphase fördernden Komplexes (engl. *Anaphase promoting complex/Cyclosome*; APC/C) vermuten lässt, welcher den proteasomalen Abbau von Proteinen während des Austritts aus der Mitose vermittelt. Ein Abbau von GFP-DYRK1A wurde auch in Überexpressions-versuchen gefunden, welcher unabhängig von der Kinaseaktivität von DYRK1A auftrat. Zusätzlich beeinträchtigte die Überexpression von Wildtyp GFP-DYRK1A die Dephosphorylierung des Retinoblastom-Proteins, eines Zellzyklus-Regulators, während des Austritts aus der Mitose, wobei die kinase-inaktive Mutante oder die C-terminale Deletionsmutante von DYRK1A diesen Effekt nicht aufwiesen.

Zusammenfassend erfolgte in dieser Studie 1) eine Charakterisierung der neu entdeckten langen Spleißvariante von DYRK4 und zugleich eine Beschreibung der Unterschiede in der Substratspezifität von DYRK4 und DYRK1A sowie 2) eine Untersuchung der Rolle von DYRK1A während des Zellzyklus und die Autophosphorylierung an Ser748.

8. References

Alt, J. R., Cleveland, J. L., Hannink, M., and Diehl, J. A. (2000). Phosphorylation-dependent regulation of cyclin D1 nuclear export and cyclin D1-dependent cellular transformation. Genes Dev *14*, 3102-3114.

Alvarez, M., Altafaj, X., Aranda, S., and de la Luna, S. (2007). DYRK1A Autophosphorylation on Serine Residue 520 Modulates Its Kinase Activity via 14-3-3 Binding. Mol. Biol. Cell *18*, 1167-1178.

Alvarez, M., Estivill, X., and de la Luna, S. (2003). DYRK1A accumulates in splicing speckles through a novel targeting signal and induces speckle disassembly. J Cell Sci *116*, 3099-3107.

Aranda, S., Laguna, A., and de la Luna, S. (2010). DYRK family of protein kinases: evolutionary relationships, biochemical properties, and functional roles. FASEB J. Available at: http://www.ncbi.nlm.nih.gov/pubmed/21048044 [Accessed November 8, 2010].

Bähler, J., and Pringle, J. (1998). Pom1p, a fission yeast protein kinase that provides positional information for both polarized growth and cytokinesis. Genes Dev. *12*, 1356-1370.

Bähler, J., and Nurse, P. (2001). Fission yeast Pom1p kinase activity is cell cycle regulated and essential for cellular symmetry during growth and division. EMBO J *20*, 1064-1073.

Bain, J., Plater, L., Elliott, M., Shpiro, N., Hastie, C. J., Mclauchlan, H., Klevernic, I., Arthur, J. S. C., Alessi, D. R., and Cohen, P. (2007). The selectivity of protein kinase inhibitors: a further update. Biochem J. *408*, 297–315.

Becker, W., and Joost, H. G. (1999). Structural and functional characteristics of Dyrk, a novel subfamily of protein kinases with dual specificity. Prog. Nucleic Acid Res. Mol. Biol *62*, 1-17.

Becker, W., and Sippl, W. (2011). Activation, regulation, and inhibition of DYRK1A. FEBS J *278*, 246-256.

Becker, W., Weber, Y., Wetzel, K., Eirmbter, K., Tejedor, F. J., and Joost, H. (1998). Sequence Characteristics, Subcellular Localization, and Substrate Specificity of DYRK-related Kinases, a Novel Family of Dual Specificity Protein Kinases. J. Biol. Chem. *273*, 25893-25902.

Bescond, M., and Rahmani, Z. (2005). Dual-specificity tyrosine-phosphorylated and regulated kinase 1A (DYRK1A) interacts with the phytanoyl-CoA alpha-hydroxylase associated protein 1 (PAHX-AP1), a brain specific protein. Int. J. Biochem. Cell Biol *37*, 775-783.

Boudrez, A., Beullens, M., Waelkens, E., Stalmans, W., and Bollen, M. (2002). Phosphorylation-dependent interaction between the splicing factors SAP155 and NIPP1. J. Biol. Chem *277*, 31834-31841.

Branchi, I., Bichler, Z., Minghetti, L., Delabar, J. M., Malchiodi-Albedi, F., Gonzalez, M., Chettouh, Z., Nicolini, A., Chabert, C., Smith, D. J., et al. (2004). Transgenic mouse in vivo library of human Down syndrome critical region 1: association between DYRK1A overexpression, brain development abnormalities, and cell cycle protein alteration. J. Neuropathol. Exp. Neurol *63*, 429-440.

Calvo, S. E., Pagliarini, D. J., and Mootha, V. K. (2009). Upstream open reading frames cause widespread reduction of protein expression and are polymorphic among humans. Proc. Natl. Acad. Sci. U.S.A *106*, 7507-7512.

Campbell, L. E., and Proud, C. G. (2002). Differing substrate specificities of members of the DYRK family of arginine-directed protein kinases. FEBS Letters *510*, 31-36.

Casanovas, O., Miró, F., Estanyol, J. M., Itarte, E., Agell, N., and Bachs, O. (2000). Osmotic stress regulates the stability of cyclin D1 in a p38SAPK2-dependent manner. J. Biol. Chem *275*, 35091-35097.

Cheng, K. C., Klancer, R., Singson, A., and Seydoux, G. (2009). Regulation of MBK-2/DYRK by CDK-1 and the Pseudophosphatases EGG-4 and EGG-5 during the Oocyte-to-Embryo Transition. Cell *139*, 560-572.

Daub, H., Olsen, J. V., Bairlein, M., Gnad, F., Oppermann, F. S., Körner, R., Greff, Z., Kéri, G., Stemmann, O., and Mann, M. (2008). Kinase-selective enrichment enables quantitative phosphoproteomics of the kinome across the cell cycle. Mol. Cell *31*, 438-448.

Deng, X., Ewton, D. Z., Mercer, S. E., and Friedman, E. (2005). Mirk/dyrk1B decreases the nuclear accumulation of class II histone deacetylases during skeletal muscle differentiation. J. Biol. Chem *280*, 4894-4905.

Deng, X., Ewton, D. Z., Pawlikowski, B., Maimone, M., and Friedman, E. (2003). Mirk/dyrk1B is a Rho-induced kinase active in skeletal muscle differentiation. J. Biol. Chem *278*, 41347-41354.

Deng, X., Mercer, S. E., Shah, S., Ewton, D. Z., and Friedman, E. (2004). The cyclin-dependent kinase inhibitor p27Kip1 is stabilized in G(0) by Mirk/dyrk1B kinase. J. Biol. Chem *279*, 22498-22504.

Diehl, J. A., Cheng, M., Roussel, M. F., and Sherr, C. J. (1998). Glycogen synthase kinase-3beta regulates cyclin D1 proteolysis and subcellular localization. Genes Dev *12*, 3499-3511.

Evans, T., Rosenthal, E. T., Youngblom, J., Distel, D., and Hunt, T. (1983). Cyclin: a protein specified by maternal mRNA in sea urchin eggs that is destroyed at each cleavage division. Cell *33*, 389-396.

Feng, W., Benko, A. L., Lee, J. H., Stanford, D. R., and Hopper, A. K. (1999). Antagonistic effects of NES and NLS motifs determine S. cerevisiae Rna1p subcellular distribution. J. Cell. Sci *112 (Pt 3)*, 339-347.

Fotaki, V., Dierssen, M., Alcantara, S., Martinez, S., Marti, E., Casas, C., Visa, J., Soriano, E., Estivill, X., and Arbones, M. L. (2002). Dyrk1A Haploinsufficiency Affects Viability and Causes Developmental Delay and Abnormal Brain Morphology in Mice. Mol. Cell. Biol. *22*, 6636-6647.

Funakoshi, E., Hori, T., Haraguchi, T., Hiraoka, Y., Kudoh, J., Shimizu, N., and Ito, F. Overexpression of the human MNB/DYRK1A gene induces formation of multinucleate cells through overduplication of the centrosome. BMC Cell Biol *4*, 12-12.

Galceran, J., de Graaf, K., Tejedor, F. J., and Becker, W. (2003). The MNB/DYRK1A protein kinase: genetic and biochemical properties. J. Neural Transm. Suppl, 139-148.

Geiger, J. N., Knudsen, G. T., Panek, L., Pandit, A. K., Yoder, M. D., Lord, K. A., Creasy, C. L., Burns, B. M., Gaines, P., Dillon, S. B., et al. (2001). mDYRK3 kinase is expressed selectively in late erythroid progenitor cells and attenuates colony-forming unit-erythroid development. Blood *97*, 901-910.

Giacinti, C., and Giordano, A. (2006). RB and cell cycle progression. Oncogene *25*, 5220-5227.

Göckler, N., Jofre, G., Papadopoulos, C., Soppa, U., Tejedor, F. J., and Becker, W. (2009). Harmine specifically inhibits protein kinase DYRK1A and interferes with neurite formation. FEBS J *276*, 6324-6337.

Gomez, B. P., Riggins, R. B., Shajahan, A. N., Klimach, U., Wang, A., Crawford, A. C., Zhu, Y., Zwart, A., Wang, M., and Clarke, R. (2007). Human X-box binding protein-1 confers both estrogen independence and antiestrogen resistance in breast cancer cell lines. FASEB J *21*, 4013-4027.

de Graaf, K., Czajkowska, H., Rottmann, S., Packman, L. C., Lilischkis, R., Lüscher, B., and Becker, W. (2006). The protein kinase DYRK1A phosphorylates the splicing factor SF3b1/SAP155 at Thr434, a novel in vivo phosphorylation site. BMC Biochem *7*, 7.

de Graaf, K., Hekerman, P., Spelten, O., Herrmann, A., Packman, L. C., Büssow, K., Müller-Newen, G., and Becker, W. (2004). Characterization of cyclin L2, a novel cyclin with an arginine/serine-rich domain: phosphorylation by DYRK1A and colocalization with splicing factors. J. Biol. Chem *279*, 4612-4624.

Guimera, J., Casas, C., Estivill, X., and Pritchard, M. (1999). HumanMinibrainHomologue (MNBH/DYRK1): Characterization, Alternative Splicing, Differential Tissue Expression, and Overexpression in Down Syndrome. Genomics *57*, 407-418.

Guo, X., Williams, J. G., Schug, T. T., and Li, X. (2010). DYRK1A and DYRK3 Promote Cell Survival through Phosphorylation and Activation of SIRT1. Journal of Biological Chemistry *285*, 13223-13232.

Gwack, Y., Sharma, S., Nardone, J., Tanasa, B., Iuga, A., Srikanth, S., Okamura, H., Bolton, D., Feske, S., Hogan, P. G., et al. (2006). A genome-wide Drosophila RNAi screen identifies DYRK-family kinases as regulators of NFAT. Nature *441*, 646-650.

Hamilton, B. T., and Snyder, J. A. (1982). Rapid completion of mitosis and cytokinesis in PtK cells following release from nocodazole arrest. Eur. J. Cell Biol *28*, 190-194.

Hanks, S. K., and Hunter, T. (1995). Protein kinases 6. The eukaryotic protein kinase superfamily: kinase (catalytic) domain structure and classification. FASEB *9*, 576-596.

Hans, F., and Dimitrov, S. (2001). Histone H3 phosphorylation and cell division. Oncogene *20*, 3021-3027.

Hendzel, M. J., Wei, Y., Mancini, M. A., Van Hooser, A., Ranalli, T., Brinkley, B. R., Bazett-Jones, D. P., and Allis, C. D. (1997). Mitosis-specific phosphorylation of histone H3 initiates primarily within pericentromeric heterochromatin during G2 and spreads in an ordered fashion coincident with mitotic chromosome condensation. Chromosoma *106*, 348-360.

Himpel, S., Panzer, P., Eirmbter, K., Czajkowska, H., Sayed, M., Packman, L. C., Blundell, H., Kentrup, H., Grötzinger, J., Joost, H. G., et al. (2001). Identification of the autophosphorylation sites and characterization of their effects in the protein kinase DYRK1A. Biochem J. *359*, 497-505.

Himpel, S., Tegge, W., Frank, R., Leder, S., Joost, H., and Becker, W. (2000). Specificity Determinants of Substrate Recognition by the Protein Kinase DYRK1A. J. Biol. Chem. *275*, 2431-2438.

Johnson, D. G., and Walker, C. L. (1999). Cyclins and cell cycle checkpoints. Annu. Rev. Pharmacol. Toxicol *39*, 295-312.

Kentrup, H., Becker, W., Heukelbach, J., Wilmes, A., Schürmann, A., Huppertz, C., Kainulainen, H., and Joost, H. (1996). Dyrk, a Dual Specificity Protein Kinase with Unique Structural Features Whose Activity Is Dependent on Tyrosine Residues between Subdomains VII and VIII. J. Biol. Chem. *271*, 3488-3495.

Kim, H., Sablin, S. O., and Ramsay, R. R. (1997). Inhibition of monoamine oxidase A by beta-carboline derivatives. Arch. Biochem. Biophys *337*, 137-142.

Kinstrie, R., Lochhead, P. A., Sibbet, G., Morrice, N., and Cleghon, V. (2006). dDYRK2 and Minibrain interact with the chromatin remodelling factors SNR1 and TRX. Biochem. J *398*, 45-54.

Kinstrie, R., Luebbering, N., Miranda-Saavedra, D., Sibbet, G., Han, J., Lochhead, P. A., and Cleghon, V. (2010). Characterization of a domain that transiently converts class 2 DYRKs into intramolecular tyrosine kinases. Sci Signal *3*, ra16.

Knudsen, E. S., and Wang, J. Y. (1996). Differential regulation of retinoblastoma protein function by specific Cdk phosphorylation sites. J. Biol. Chem *271*, 8313-8320.

Kyng, K. J., May, A., Kølvraa, S., and Bohr, V. A. (2003). Gene expression profiling in Werner syndrome closely resembles that of normal aging. Proc. Natl. Acad. Sci. U.S.A *100*, 12259-12264.

Leder, S., Weber, Y., Altafaj, X., Estivill, X., Joost, H. G., and Becker, W. (1999). Cloning and characterization of DYRK1B, a novel member of the DYRK family of protein kinases. Biochem. Biophys. Res. Commun *254*, 474-479.

Lee, P., Paik, S., Shin, C., Huh, W., and Hahn, J. (2011). Regulation of yeast Yak1 kinase by PKA and autophosphorylation-dependent 14-3-3 binding. Mol. Microbiol *79*, 633-646.

Leypoldt, F., Lewerenz, J., and Methner, A. (2001). Identification of genes up-regulated by retinoic-acid-induced differentiation of the human neuronal precursor cell line NTERA-2 cl.D1. J. Neurochem *76*, 806-814.

Li, K., Zhao, S., Karur, V., and Wojchowski, D. M. (2002). DYRK3 activation, engagement of protein kinase A/cAMP response element-binding protein, and modulation of progenitor cell survival. J. Biol. Chem *277*, 47052-47060.

Lin, B. T., and Wang, J. Y. (1992). Cell cycle regulation of retinoblastoma protein phosphorylation. Ciba Found. Symp *170*, 227-241; discussion 241-243.

Lippincott-Schwartz, J., Snapp, E., and Kenworthy, A. (2001). Studying protein dynamics in living cells. Nat. Rev. Mol. Cell Biol *2*, 444-456.

Lochhead, P. A., Sibbet, G., Kinstrie, R., Cleghon, T., Rylatt, M., Morrison, D. K., and Cleghon, V. (2003). dDYRK2: a novel dual-specificity tyrosine-phosphorylation-regulated kinase in Drosophila. Biochem J. *374*, 381-391.

Lochhead, P. A., Sibbet, G., Morrice, N., and Cleghon, V. (2005). Activation-Loop Autophosphorylation Is Mediated by a Novel Transitional Intermediate Form of DYRKs. Cell *121*, 925-936.

Lord, K. A., Creasy, C. L., King, A. G., King, C., Burns, B. M., Lee, J. C., and Dillon, S. B. (2000). REDK, a novel human regulatory erythroid kinase. Blood *95*, 2838-2846.

Ludlow, J. W., Glendening, C. L., Livingston, D. M., and DeCarprio, J. A. (1993). Specific enzymatic dephosphorylation of the retinoblastoma protein. Mol. Cell. Biol. *13*, 367-372.

Maddika, S., and Chen, J. (2009). Protein kinase DYRK2 is a scaffold that facilitates assembly of an E3 ligase. Nat Cell Biol *11*, 409-419.

Martí, E., Altafaj, X., Dierssen, M., de la Luna, S., Fotaki, V., Alvarez, M., Pérez-Riba, M., Ferrer, I., and Estivill, X. (2003). Dyrk1A expression pattern supports specific roles of this kinase in the adult central nervous system. Brain Res *964*, 250-263.

Mashima, T., Naito, M., Fujita, N., Noguchi, K., and Tsuruo, T. (1995). Identification of actin as a substrate of ICE and an ICE-like protease and involvement of an ICE-like protease but not ICE in VP-16-induced U937 apoptosis. Biochem. Biophys. Res. Commun *217*, 1185-1192.

Mercer, S. E., and Friedman, E. (2006). Mirk/Dyrk1B: A Multifunctional Dual-Specificity Kinase Involved in Growth Arrest, Differentiation, and Cell Survival. CBB *45*, 303-315.

Moriya, H., Shimizu-Yoshida, Y., Omori, A., Iwashita, S., Katoh, M., and Sakai, A. (2001). Yak1p, a DYRK family kinase, translocates to the nucleus and phosphorylates yeast Pop2p in response to a glucose signal. Genes Dev *15*, 1217-1228.

Nagy, Z. (1999). Mechanisms of neuronal death in Down's syndrome. J. Neural Transm. Suppl *57*, 233-245.

Nagy, Z., Esiri, M. M., Cato, A. M., and Smith, A. D. (1997). Cell cycle markers in the hippocampus in Alzheimer's disease. Acta Neuropathol *94*, 6-15.

Nakai, K., and Horton, P. (2007). Computational prediction of subcellular localization. Methods Mol. Biol *390*, 429-466.

Ohno, M., Fornerod, M., and Mattaj, I. W. (1998). Nucleocytoplasmic transport: the last 200 nanometers. Cell *92*, 327-336.

Ohtani, K., DeGregori, J., and Nevins, J. R. (1995). Regulation of the cyclin E gene by transcription factor E2F1. Proc. Natl. Acad. Sci. U.S.A *92*, 12146-12150.

Okui, M., Ide, T., Morita, K., Funakoshi, E., Ito, F., Ogita, K., Yoneda, Y., Kudoh, J., and Shimizu, N. (1999). High-Level Expression of the Mnb/Dyrk1A Gene in Brain and Heart during Rat Early Development. Genomics *62*, 165-171.

Pagano, M., Bain, J., Kazimierczuk, Z., Sarno, S., Ruzzene, M., Di Maira, G., Elliott, M., Orzeszko, A., Cozza, G., Meggio, F., et al. (2008). The selectivity of inhibitors of protein kinase CK2: an update. Biochem. J. *415*, 353.

Papadopoulos, C., Arato, K., Lilienthal, E., Zerweck, J., Schutkowski, M., Chatain, N., Müller-Newen, G., Becker, W., and de la Luna, S. (2011). Splice Variants of the Dual Specificity Tyrosine Phosphorylation-regulated Kinase 4 (DYRK4) Differ in Their Subcellular Localization and Catalytic Activity. J. Biol. Chem *286*, 5494-5505.

Park, J., Oh, Y., Yoo, L., Jung, M., Song, W., Lee, S., Seo, H., and Chung, K. C. (2010). DYRK1A phosphorylates p53 and inhibits proliferation of embryonic neuronal cells. J Biol Chem. Available at: http://www.ncbi.nlm.nih.gov/pubmed/20696760 [Accessed August 16, 2010].

Park, J., Song, W., and Chung, K. C. (2009). Function and regulation of Dyrk1A: towards understanding Down syndrome. Cell. Mol. Life Sci *66*, 3235-3240.

Pérez-Sala, D., and Mollinedo, F. (1995). Inhibition of N-linked glycosylation induces early apoptosis in human promyelocytic HL-60 cells. J. Cell. Physiol *163*, 523-531.

Peters, J. (2006). The anaphase promoting complex/cyclosome: a machine designed to destroy. Nat. Rev. Mol. Cell Biol *7*, 644-656.

Raich, W. B., Moorman, C., Lacefield, C. O., Lehrer, J., Bartsch, D., Plasterk, R. H. A., Kandel, E. R., and Hobert, O. (2003). Characterization of Caenorhabditis elegans homologs of the Down syndrome candidate gene DYRK1A. Genetics *163*, 571-580.

Reimertz, C., Kögel, D., Rami, A., Chittenden, T., and Prehn, J. H. M. (2003). Gene expression during ER stress-induced apoptosis in neurons: induction of the BH3-only protein Bbc3/PUMA and activation of the mitochondrial apoptosis pathway. J. Cell Biol *162*, 587-597.

Rogers, S., Wells, R., and Rechsteiner, M. (1986). Amino acid sequences common to rapidly degraded proteins: the PEST hypothesis. Science *234*, 364-368.

Rubin, E., Mittnacht, S., Villa-Moruzzi, E., and Ludlow, J. W. (2001). Site-specific and temporally-regulated retinoblastoma protein dephosphorylation by protein phosphatase type 1. Oncogene *20*, 3776-3785.

Sacher, F., Möller, C., Bone, W., Gottwald, U., and Fritsch, M. (2007). The expression of the testis-specific Dyrk4 kinase is highly restricted to step 8 spermatids but is not required for male fertility in mice. Mol. Cell. Endocrinol *267*, 80-88.

Sheaff, R. J., Groudine, M., Gordon, M., Roberts, J. M., and Clurman, B. E. (1997). Cyclin E-CDK2 is a regulator of p27Kip1. Genes & Development *11*, 1464 - 1478.

Sherman, M. Y., and Goldberg, A. L. (2001). Cellular defenses against unfolded proteins: a cell biologist thinks about neurodegenerative diseases. Neuron *29*, 15-32.

Sitz, J., Baumgärtel, K., Hämmerle, B., Papadopoulos, C., Hekerman, P., Tejedor, F., Becker, W., and Lutz, B. (2008). The down syndrome candidate dual-specificity tyrosine phosphorylation-regulated kinase 1A phosphorylates the neurodegeneration-related septin 4. Neuroscience *157*, 596-605.

Sitz, J. H. (2003). Zur Funktion der Kinase Dyrk1A im Gehirn der adulten Maus. Available at: http://edoc.ub.uni-muenchen.de/1256/ [Accessed February 27, 2011].

Skurat, A. V., and Dietrich, A. D. (2004). Phosphorylation of Ser640 in muscle glycogen synthase by DYRK family protein kinases. J. Biol. Chem *279*, 2490-2498.

Souza, G., Lu, S., and Kuspa, A. (1998). YakA, a protein kinase required for the transition from growth to development in Dictyostelium. Development *125*, 2291-2302.

Standart, N., Minshull, J., Pines, J., and Hunt, T. (1987). Cyclin synthesis, modification and destruction during meiotic maturation of the starfish oocyte. Dev. Biol *124*, 248-258.

Su, A. I., Wiltshire, T., Batalov, S., Lapp, H., Ching, K. A., Block, D., Zhang, J., Soden, R., Hayakawa, M., Kreiman, G., et al. (2004). A gene atlas of the mouse and human protein-encoding transcriptomes. Proc Natl Acad Sci U S A *101*, 6062-6067.

Taira, N., Nihira, K., Yamaguchi, T., Miki, Y., and Yoshida, K. (2007). DYRK2 is targeted to the nucleus and controls p53 via Ser46 phosphorylation in the apoptotic response to DNA damage. Mol. Cell *25*, 725-738.

Taira, N., Yamamoto, H., Yamaguchi, T., Miki, Y., and Yoshida, K. (2010). ATM augments nuclear stabilization of DYRK2 by inhibiting MDM2 in the apoptotic response to DNA damage. J. Biol. Chem *285*, 4909-4919.

Tamrakar, S., Rubin, E., and Ludlow, J. W. (2000). Role of pRB dephosphorylation in cell cycle regulation. Front. Biosci *5*, D121-137.

Tang, C. C., Fu, R., Wu, K., Hsu, W., and Tang, T. K. (2009). CPAP is a cell-cycle regulated protein that controls centriole length. Nat. Cell Biol *11*, 825-831.

Tejedor, F., Zhu, X. R., Kaltenbach, E., Ackermann, A., Baumann, A., Canal, I., Heisenberg, M., Fischbach, K. F., and Pongs, O. (1995). minibrain: A new protein kinase family involved in postembryonic neurogenesis in Drosophila. Neuron *14*, 287-301.

Varjosalo, M., Björklund, M., Cheng, F., Syvänen, H., Kivioja, T., Kilpinen, S., Sun, Z., Kallioniemi, O., Stunnenberg, H. G., He, W., et al. (2008). Application of active and kinase-deficient kinome collection for identification of kinases regulating hedgehog signaling. Cell *133*, 537-548.

Vlach, J., Hennecke, S., and Amati, B. (1997). Phosphorylation-dependent degradation of the cyclin-dependent kinase inhibitor p27. EMBO J *16*, 5334-5344.

Wang, J. Y. (2000). Regulation of cell death by the Abl tyrosine kinase. Oncogene *19*, 5643-5650.

Wang, X., Wei, Y., Yuan, S., Liu, G., Lu, Y., Zhang, J., and Wang, W. (2005). Potential anticancer activity of tanshinone IIA against human breast cancer. Int. J. Cancer *116*, 799-807.

Wegiel, J., Gong, C., and Hwang, Y. (2011). The role of DYRK1A in neurodegenerative diseases. FEBS J *278*, 236-245.

Woods, Y. L., Cohen, P., Becker, W., Jakes, R., Goedert, M., Wang, X., and Proud, C. G. (2001). The kinase DYRK phosphorylates protein-synthesis initiation factor eIF2Bepsilon at Ser539 and the microtubule-associated protein tau at Thr212: potential role for DYRK as a glycogen synthase kinase 3-priming kinase. Biochem. J *355*, 609-615.

Yabut, O., Domogauer, J., and D'Arcangelo, G. (2010). Dyrk1A Overexpression Inhibits Proliferation and Induces Premature Neuronal Differentiation of Neural Progenitor Cells. J. Neurosci. *30*, 4004-4014.

Zarkowska, T., and Mittnacht, S. (1997). Differential phosphorylation of the retinoblastoma protein by G1/S cyclin-dependent kinases. J. Biol. Chem *272*, 12738-12746.

Zhang, D., Li, K., Erickson-Miller, C. L., Weiss, M., and Wojchowski, D. M. (2005). DYRK gene structure and erythroid-restricted features of DYRK3 gene expression. Genomics *85*, 117-130.

Zieve, G. W., Turnbull, D., Mullins, J. M., and McIntosh, J. R. (1980). Production of large numbers of mitotic mammalian cells by use of the reversible microtubule inhibitor nocodazole. Nocodazole accumulated mitotic cells. Exp. Cell Res *126*, 397-405.

Zou, Y., Ewton, D. Z., Deng, X., Mercer, S. E., and Friedman, E. (2004). Mirk/dyrk1B kinase destabilizes cyclin D1 by phosphorylation at threonine 288. J. Biol. Chem *279*, 27790-27798.

9. Curriculum Vitae

Personal Information

Name :	Papadopoulos
Forename :	Chrisovalantis
Nationality :	Greek
Date of Birth :	31/01/1981
Place of Birth :	Wesel, Germany
Marital status :	single

Education

10/2008 – 05/2011 Continuation of doctoral studies at the Institute of Pharmacology and Toxicology, RWTH Aachen University (supervisor: Prof. Walter Becker); Title: Identification and characterization of a new splice variant of the protein kinase DYRK4 and the role of DYRK1A during mitotic exit; Mark: summa cum laude

04/2008 – 09/2008 Half year fellowship of the DAAD (German Academic Exchange Service) at the Center of Genomic Regulation (CRG) (Barcelona, Spain) (supervisor: Dr. Susana de la Luna); Topic: Dysregulation of neuronal signaling pathways caused by additional copy of the *DYRK1A* gene in trisomy 21

01/2008 2 weeks research stay at the Instituto de Neurociencias CSIC-UMH in the Group for Molecular Neurogenetics of Francisco J. Tejedor in San Juan, Alicante (Spain)

04/2007 – 03/2008 PhD student at the Institute of Pharmacology and Toxicology, RWTH Aachen University (supervisor: Prof. Walter Becker)

03/2007 Diploma in Biology at the Institute of Pharmacology and Toxicology, RWTH Aachen University (supervisor: Prof. Walter Becker); experimental part at the CRG (Barcelona, Spain); Title: Functional Characterisation of the Protein Kinase DYRK4; Degree: Diplom-Biologe (Overall mark: very good)

10/2001 – 03/2007 RWTH Aachen University; field of study: biology

10/2000 – 09/2001 RWTH Aachen University; field of study: mathematics

08/1991 – 06/2000 Andreas-Vesalius-Gymnasium Wesel; secondary highschool Qualification: A levels, High School Diploma

10. Publication List

Original Articles

Papadopoulos C, Arato K, Lilienthal E, Zerweck J, Schutkowski M, Chatain N, Müller-Newen G, Becker W, de la Luna S.
Splice variants of the dual-specificity tyrosine phosphorylation-regulated kinase 4 (DYRK4) differ in their subcellular localization and catalytic activity.
J Biol Chem. 286 (2011):5494-5505.

Göckler N, Jofre G, Papadopoulos C, Soppa U, Tejedor FJ, Becker W.
Harmine specifically inhibits protein kinase DYRK1A and interferes with neurite formation.
FEBS J. 276 (2009):6324-6337.

Sitz JH, Baumgärtel K, Hämmerle B, Papadopoulos C, Hekerman P, Tejedor FJ, Becker W, Lutz B.
The Down syndrome candidate dual-specificity tyrosine phosphorylation-regulated kinase 1A phosphorylates the neurodegeneration-related septin 4.
Neuroscience. 157 (2008):596-605.

Minireview

Soppa U, Papadopoulos C, Becker W.
Implications of the elevated activity of protein kinase DYRK1A in Down syndrome
Biotech international 22 (2010):12-15.

Oral Communication at symposia and meetings

Papadopoulos C, Arató K, Chatain N, Müller-Newen G, Becker W, de la Luna S.
Two novel isoforms of DYRK4 differ in subcellular localization and their expression pattern.
Naunyn-Schmiedeberg's Archives of Pharmacology 381 (2010):30-30.

Papadopoulos C, Kiesgen S.
Is DYRK1A phosphorylation on Ser748 regulated during cell cycle?
DYRK1A Joint Meeting at Instituto de Neurociencias CSIC-UMH in San Juan, Alicante (Spain), January 2010

Poster Presentation at symposia and meetings

Papadopoulos C, Pruessmeyer J, Soppa U, Becker W, Ludwig A.
The protein kinase DYRK1A increases alpha-secretase activity in neuronal cells and accelerates alpha-cleavage of amyloid precursor protein.
10th International Conference on Alzheimer's & Parkinson's Diseases (AD/PD) 2011, Barcelona, Spain.
Neurodegenerative Dis. 8(Suppl. 1) (2011):1-1.

Papadopoulos C, Arató K, Lilienthal E, Zerweck J, Schutkowski M, Becker W, de la Luna S.
Biochemical Characterization of DYRK4.
Trinational Fall Meeting 2009 on Signal Transduction and Disease, Aachen, Germany

Göckler N, Jofre G, Papadopoulos C, Tejedor FJ, Becker W.
Harmine specifically inhibits protein kinase DYRK1A and interferes with neurite formation.
Trinational Fall Meeting 2009 on Signal Transduction and Disease, Aachen, Germany